STUTZMAN

NATIONAL ACADEMIES OF SCIENCE AND ENGINEERING

NATIONAL RESEARCH COUNCIL

of the

UNITED STATES OF AMERICA

UNITED STATES NATIONAL COMMITTEE

International Union of Radio Science

National Radio Science Meeting

13-16 January 1986

Sponsored by USNC/URSI
in cooperation with
Institute of Electrical and Electronics Engineers

University of Colorado
Boulder, Colorado
U.S.A.

NOTE:

Programs and Abstracts of the USNC/URSI Meetings are available from:

USNC/URSI
National Academy of Sciences
2101 Constitution Avenue, N.W.
Washington, DC 20418

at $2 for meetings prior to 1970, $3 for 1971-71 meetings, and $5 for 1976-86 meetings.

The full papers are not published in any collected format; requests for them should be addressed to the authors who may have them published on their own initiative. Please note that these meetings are national. They are not organized by the International Union, nor are the programs available from the International Secretariat.

MEMBERSHIP

United States National Committee

INTERNATIONAL UNION OF RADIO SCIENCE

Chairman:	Robert K. Crane*
Vice Chairman:	Sidney A. Bowhill*
Secretary:	Chalmers M. Butler*
Immediate Past Chairman:	Prof. Thomas B. A. Senior*

Members Representing Societies, Groups, and Institutes:

American Geophysical Union	Dr. Donald A. Gurnett
American Astronomical Society	Dr. David E. Hogg
IEEE Antennas & Propagation Society	Dr. W. Ross Stoner
IEEE Communications Society	Prof. Raymond Pickholtz
IEEE Geophysics and Remote Sensing Society	Dr. Robert E. McIntosh

Liaison Representatives from Government Agencies:

National Telecommunications & Information Administration	Dr. Douglass D. Crombie
National Science Foundation	Dr. Vernon Pankonin
National Aeronautics & Space Administration	vacant
Federal Communications Commission	Mr. William A. Daniel Mr. William J. Cook
Department of Defense	Dr. George L. Salton
Department of the Army	Lt. Col. Robert Clayton, Jr. Mr. Earl J. Holliman
Department of the Navy	vacant
Department of the Air Force	Dr. Allan C. Schell

Members-at-Large:

Dr. David C. Chang
Dr. Donald T. Farley
Mr. John A. Klobuchar
Dr. Edmund K. Miller
Dr. Ray J. King
Dr. Arthur D. Spaulding

Chairmen of the USNC/URSIC Commissions:

Commission A	Dr. Norris S. Nahman
Commission B	Dr. Akira Ishimaru
Commission C	Dr. Jay W. Schwartz
Commission D	Drs. K. J. Button & A. A. Oliner
Commission E	Dr. Joel M. Morris
Commission F	Dr. Richard K. Moore
Commission G	Dr. Kung Chie Yeh
Commission H	Dr. Kenneth J. Harker
Commission J	Dr. William J. Welsh

Officers of URSI resident in the United States:
(including Honorary Presidents)

President	Prof. William E. Gordon*
Honorary President	Prof. Henry G. Booker*

Chairmen and Vice Chairmen of Commissions of URSI resident in the United States:

Vice Chairman of Commission B	Prof. Thomas B. A. Senior
Vice Chairman of Commission F	Dr. Robert K. Crane
Vice Chairman of Commission G	Dr. Jules Aarons

Foreign Secretary of the U.S. National Academy of Sciences	Dr. Walter A. Rosenblith
Chairman, National Research Council, Commission on Physical Sciences, Mathematics, and Resources	Dr. Herbert Friedman
Chairman, National Research Council, Board on Physics and Astronomy	Prof. Hans Frauenfelder
NRC Staff Officer	Dr. Robert L. Riemer
Honorary Members	Dr. Harold H. Beverage Dr. Ernst Weber

* Member of USNC/URSI Executive Committee

DESCRIPTION OF THE
INTERNATIONAL UNION OF RADIO SCIENCE

The International Union of Radio Science is one of 18 world scientific unions organized under the International Council of Scientific Unions (ICSU). It is commonly designated as URSI (from its French name, Union Radio Scientifique Internationale). Its aims are (1) to promote the scientific study of radio communications, (2) to aid and organize radio research requiring cooperation on an international scale and to encourage the discussion and publication of the results, (3) to facilitate agreement upon common methods of measurement and the standardization of measuring instruments, and (4) to stimulate and to coordinate studies of the scientific aspects of telecommunications using electromagnetic waves, guided and unguided. The International Union itself is an organizational framework to aid in promoting these objectives. The actual technical work is largely done by the National Committee in the various countries.

The officers of the International union are:

President:	Dr. A. P. Mitra (India)
Past President:	Prof. W. E. Gordon (U.S.A.)
Vice Presidents:	Dr. Ing. H. J. Albrecht (F.R.G.) A. L. Cullen (U.K.) S. Okamura (Japan) Prof. V. Zima (Czechoslavakia)
Secretary-General:	J. Van Bladel (Belgium)
Honorary Presidents:	G. Beynon (U.K.) H. G. Booker (U.S.A.) W. Dieminger (West Germany) I. Koga (Japan J. A. Ratcliffe (U.K.)

The Secretary-General's office and the headquarters of the organization are located at Avenue Albert Lancaster, 32, B-1180 Brussels, Belgium. The Union is supported by contributions (dues) from 38 member countries. Additional funds for symposia and other scientific activities of the Union are provided by ICSU from contributions received for this purpose from UNESCO.

The International Union, as of the XXth General Assembly held in Washington, DC in August 1981, has nine bodies called Commissions for centralizing studies in the principal technical fields.

Every three years the International Union holds a meeting called the General Assembly. The next is the XXIIst, to be held in 1987. The Secretariat prepares and distributes the Proceedings of these General Assemblies. The International Union arranges international symposia on specific subjects pertaining to the work of one or several Commissions and also cooperates with other Unions in internatioanl symposia on subjects of joint interest.

Radio is unique among the fields of scientific work in having a specific adaptability to large-scale international research programs, since many of the phenomena that must be studied are worldwide in extent and yet are in a measure subject to control by experimenters. Exploration of space and the extension of scientific observations to the space environment are dependent on radio for their research. One branch, radio astronomy, involves cosmic phenomena. URSI thus has a distinct field of usefulness in furnishing a meeting ground for the numerous workers in the manifold aspects of radio research; its meetings and committee activities furnish valuable means of promoting research through exchange of ideas.

Session A-1 0855-Mon. CR1-42

EM MEASUREMENTS FOR SATELLITE COMMUNICATIONS

Chairman: H. M. Cronson, The MITRE Corp., Bedford, MA 01730

A1-1 0900 CALIBRATION OF AN EHF SATELLITE COMMUNICATION TERMINAL

L. W. Rispin and A. J. Simmons
M.I.T. Lincoln Laboratory
P. O. Box 73
Lexington, Massachusetts 02173

An experimental satellite communications package operating in the EHF frequency range (≈ 44 GHz uplink, ≈ 21 GHz downlink) is being built by Lincoln Laboratory for launch within the next couple of years. To measure the link performance of this satellite, as well as future EHF satellites in this band, a calibration terminal has been built at Lincoln Lab. To perform RF calibration of the terminal itself, automated transmitting and receiving systems have been installed on two nearby towers.

The RF portion of the terminal itself consists of an eight-foot dish and pedestal with a five-horn tracking feed for 21 GHz and a single beam transmitting feed for 44 GHz. The two frequencies are diplexed by means of a flat, frequency-selective reflector located near the feedhorns. It is made up of printed, crossed resonant dipoles sandwiched between two dielectric sheets. Mounted on the back of the antenna are calibrated transmitter, receiver and a noise source.

The main boresight tower contains a two-foot, 21 GHz transmitting dish and two one-foot, 44 GHz dishes, one transmitting, the other receiving. All antennas are circularly polarized. With the three antennas in the boresight tower are transmitting sources at both frequencies as well as a 44 GHz detector and power meter. Remotely controllable precision attenuators are used for power level setting. Since this tower was slightly closer than the desired far-field distance, a secondary more distant tower was also used for initial antenna gain and pattern measurement.

The boresight tower is used for determining pointing direction, G/T and EIRP of the eight-foot terminal. The latter two quantities are each measured in two ways, by measuring the link performance and by independent measurement of antenna gain, noise figure, and RF power input to the antenna. The expected accuracy of calibration is about 1 dB in either G/T or EIRP. All equipment is controlled and monitored via telephone line.

The talk will describe the equipment used in the measurement as well as some of the measurement results.

Test antenna site was field probed to determine if plane wave was present from source(s).
±0.4dB gain error
EIRP can be measured by back solving Friis eqn.

A1-2
0920

DEVELOPMENT OF AIRBORNE EHF SATCOM TERMINALS

Allen L. Johnson
Avionics Laboratory
AFWAL/AAAI
Wright-Patterson AFB, OH 45433

15 Sept 1985

In an effort to provide additional link reliability for the command and control communications between the National Command Authority and the Nuclear Capable Forces of bomber, missiles and submarines, the Avionics Laboratory undertook the development of an EHF (36-38 GHz) airborne satellite communication (SATCOM) terminal. The initial terminal (AN/ASC-22) provided a 1000 watt CW transmitter, a 36" stabilized steerable antenna and a low noise receiving system to operate with the Lincoln Experimental Satellites (LES 8, LES 9). Data rates of 75, 2400 and 19,200 bps were provided by a processor controlled modulator/demodulator. Wide band frequency hopping provided the spread spectrum modulation technique. The system employed passive antenna pointing, satellite commanding capability and multichannel receiving capability.

A second generation dual band system (AN/ASC-28) was subsequently developed to operate in the 7-8 GHz band over the DSCS II satellite and in an EHF band (36-38 or 40-45 GHz) over LES 8/9 and the proposed Strategic Satellite System (SSS).

A third generation terminal (AN/ASC-30) has recently been developed which provides a transmit capability of 8 GHz or 44 GHz and a receiver at 7 GHz or 20 GHz to operate with DSCS or the MILSTAR satellites.

During a six-year flight test evaluation of three generations of EHF airborne SATCOM terminals over 1000 hours of airborne EHF operation has been achieved. The paper describes the flight test results including the reliability of the EHF terminals.

Propagation problems for EHF satellite communication have turned out to be less severe than anticipated. Multipath fading is experienced only when operating at very low elevation angles to the satellite. Rain attenuation on the ground of 25 dB has been recorded, but only for short periods of intense rain. Precipitation attenuation during takeoff, climbout and at altitude has been predicted and verified with extensive measurements.

A1-3
0940

ERROR ANALYSIS OF IN-ORBIT MEASUREMENTS ON COMMUNICATIONS SATELLITES: Keneth Fullett and Vasilis Riginos, COMSAT Laboratories, Clarksburg, MD 20734

The characteristics of communications satellites are measured in-orbit during initial acceptance and during anomaly investigations on an operational satellite. Measurements are performed by transmitting known signals to the spacecraft and comparing the power and phase of these with the returned signals re-transmitted from the satellite. These measurements contain many sources of error. These sources can be subdivided into those originating from the space segment and the earth station. The space segment errors are due to inaccuracies in the atmospheric loss model, spacecraft antenna pointing, and spacecraft position. Earth station errors are due to inaccuracies in the measurement equipment, earth station antenna pointing, and calibration.

This paper will analyze inaccuracies due to the earth station measurement equipment, and calibration, of a spectrum analyzer based in-orbit test system. The analysis covers both frequency and power measurements excluding the contributions of the earth station antenna.

Total down-link uncertainty for absolute measurements ~ 0.4 dB

Punch line: specifying antenna gains to 0.1 dB is ridiculous

A1-4
1020

AN EHF/SHF TERMINAL FOR SATELLITE COMMUNICATIONS MEASUREMENTS

Brian B.T. Spink
Rome Air Development Center
Griffiss AFB NY 13441-5700

C.P. Alkons and D.L. Zimmerman
The MITRE Corporation
MS/R350
Burlington Road
Bedford MA 01730

A SATCOM EHF/SHF research terminal is being developed at the Rome Air Development Center (RADC), Griffiss AFB NY. The terminal will be used for satellite communications measurements with future EHF satellite systems, such as the British SKYNET system. The terminal will be assembled from modular, state-of-the-art advanced development model subsystems, and will be housed in a transportable shelter.

The terminal will be used in proof-of-concept experiments to evaluate new technology developments and will add a significant new capability for the military services in the design, test, and measurements of future SATCOM systems. Terminal availability for measurements is planned for late 1985 to early 1986. This paper discusses the configuration, functions, and measurement capabilities of the RADC terminal.

Built a transportable satellite testbed

20 GHz LNA
>30 dB gain 3.6 dB NF
IP_3 = 20 dB 1dB compression: −15.6 dB

Built a synthesizer 11.7 ± 0.5 GHz

A1-5 Discussion
1040

With Milstar as long as you have enough uplink power (above a threshold) you get perfect downlinks. This is unlike normal transponder operation.

Session B-1 0855-Mon. CR2-28

SCATTERING - I

Chairman: R. W. Ziolkowski, Lawrence Livermore National Laboratory, Livermore, CA 94550

B1-1

0900 COMPLEX POLE PATTERNS OF CONDUCTING SPHEROIDS AND FINITE CYLINDERS

Barbara L. Merchant
Naval Research Laboratory
Washington, DC 20375
Anton Nagl and Herbert Überall
Department of Physics
Catholic University of America
Washington, DC 20064, and
Philip J. Moser
Corporate Technology Center
Sperry Corp.
Reston, VA 22091

Using a modification of the Waterman T-matrix code, we obtain comprehensive sets of pole patterns of the radar scattering amplitude in the complex frequency plane for perfectly conducting spheroids and finite-length cylinders, in the spirit of the Singularity Expansion Method (SEM). This completes our earlier study (P. J. Moser et al., Proc. IEEE, vol. 72, p. 1652, 1984) in which the non-axial vibration resonances (corresponding to the scattering poles) were interpreted as those of helical surface waves, for the cylinder case. Here, only a discrete number of pitch angles of the helix are allowed, due to the finite length of the cylinder, and in addition, a refraction effect occurs when the tangentially incident wave generates the helical wave on the cylinder. For the case of spheroids, the poles correspond to the resonances of a discrete set of quasi-helicoidal waves propagating along geodesics. Previous studies of these spheroidal poles (L. Marin, IEEE Trans. Antennas Prop., vol. AP-22, p. 266, 1974) had only been able to obtain TM poles, and of these only those corresponding to axial propagation. Here both TM and TE poles are obtained for both axial and (quasi-) helicoidal propagation, for spheroids and cylinders of length-to-diameter ratios up to 5:1 (higher for axial poles). Work at Catholic University supported by the Sperry Corporation.

B1-2
0920

RESONANCE FREQUENCIES OF CONDUCTING SPHEROIDS AS OBTAINED FROM THE PHASE MATCHING OF SURFACE WAVES

Barbara L. Merchant
Naval Research Laboratory
Washington, DC 20375
Anton Nagl and Herbert Überall
Department of Physics
Catholic University of America
Washington, DC 20064

The complex resonance frequencies of conducting spheroids have been obtained by us (P. J. Moser et al., Proc. IEEE vol. 72, p. 1652, 1984, and this conference) for both TE and TM modes, for deformations up to 5:1. We show that these resonances originate from a phase matching of repeatedly circumnavigating surface waves, and we develop a quantitative model of this phenomenon. The propagation constants vary continuously during the passage of the waves over the curved surface along a geodesic, depending to first order on the local longitudinal curvature of the path. This longitudinal curvature dependence was obtained in a calculation of Franz and Galle (Zeits. f. Naturf., vol. 10a, p. 374, 1955) in terms of a power series expansion in $k^{2/3}$, comprising five terms of the series. Using this, we formulate the phase matching as an integral condition over the closed path, in the sense of Fermat's principle, and obtain the resonance frequencies as the complex values of k which satisfy this phase matching integral. They are found to compare, by and large, reasonably well with the values obtained by our previous T- matrix calculation, indicating the basic correctness of our physical phase-matching model. (Work at Catholic University supported by the Sperry Corporation).

B1-3
0940

ELECTROMAGNETIC SCATTERING BY
DIELECTRIC PROLATE SPHEROIDS

B. P. Sinha and M. Francis R. Cooray
Faculty of Engineering and Applied Science
Memorial University of Newfoundland
St. John's, NF, Canada A1B 3X5

The multipole expansion technique applied by Sinha and MacPhie (Radio Sci, 12, 171-184, 1977) to the scattering from a single infinitely conducting prolate spheroid of a plane electromagnetic wave with arbitrary polarization and angle of incidence is extended to obtain the solution for EM plane wave scattering by a prolate spheroid composed of homogeneous and perfect dielectric material of dielectric constant ε_{R2}. The dielectric prolate spheroid is assumed to be embedded in a nonlossy infinite, homogeneous and isotropic medium of dielectric constant ε_{R1} which contains the plane electromagnetic wave of arbitrary polarization incident on the prolate spheroid at an arbitrary angle of incidence. The medium and the scatterer are assumed to be nonferromagnetic (magnetic permeabilities μ_1 and μ_2 each $\simeq \mu_0$, the permeability of the free space) with no free charge in either region. Since in the present problem the tangential components of both E and H fields must be continuous simultaneously across the spheroid surface ($\xi=\xi_0$, a constant), in addition to $\vec{M}^{(a)}$ vectors [$\vec{M}^{(a)}_{mn}$ = $\vec{\nabla}\phi_{mn}(h;\xi,\eta,\phi)x\hat{a}$, $\hat{a}=(\hat{x},\hat{y},\hat{z})$] which generate modal expansion of E fields, $\vec{N}^{(a)}$ vectors [$\vec{N}^{(a)}_{mn} = \frac{1}{k}\vec{\nabla} \times \vec{M}^{(a)}_{mn}$] are used to expand H fields.

The $\vec{M}$ and $\vec{N}$ vectors employed are the generalized exponential prolate spheroidal vector wave functions developed by Sinha and MacPhie (Quart. Appl. Math., 38, 143-158, 1980; IEEE Trans. AP, 31, 294-304, 1983).

The general solution is obtained in the form $\underline{S} = [G]\underline{I}$, where $\underline{S}$ and $\underline{I}$ are respectively the column vectors of coefficients of the series expansions of the scattered and transmitted fields taken together and the incident field. [G] is the transformation matrix which depends only on the scatterer. Numerical results in the form of curves of scattering cross-sections are given for variety of prolate spheroids composed of dielectric materials of different refractive indices.

B1-4
1000

CURRENT DISTRIBUTION ON A THIN WIRE IN A MULTIMODE RECTANGULAR CAVITY

D.I. Wu and D.C. Chang
Electromagnetics Laboratory
Department of Electrical and Computer Engineering
University of Colorado
Campus Box 425
Boulder, CO 80309

The use of a mode-stirred chamber in EMI testing is becoming widely accepted since it has been shown experimentally that the chamber exhibits a unique uniformity feature that allows for repeatable measurement data. A mode-stirred chamber is an electrically large rectangular cavity with a rotating scatterer. As part of an on-going effort to analyze the fields inside such a cavity, we begin with a simple structure of a thin wire scatterer with finite radius. The scattered field is found in terms of the unknown induced current on the scatterer, which in turn can be found by formulating and solving the electric-field integral equation in the usual manner.

It is well known that the kernel of the integral equation, i.e. the Green's function, for a rectangular cavity consists of a triple summation of orthogonal mode functions. When the observation point is very close to the source point, the modal Green's function requires an exceedingly, if not impractically, large amount of computation time. To alleviate this difficulty, we approximate the modal Green's function with a ray-mode representation, which consists of a finite mode sum and a sum over all the images. This representation is effective because it allows for the disposal of all the far away image terms without suffering an unacceptable loss of numerical accuracy. Using piecewise sinusoidal functions as the testing as well as the expansion functions for the current, the integral equation reduces to a matrix equation involving simple sine, cosine and known exponential integrals.

The solution to the integral equation shows that while there is still a "resonant" phenomenon for a thin wire in a cavity, the resonant lengths are now shifted. Depending on the incident field, this resonant mode may or may not be very pronounced. Typically, the induced current has large amplitude, and its distribution is very similar to that of the free space result. When the resonant mode is not excited properly, however, the distribution can take on any arbitrary shape, but its amplitude is usually negligible.

B1-5
1020

STATIC CAPACITANCE OF A LARGE MICROSTRIP PATCH OF ARBITRARY SHAPE

Edward F. Kuester
Electromagnetics Laboratory
Department of Electrical and Computer Engineering
University of Colorado, Campus Box 425
Boulder, CO 80309

The determination of the static capacitance of microstrip patches has presented a challenging problem in the numerical solution of an integral equation. Because of the singular nature of the unknown charge density function at the edge of the patch, moment and finite-element methods must be applied carefully to this problem. The circular patch has been most extensively and accurately analyzed of all patch shapes, but this is so because rotational symmetry considerably simplifies the formulation of the problem. Other shapes, notably the rectangle, have been studied, and results obtained by different numerical methods have not always been close to each other. Empirical formulas for the rectangle are available, but are not reliable over all parameter ranges.

In this paper, we will obtain an explicit, closed-form approximation to the capacitance of an arbitrary patch. This is accomplished by modeling the "aperture" electric field (in the top plane of the substrate beyond the edge of the patch) locally as that of a semi-infinite plane conductor above a grounded slab. The idea is similar to one used by Leppington and Levine (Proc. Camb. Phil. Soc., 68, 235-254, 1970) and uses the edge fields from the known solution to the half-plane edge problem (Lebedev, Sov. Phys. Tech. Phys., 3, 1234-1243, 1958; Chew and Kong, Math. Proc. Camb. Phil. Soc., 89, 373-384, 1981). The formula obtained depends on only three parameters of the patch shape: the area S, the perimeter P, and the Neumann self-inductance of a thin wire bent into the shape of the perimeter. It is a correction and generalization of a result of Soibel'man (Siberian Math. J., 25, 966-978, 1984) for the case of an air substrate. The explicit form of the edge correction has implications for the validity of "effective width" techniques in analyzing microstrip structures.

B1-6
1040

DECONVOLUTION OF SCATTERING DATA WITH A METHOD BASED ON A COMBINATION OF TIKHONOV REGULARIZATION AND THE SINGULAR VALUE DECOMPOSITION

Byron Drachman
Department of Mathematics
Edward Rothwell
Department of Electrical Engineering
Michigan State University
East Lansing, Michigan 48824

Let $r(t)$ be the response of a target with impulse response $h(t)$ illuminated by a time limited excitation waveform $e(t)$, $0 \leq t \leq T$. If $r(t)$ and $e(t)$ are assumed known quantities, then extracting $h(t)$ from the convolution

$$r(t) = \int_0^T e(t')h(t - t')dt'$$

is the deconvolution problem, known to be ill-conditioned.

Discretization of the above problem leads to an ill-conditioned matrix problem. Two available methods to solve the equation are 1) introduction of a parameter λ and Tikhonov-regularization, and 2) singular value decomposition with small singular values discarded in order to regularize the problem.

We show the connection between the two methods, discuss how to choose λ, combine the two approaches into a third algorithm that incorporates the best features of each, and apply and compare the three algorithms using data from measured experimental quantities.

B1-7
1100

AN APPROACH TO TIME-DOMAIN INVERSE SCATTERING AND RADAR SIGNAL PROCESSING USING THE "ANALYTIC SIGNAL"

W. Ross Stone
IRT Corporation
1446 Vista Claridad
La Jolla, CA 92037

Much of the theory for inverse scattering has been developed under the assumptions of coherent, monochromatic radiated and measured fields. However, many practical inverse scattering applications employ pulsed probing waves and time-domain processing of the scattered field. This is true of many radars, both bistatic and monostatic. Although some monochromatic results can be extended to the time domain by their application across a spectrum of frequencies, this has not often been done. D. Gabor (J. Inst. Ele. Engrs. (London), Vol. 93, pp. 429-457, 1946) defined an "analytic signal" by replacing the usual real expression for a time-domain signal with a complex form. In a companion paper (in the Pulse Measurements session) the author has derived a relationship between this analytic form of a time-domain signal and a one-dimensional hologram. This paper extends this result to the multi-dimensional case, and shows the relationship to a multi-dimensional hologram. Using this result and a technique developed by Gammel, it shown how the information present in the signals received by a radar array relates to the (multi-dimensional) holographic image which would be obtained if the same array were operated as a coherent imaging array. In 1981 the author presented the relationship between the solution to the inverse scattering problem in the short wavelength limit and holography. This result is combined with the result of the present paper to provide a solution to the inverse scattering problem in the time domain.

Previously, it has been assumed that in order to use an array for coherent imaging, it is necessary to record two quadrature signals at each element. This usually implies a doubling of the receiving electronics required, or a very sophisticated sampling method. One of the significant features of these results is to show that it should be possible to obtain the same information without increasing the electronics, and to do so in real time with an analogue implementation that is little more than a rearrangement of the electronics usually present.

B1-8
1120

GREEN'S FUNCTION FOR THE FOURIER SPECTRA OF THE FIELDS FROM TWO-DIMENSIONAL SOURCES OR SCATTERERS IN UNIFORM MOTION

D. De Zutter
Electromagnetism and Acoustics Laboratory
University of Ghent, Sint-Pietersnieuwstr. 41
9000 Ghent, Belgium

The fields from moving harmonic sources, detected by a stationary observer, turn out to be rather complicated functions of time (J. Van Bladel, Relativity and Engineering, Springer-Verlag, 1984). These time-signals exhibit both amplitude and phase modulation. In this contribution attention is focussed on the frequency content of such signals emitted by two-dimensional sources.

First, a representation of the moving sources in terms of a scalar and vector potential, in a reference frame in which the sources are at rest, is presented. Subsequently, Green's functions pertaining to the Fourier spectra of the radiated fields are found. The final results give the spectra of the radiated electric and magnetic fields detected by a stationary observer, in the form of space integrals of these Green's functions multiplied with the source current density, over the cross-section of the volume occupied by the sources. In this way, the radiated fields are not required as an intermediate step in the evaluation of their Fourier spectra.

The proposed method is completely general. It applies to sources with arbitrary relativistic but constant velocity, and is equally valid for observers located in the near-field or in the far-field. Numerical results are presented for a moving line source.

The Green's function approach shows that a meaningfull definition of instantaneous frequency and Doppler shift can only be given in the far-field. Consequently, the so-called inverse Doppler effect (N. Engheta, A. Mickelson and C.H. Papas, Trans. Ant. Prop., AP-28, 519-522, 1980) can be severely criticized.

The proposed method also applies to the Fourier spectra of the fields scattered by a moving two-dimensional body. In that case the incident fields are transformed to the frame in which the scatterer is at rest. In that frame the scatterer can be replaced by the induced current and charge densities, which are the sources of the scattered fields. Combining this approach with the Green's function for moving two-dimensional sources, allows us to draw general conclusions about the Fourier spectra of the scattered fields, especially in the far-field region. The obtained results confirm the conclusions formulated in (D. De Zutter, Applied Scientific Research, 36, 241-269). As a final example, the Fourier spectra of the fields scattered by a moving dielectric circular cylinder, immersed in an incident plane E-wave, are analysed in some detail.

B1-9
1140

INTEGRAL EQUATION FOR THE FIELDS INSIDE A DIELECTRIC CYLINDER IN AN INCIDENT E-WAVE

D. De Zutter and L. Knockaert
Electromagnetism and Acoustics Laboratory
University of Ghent, Sint-Pietersnieuwstr. 41
9000 Ghent, Belgium

In a recent paper (E. Marx, Trans. Ant. Prop., AP-32, 166-172, 1984) it was shown by Marx that the determination of the scattered and transmitted transient electromagnetic waves due to a homogeneous dielectric body can be reduced to the solution of a single integral equation. In the present paper we restrict ourselves to the scattering of a time-harmonic E-wave by a dielectric cylinder. For this case we show that two alternative formulations exist that solve the problem by a single integral equation. A first formulation is particularly suited for the determination of the fields inside the dielectric. The second formulation yields the result by Marx and is better suited for the calculation of the scattered fields.

The geometry of the problem is shown in the figure below. We introduce a new unknown ζ defined on c by:

$$\int_c G(\bar{r}/\bar{r}'')\ \zeta(\bar{r}'')\ dc(\bar{r}'') = E(\bar{r}) \qquad (1)$$

$$G = \frac{j}{4} H_0^{(2)}(k|\bar{r}-\bar{r}''|) \text{ and } k=[\omega^2\mu(\varepsilon+\sigma/j\omega)]^{1/2}$$

The observation point $\bar{r}$ is either located inside the cylinder or lies on the boundary c and E denotes the total electric field. After some calculations one can prove that the following integral equation is satisfied by ζ:

$$\int_c K(\bar{r}',\bar{\tau})\ \zeta(\bar{\tau})\ dc(\bar{\tau}) = E^i(\bar{r}')$$

$$K(\bar{r}',\bar{\tau}) = G_0(\bar{r}'/\bar{\tau})/2 + G(\bar{r}'/\bar{\tau})/2 \qquad (2)$$

$$+ \int [G(\bar{r}/\bar{\tau})\ \frac{\partial G_0}{\partial n}(\bar{r}/\bar{r}') - \frac{\partial G}{\partial n}(\bar{r}/\bar{\tau}) G_0(\bar{r}/\bar{r}')]dc(\bar{r})$$

The source term is simply the incident electric field. G_0 is the scalar Green's function for the medium outside the cylinder. After solving for ζ from (2), substitution in (1) gives the field inside the cylinder.

As an alternative to the substitution introduced in (1), we can define a new variable ξ as follows:

$$\int_c G_0(\bar{r}/\bar{r}'')\ \xi(\bar{r}'')\ dc(\bar{r}'') = E^{sc}(\bar{r}) \qquad (3)$$

In this case the observation point $\bar{r}$ is either located outside or on the boundary c. This approach gives rise to an integral equation with a much more complicated source term found by Marx.

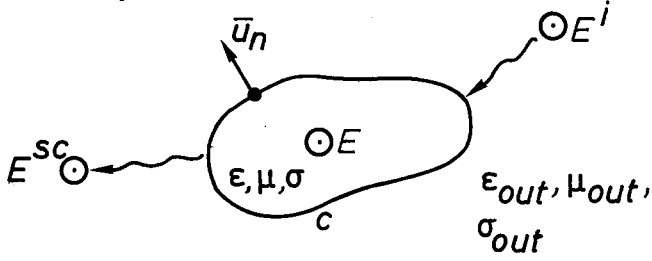

Session E-1 0855-Mon. CR1-40

NOISE AND INTERFERENCE ANALYSIS

Chairman: Joel Morris, School of Engineering, Howard University, Washington, DC 20059

E1-1
0900

SECOND ORDER NON-GAUSSIAN NOISE DISTRIBUTIONS, WIRH APPLICATIONS TO ZMNL SYSTEM OUTPUTS*

David Middleton
127 East 91 Street
New York,N.Y. 10128

The canonical first-order Class Aand B models of general nongaussian noise and interference developed by the author since 1974(D. Middleton,IEEE Trans. Electromag. Compat.,EMC-25,76-106, 1983 and refs. therein),are extended to general second-order dist--tibutions. These explicitly contain all associated second-order correlations,as well as those of a general additive gaussian com--ponent,as well. The derivations are extended to include not only received noise processes,but nongaussian space-time fields them--selves,which are sampled by spatial arrays and apertures.

With these specific second-order nongaussian distributions (and their associated pdf's) it is now possible to extend the "classical" second-order theory of output signal-to-noise ratios, spectra,and covariance functions following zero-memory non-linear ZMNL) devices(cf.,D. Middleton,Introduction to Statistical Commun--ication Theory,McGraw-Hill,New York,1960),to include explicitly the many important applications where the interference(which may or may not accompany a desired signal) is highly nongaussian.

Because of the statistical-physical construction of these analytic nongaussian noise field and process models,the rôles of the physical processes involved may be directly observed in the output results. The general results outlined here are illustrated by several examples,e.g.,nongaussian noise through nonlinear devices,etc.

---

* Work supported under Contract N00014-84-C-0417(P00001) with the Office of Naval Research,Code 411 SP.

E1-2
0920

STUDY OF THE AMPLITUDE PROBABILITY DISTRIBUTION OF EMI FIELDS IN A CAVITY USING COMPUTER SIMULATION

Yasuo Kuga and Akira Ishimaru
Department of Electrical Engineering
University of Washington
Seattle, WA 98195

The estimation of the maximum electromagnetic interference field strength is important in many EMI problems. It is not practical, however, to measure the field at all necessary points. Since it is not possible to measure the field strength at every point, the measurement must be made at a small number of points, and the maximum field strength must be estimated from the measured data. The important question is, therefore, how to choose these measurement points, how many points are necessary and sufficient, what measurements need to be made, and how to process the measured data in order to obtain the estimated field.

As the first step to EMI problems, we used a two-dimensional cavity model and conducted computer simulation studies of a field inside a cavity. Fields were calculated by using randomly distributed noise sources for rectangular and circular cavities. The statistical data of the calculated fields were obtained. We then used the concept of a multi-element probe to measure the maximum field. The multi-element probe consists of either 5 or 9 detectors. It is shown that for the same number of measurements the multi-element probe can improve the probability of finding the maximum field in the cavity compared with a single element probe.

In the EMI problem it is also important to know the distribution function of the interference field. The amplitude probability distribution (APD) function of the simulation data was compared with the Rayleigh, lognormal, K, and I-K distributions. The I-K distribution which is the generalized form of K distribution seems to be the most useful in our studies.

E1-3
0940

RADIO NOISE DUE TO CORONA ON A MULTICONDUCTOR POWER LINE ABOVE A DISSIPATIVE EARTH

Robert G. Olsen
Electrical & Computer Engineering Department
Washington State University
Pullman, WA 99164-2210

A variety of methods for predicting the radio noise due to corona on power line conductors have been developed. These methods can be separated into two categories. The first category includes methods which are completely experimental. In these, long term measurements are made on one or more "base case" power lines. Predictions for other power lines and other weather conditions are made by extrapolating from base case results according to experimentally derived correction factors. The second category includes methods which are partly experimental and partly analytic. In each of these, it is assumed that the corona injects a pulsing current into each conductor at a large number of points along the power line. Experiments are used to determine this current as a function of weather conditions, bundle geometry and surface gradient. Analytic techniques are then used to predict the fields associated with these injected currents. The latter category of techniques are called "analytic."

In this paper a new, more accurate analytic theory of radio noise has been developed. Its most outstanding characteristics are: 1. It exhibits a change in slope of the lateral profile due to earth conduction effects which is consistent with experimental results and 2. It can be used to show the relationship between rod and loop measurements of noise fields. The new theory has been compared to existing noise theories both analytically and numerically. It has been shown to be valid for conductor spacings of up to one eight of a wavelength and measurement points of up to a third of a wavelength from the line. The validity of other analytic theories has been shown to be more restricted.

E1-4
1000

MODELING OF A SHAPED-BEAM SATELLITE ANTENNA PATTERN FOR INTERFERENCE ANALYSIS

Hiroshi Akima
U.S. Department of Commerce
Natl. Telecommunications and Information Admin.
Institute for Telecommunication Sciences
Boulder, Colorado 80303

For efficient use of the geostationary satellite orbit, mutual interference among satellite systems must be analyzed in the planning stage of the systems. To save the transmitter power, many antennas of satellites in the fixed-satellite service use so-called shaped-beam emission patterns, each approximating the desired service area. Modeling a shaped-beam pattern is needed in the analysis of mutual interference.

Typically, a shaped-beam antenna pattern is given graphically on a map of the earth with several contour lines, each corresponding to a gain value. A possible way of using such contour lines with a computer is to approximate each contour line with a polygon and use the coordinates of the polygon points as the input data. We present a simple method for calculating the gain value at an arbitrary earth point.

A method of bivariate interpolation for scattered data points such as the one developed by Akima (ACM-TOMS, 4, 148-159, 1978) could be used, but such a method usually requires a large storage and long calculation time. Such a method does not take full advantage of the fact that the data points are grouped by gain values.

The method we have developed is based on the distance between the point for which we wish to calculate the gain and the polygon that approximates the contour. When the point lies between two polygons, the method linearly interpolates the gain with respect to the distances to the polygons. When the point lies inside the inner-most polygon, the method uses quadratic interpolation with the distances from the maximum gain point to the point in question and to the polygon. When the point lies outside the outer-most polygon, the method uses linear extrapolation with the two outer-most polygons. The results are continuous and free from undulations. The method can easily handle multiple maximum gain points and multiple contours for a single gain value. Perhaps the only disadvantage is that the results are not smooth, but this is not considered serious in many applications.

The method has been implemented in a computer program and is used in the U.S. preparatory effort for the 1985/88 WARC (World Administrative Radio Conference). At their request, the program has been sent to the ITU (International Telecommunication Union) which convenes the conference.

Session G-1/H-1 0855-Mon. CR2-26

NONLINEAR INTERACTION OF HIGH POWER RADIO WAVES - I

Chairman: S. Ganguly, Center for Remote Sensing, Falls Church, VA 22046

G1/H1-1
0900

HIGH POWER ELECTRON TEMPERATURE MODIFICATION OF THE LOWER IONOSPHERE

A. J. Ferraro and H. S. Lee
Communications and Space Sciences Laboratory
Department of Electrical Engineering
The Pennsylvania State University
University Park, PA 16802

In this presentation a review is given of research activities, especially at the Communications and Space Sciences Laboratory, involving modification of the ionospheric electron temperature by ground-based high and very high power HF transmitting sources. Early experiments to be discussed were based upon the well-known Luxembourg effect which was used as a diagnostic tool to support proposed chemical models of D-region formation. Through the years, numerous experiments and theoretical investigations emerged from the concept of ohmic heating via ground-based HF emitters; most of these were devoted toward understanding the physics of ionospheric formation and few were related to specific missions involving propagation and communications. Most notable are recent investigations into generation of ELF/VLF signals by modulating the dynamo current system with very high powers from the Arecibo Observatory. Signal detection of this generated ELF/VLF and the theoretical model of coupling of the ELF/VLF fields into the earth-ionospheric waveguide are presented.

G1/H1-2 0920 SPONTANEOUS GENERATION OF ULF/ELF/VLF CURRENT LOOPS IN THE IONOSPHERE

K. Papadopoulos
Science Applications International Corporation
1710 Goodridge Drive
McLean, VA 22102

Nonlinear processes resulting in the formation of spontaneous oscillatory current loops in the ionosphere through the use of ground based heaters are presented. The loops result in the generation of electromagnetic waves in the ULF/ELF/VLF range which propagate either into the earth's magnetosphere, or couple into earth-ionosphere waveguide. Emphasis will be given to

(i) thermoelectric current loop generation
(ii) stimulated beat frequency excitation
(iii) current loop generation by resonance absorption.

The theoretical models will be compared with recent experimental results in Arecibo. Future experiments using available and projected HF facilities as well as shuttle base transmitters will be discussed.

Permanent Address: University of Maryland, College Park, MD 20742

G1/H1-3
1000

ENERGIZATION OF CHARGED PARTICLES IN THE SUPRAURORAL REGION

Tom Chang
Center for Space Research
MIT
Cambridge, MA 02139

The generation of lower hybrid waves below field-aligned potential drops and the effect of the resulting turbulence on the ion and electron populations in the suprauroral region are studied numerically and analytically in terms of an electron-ion plasma which is destabilized by a weak electron beam traveling along the magnetic field. In the calculated evolution of the plasma, we discern the resonant and non-resonant quasilinear processes, as well as the effects of parametic and nonlinear mode-mode couplings. Estimate of suprauroral acceleration of charged particles are made using simulation and model (nonlinear Schroedinger equation) calculations.

G1/H1-4 PARAMETRIC EXCITATION OF WHISTLER WAVES BY HF HEATER
1020

S.P. Kuo
Polytechnic Institute of New York, Long Island Center
Farmingdale, New York 11735
M.C. Lee
Research Laboratory of Electronics
Massachusetts Institute of Technology
Cambridge, Massachusetts 02139

The possible excitation of whistler waves by HF heating in the auroral ionospheric F region is examined. This process can be described by the stimulated scattering of an upgoing left-hand circularly polarized HF pump wave (for a downward earth's magnetic field) into an upgoing Langmuir wave and a downgoing whistler wave. While the source of the whistler wave is the induced current density driven by the HF pump field in the density perturbation of the excited Langmuir wave, that for the Langmuir wave is provided by the ponderomotive force resulting from the total radiation fields of the HF pump wave and the excited whistler wave. The instability threshold for a uniform medium model has the expression of $|e\varepsilon_{th}/m| = (\nu_e/2^{\frac{1}{2}})(\omega_o - \Omega_e)(\omega\omega_\ell kk_\ell)^{\frac{1}{2}}/\Omega_e$, where ω_o, $\omega(k)$, $\omega_\ell(k_\ell)$, ν_e, $e(m)$, Ω_e, and ε_{th} have their conventional meanings of the HF pump wave frequency, the whistler wave frequency (number), the Langmuir wave frequency (number), the electron collision frequency, the electric charge (electron mass), the electron gyrofrequency, and the threshold electric field of the HF pump wave, respectively. The analysis has been extended to take into account the background ionospheric inhomogeneity. The results of this study will be presented in the meeting.

G1/H1-5 1040 CONSTRAINTS BY AERONOMY ON THE PLASMA PHYSICS OF HF HEATER ACCELERATED ELECTRONS

Herbert C. Carlson, Jr.
Ionospheric Physics Division
Air Force Geophysics Laboratory
Hanscom AFB MA 01731

The processes leading to electron acceleration by a strong HF pump wave in the ionosphere, and the possible (feedback) influence of such fluxes on HF induced instabilities in that ionospheric plasma, are of considerable interest. Future experimental and theoretical work addressing the problem of heater accelerated electrons in the ionosphere must make adequate allowance for significant constraints imposed by purely aeronomic considerations. These include electron scattering and angular redistribution, depth of penetration, time of flight, dominating cross sections, and background flux conditions. These are all discussed here within the context of consequences: for the flux itself, and for diagnostics available to measure and study these fluxes under various ambient ionospheric conditions.

G1/H1-6
1100

THE NONLINEAR INTERACTIVE SIDEBAND OF TWO POWERFUL WAVES AT CLOSELY SPACED FREQUENCIES IN THE IONOSPHERE

Zhong-hao Huang and William E. Gordon
Department of Space Physics & Astronomy
Rice University
Houston, TX 77251-1892

The theory and experiment of nonlinear interactive sidebands using two powerful waves at closely spaced frequencies in the ionosphere are described. When the ionosphere is illuminated with two strong HF signals of slightly different frequencies, the nonlinear mixing process arises because of the ponderomotive force. The HF signals reflect from the ionosphere and contain sidebands which are multiples of the difference frequency between the two pump waves. It is shown that the amplitudes of the sidebands, which depend on the modulation index, are related to (1) the effective HF power; (2) the HF frequency; (3) the temperature of the electrons; (4) the integral of the electron density of the ionosphere; and (5) the difference frequency of the two HF pump waves.

G1/H1-7
1120

IONOSPHERE HEATING IN THE USSR

Dr. D.B. Newman, Jr.
Department of Electrical Engineering and Computer Science
The George Washington University
Washington, D.C. 20052

Researchers in the USSR have used HF radio waves to heat the ionosphere since 1973 at facilities near Moscow, Gorkiy and Apatity. Their work includes field aligned scatter experiments and generating low-frequency electromagnetic radiation during periodic heating of the ionosphere. This talk presents some of the results of their work, based on a survey of the literature.

G1/H1-8 1140 TEMPORAL EVOLUTION OF THE HF-ENHANCED PLASMA LINE IN THE ARECIBO F REGION

F. T. Djuth[1], C. A. Gonzales[2], H. M. Ierkic[3], S. Ganguly[4]

[1]Space Sciences Laboratory, The Aerospace Corporation, El Segundo, CA 90245
[2]IBM Thomas Watson Laboratories, Yorktown Heights, NY 10598
[3]Arecibo Observatory, Arecibo, Puerto Rico 00612
[4]Center for Remote Sensing, Falls Church, VA 22046

The temporal development of the so-called HF-enhanced plasma line (HFPL) has been studied in detail using the high-power high-frequency (HF) facility located near Arecibo, Puerto Rico. Observations were made with the Arecibo 430 MHz radar. In the current work, attention is focused on the evolution of the HFPL spectrum subsequent to the onset of the HF wave in the F-region plasma. The development of the HFPL spectrum is examined for several different HF pulse lengths and HF duty cycles. In this regard, low duty cycles tend to consistently produce a different spectral evolution than high duty cycles. Broad, diffuse HFPL spectra are observed with low HF duty cycles, whereas sharply defined nonlinear Landau damping cascades develop at high duty cycles. Under a variety of observing conditions, the Arecibo HFPLs are observed to develop dominant decay line peaks within a few ms of HF turn-on in the plasma. In addition, at early times during periods of slow HFPL growth, and also for very low HF power levels, weak flat-top and/or double-humped spectral features are observed that can be attributed to radio wave scattering off of ion-acoustic waves. During periods of strong HFPL excitation, weak spectral signatures are occasionally observed in the band 430 MHz $\pm$ (f_{HF} + δ), where f_{HF} is the HF frequency and δ = 10-100 kHz. The origin of this structure is currently not known. Finally, the temporal development of the 430 MHz spectra is closely examined during the so-called plasma line overshoot. A diffuse spectral cascade is evident within a few ms of the onset of the HF wave in the plasma, and dominant decay line peaks quickly develop thereafter. Processes involving direct conversion of the HF wave into Langmuir waves and/or soliton formation do not appear to be the dominant processes responsible for the 430 MHz HFPLs observed in the Arecibo F region. The measured HFPL spectra are in qualitative agreement with the predictions of nonlinear Landau damping theory, but the experimental observations do not match the theoretical predictions in every detail.

Session J-1 0855-Mon. CR2-6

RADIO AND RADAR STUDIES OF THE SOLAR SYSTEM

Chairman: J. R. Fischer, NRAO, Greenbank, WV 24944

J1-1
0900

THE GOLDSTONE SOLAR SYSTEM RADAR

R. F. Jurgens, S. Brokl, K. Farazian, C. Franck
Jet Propulsion Laboratory
4800 Oak Grove Drive, 238-420
Pasadena, CA 91103

A new all-digital high speed data acquisition system is the heart of the Goldstone Solar System Radar. The system consists of four complex channels wth 512 range gates clocked at a rate of 50 Mhz. A VAX 11/780 computer provides the control for this system. An FPS 5210 array processor is used as a programmable I/D device for collection and buffering of data into the VAX. A Hydrogen Maser frequency standard provides 1 x 10 frequency stability and master timing to the system. A Polynomial Driven Time Base and Pseudo-noise Generator (PDPG) is used to drift the time base according to the Doppler predict and provides codes of length (2-1) when $1 < N < 24$ at clock rates up to 10 Mhz.

An intermediate frequency (IF) carrier at 7.5 Mhz is sampled using 8 bit analog to digital (A/D) flash converters. The output of the A/D converters feeds all digital Anti-Dispersion Filters (ADFs). After the (ADFs) Digital Complex Mixers (DCMs) heterodyne the IF signal down to baseband, the A/D, ADFs and DCMs operate with 50 Mhz clocks. The signal then passes through Complex Baud Filters (CBFs). These devices resample and lower the data rate for subsequent processing. The signal then goes to a baseband multiplexer for distribution to correlator-accumulator modules. The multiplexer and correlator assembly can be configured in many ways depending on the needs of a particular experiment. The system is used as a three station interferometer at S band (2320 Mhz) and is capable of resolving 1 km resolution pixel data at the planet Venus or 20 km at Mercury.

Additionally, it can operate as a two station interferometer at X band (8495 Mhz) with 8 km resolution at Mercury or 8 x 8 km doppler at the planet Mars. The system can operate in the CW mode with two station dual polarization at X band for precision observation of asteroids, comets and the outer planets.

J1-2
0920

OBSERVATIONS OF TITAN AND THE GALILEAN SATELLITES WITH THE OVRO MM-ARRAY AND THE VLA

D.O. Muhleman, G.L. Berge, D.J. Rudy and M.W. Spencer
Geological and Planetary Sciences, California Institute of Technology, Pasadena, CA 91125

The major satellites of the solar system are grossly unlike the Moon and the terrestrial planets. The surfaces of the Galilean Satellites have been photographed from Voyager with very high resolution but the surface of Titan has not been seen because the body has an atmosphere more massive than the Earth's with aerosol clouds that tower to altitudes 25% of its radius. We are reporting observations of the surfaces for Galilean Satellites and the surface and atmosphere of Titan made with the OVRO 3-element, MM array at a wavelength of 2.7 mm and the VLA at 1.3, 2.0 and 6 cm. Carbon monoxide was clearly detected in Titan's atmosphere and cyanoacetylene was marginally detected. The VLA measurements of the Galilean Satellites reveal greatly depressed brightness temperatures which, we will argue, are caused by isotropic scattering in their "ice blocky" surface. The surface emission polarization of Titan, Europa, Ganymede and Callisto were also measured at the VLA in an (only partially successful) attempt to determine the surface dielectric constants. In Titan's case, a strong determination of the surface emissivity or polarization can tightly constrain the discussions on the nature of its surface. Persuasive theoretical arguments show that it is likely that Titan's surface is either covered with an ocean of liquid ethane or that the surface is composed of ice mountains and great lakes of the hydrocarbon. We find that the emissivity of Titan at cm-wavelengths is $0.85 \pm .05$ while that of the icy Galilean Satellites ranges from 0.5 to 0.6. The emissivity of liquid ethane is 0.95. The ultimate test of the ocean hypothesis is to measure the microwave polarization pattern of the surface emission either with the VLA or, ultimately, from a spacecraft. For the latter, we will have to wait to at least 2002.

J1-3 0940 LUNAR AND VENUSIAN BRIGHT RINGS: T. W. Thompson, Planetary Science Institute, Pasadena, CA 91101

J1-4
1000

VERY LARGE ARRAY OBSERVATIONS OF MARS

D.J. Rudy, G. L. Berge, D. O. Muhleman
Division of Geological and Planetary Sciences
California Institute of Technology 170-25
Pasadena, California 91125

Observations of Mars were made at the Very Large Array in New Mexico on November 5 and 7, 1983, and on February 1 and 2, 1985. The observations were made at 2 and 6 cm. while the array was in it's largest configuration. For the 1983 observations the Earth was high in the Martian sky (24°N) and so the viewing geometry was ideal for observations of the North Polar Region. The season in the north was late spring(L_s=60°) and so the seasonal polar cap was still receding. The 1985 set of observations were taken when the Earth was high in the southern sky(26°S) so as to complement the first set of observations. The southern season during this time was mid-summer(L_s=304°). Since the total integration times for the data sets were 8 hours and 11 hours for the observations made in 1983 and 1985 respectively, the data are smeared in latitude.

The data, which are in the form of visibilities, were self-calibrated, mapped, and cleaned using the AIPS image processing system developed by NRAO. The final images were then fit with various models in order to determine the extent of the polar regions, the sub-surface dielectric constant, and the radio absorption length. Eventually it is hoped to get these last two parameters as a function of latitude, and possibly obtain a sub-surface density, also as a function of latitude.

The whole-disk temperatures give us confidence that the absolute calibration is off by only 2 or 3%. The results of fitting the North Polar Cap are:

Wave.	Disk	Cap	Latitude
2 cm	203.9K±0.5	146.3K±2.0	69.3°N±0.3
6 cm	197.7K±0.5	142.6K±3.0	69.0°N±0.5

where Disk is the brightness temperature below the given Latitude, Cap is the brightness temperature above the given latitude, and the latitude is the best fit extent of the North Polar Cap. The values for the South Polar Cap will be given at the conference. Currently, we are fitting the sub-earth dielectric constant and radio absorption length to the data and these results will also be presented.

J1-5 JUPITER'S ZONE-BELT STRUCTURE AT RADIO WAVELENGTHS.
1020

Imke de Pater
Radio astron. lab.
601 Campbell Hall
University of California
Berkeley, CA 94720

Despite the fact that the first telescopic observations of the planet Jupiter centuries ago revealed the familiar zones and belts on its disk, the difference between these two banded structures is still unexplained. Two competing theories, based upon different data, exist: a) at 5 micrometers the relatively high brightness temperatures of the belts as compared to the zones suggest that the brown belts are regions in the atmosphere devoid of clouds at the level where ammonia condenses b). Polarization data of reflected sunlight and absorption features in this spectrum due to methane bands indicate no systematic differences between belts and zones.

Since the main constituent of all the cloud layers is ammonia, a detailed analysis of the spatial and vertical distribution of this gas in the cloud layers may yield a clue to the differences between the zone-belt regions seen at optical and infra-red wavelengths. With this in mind, high resolution images of Jupiter were obtained with the VLA at 1.3, 2, 6 and 20 cm wavelengths. At these wavelengths we probe the atmosphere at pressure levels between about 0.5 atm (at 1.3 cm) and 10 atm (at 20 cm); this covers the major regions of cloud formation.

After elaborate image processing (cleaning and self calibration of the data was not "standard": in addition to the "normal" planetary problems which concern the large plateau of emission, the data were taken in 2 different array configuarations; at 6 and 20 cm the bulk of radiation is synchrotron rather than thermal emission, an emission component which varies with Jupiter's rotational aspect) good maps were obtained at all four wavelenghs, with a resolution between 1.2 and 3.5" (depending on wavelength). Belts are clearly seen as bright regions on the shorter wavelength maps, which indicates a lack of ammonia gas in these regions. Simulation of the data show that the belt-zone structure gives information not only on the cloud structure, but also on the its dynamics.

J1-6
1040

VERY LARGE ARRAY OBSERVATIONS OF SATURN'S RINGS

A. W. Grossman, D. O. Muhleman,
G. L. Berge, T. E. Dowling
Division of Geological and Planetary Sciences
California Institute of Technology 170-25
Pasadena, California 91125

We observed Saturn and the Rings at 2 cm and 6 cm in the C configuration at the VLA in April, 1983 when B = 15.7 degrees. Synthesis maps produced by self-calibration and cleaning provide a resolution of 1.5 arcseconds at 2 cm and 4.0 arcseconds at 6 cm. These maps reveal the rings extending on either side of the disk and as a cusp occulting the disk in front. A model consisting of five constant temperature regions including the disk, cusp, and three rings were fit to the data. The resulting brightness temperatures in degrees kelvin are pesented in the following table:

	Disk	Cusp	A ring	B ring	C ring
T_b 2 cm	146.8 ±0.1	50.8 ±0.3	2.2 ±0.3	5.7 ±0.3	1.4 ±0.4
T_b 6 cm	180.1 ±0.1	63.8 ±0.3	4.1 ±0.4	6.2 ±0.4	6.8 ±0.6

These results agree with previous observatins (F.P. Schloerb, D.O. Muhleman, G.L. Berge, *Icarus* **39**, 214-231, 1979), however, these values include only the formal error and do not account for any systematic error. The computed averaged optical depth of the rings as they cross the disk (cusp) is 0.31 at both wavelengths. This is consistent with a model of ring particles which are good scatters, poor absorbers, and large compared to these wavelengths. Clearly the brightness temperature of the rings is much less than their equilibrium blackbody temperature of about 80K. This implies a very low emissivity for the ring particles, and suggests a composition of water ice. In addition, the low brightness temperature implies that only a small fraction of particles are large compared to the absorption length which is about 100 meters for 80K pure ice at a wavelength of 2 cm. Furthermore, the similarity of the ring temperatures at both wavelengths suggests that the observed radiation is mostly due to scattered emission from the disk rather than direct emission from the rings. Currently we are fitting scattering models with power law particle size distributions.

J1-7
1100

INTERFEROMETRIC OBSERVATIONS OF SATURN AND ITS RINGS AT A WAVELENGTH OF 2.6 MM

T. Dowling, D. Muhleman, G. Berge, and A. Grossman
California Institute of Techology 170-25
Pasadena, California 91125

We have observed Saturn and its rings at a wavelength of 2.6 mm with the Owens Valley Radio Astronomy Observatory (OVRO) 3-element interferometer array. Here we analyze 454 visibility points taken in June 1984, when the ring opening angle, B, was 19°, and 281 points taken in June 1985, when B was 23°. The combined coverage yields a synthetic beam with a FWHM of 3 arcseconds. A map made by scaling and combining the 1985 data to the 1984 data, ignoring the change in B, shows ring features with possible forward scattering at the 2-σ level. The combined data set has been fit to a model consisting of a disk brightness temperature, Td, ring temperatures, Ta, Tb and Tc, and a 'cusp' temperature, Tcusp, which corresponds to the region where the rings cross Saturn's disk. The result is:

$$T_d = 160\pm2 \quad T_a = 7\pm5 \quad T_b = 29\pm5 \quad T_c = 31\pm7 \quad T_{cusp} = 82\pm5$$

The errors quoted do not include systematic errors. The solution for Tcusp is sensitive to the pointing, and the data do not permit a separation of the rings in the cusp region. The optical depth τ averaged over the three rings is 0.36, which is not significantly different than the value of 0.31 found by Grossman, et al. (this conference) for 2 and 6 cm. This independence of τ with wavelength adds to the theory that extinction by the rings is due primarily to scattering, and that the ring particles are larger than 6 cm. Earlier calculations by Muhleman (*Planetary Rings*, 59-70, 1982) suggest that about 8K of the observed ring flux can be attributed to scattered disk emission, and therefore the rest must be emission from the rings. Our solution for the separate ring temperatures is preliminary, and the high temperature found for Tc is probably due to inadequate coverage of the visibility plane. We plan to continue our observations of Saturn at OVRO with shorter and longer baselines, increasing our resolution and sensitivity to the rings.

J1-8
1120 GEOLOGY OF THE VENUSIAN SURFACE BY RADAR: S. H. Zisk, MIT Haystack Observatory, Westford, MA 01886

J1-9
1140

VLA OBSERVATIONS OF URANUS AT 2.0 CM

G.L. Berge and D.O. Muhleman, Division of Geological and Planetary Sciences, California Institute of Technology, Pasadena, CA 91125
R.P. Linfield, Jet Propulsion Laboratory, California Institute of Technology, Pasadena, CA 91109

We observed Uranus at 2 cm on 30 April, 1985 using the Very Large Array in its B configuration. Our goals were to obtain a good-quality radio image with well-calibrated brightness for atmospheric studies and to obtain an accurate position relative to QSO positions for general ephemeris improvement and as an aid to Voyager spacecraft navigation by VLBI.

For phase and secondary flux calibrators we chose two QSO's having accurate VLBI positions that were close to Uranus and straddled it in position: 0T-111 and P1657-261. We took special care in the manner that positions were specified as input to the VLA. For the Uranus ephemeris we used JPL-DE200. We treated all sources as moving sources and supplied the geocentric position, rates, and horizontal parallax at an epoch that was the approximate center of each scan. The flux densities were tied to 3C286, our primary flux calibrator (3.45 Jy), at a time when its zenith angle matched those of the other two calibrators.

After performing rather standard calibration and mapping procedures, we obtained a good image. There is just one obvious feature: a small, but significant asymmetry such that the highest apparent brightness is centered on the pole rather than on the subearth point. This has been seen previously, but was less pronounced in 1985 because of the small projected distance between pole and subearth point (0".25 as compared to the radius of 1".94).

Further analysis of the visibilities was done by fitting to them a uniform disk model with disk temperature and position offset as the only unknowns. Since it is the position offset of the disk center that is desired, a small correction was applied to remove the effect of the asymmetry. The numerical results were:

$$T_D = 191 \pm 8 \text{ K}$$
$$\Delta\alpha \cos\delta = -0".399 \pm 0".030$$
$$\Delta\delta = -0".041 \pm 0".035$$

where the uncertainties reflect a realistic estimate of systematic errors; the formal errors are small by comparison. Work is still in progress to recover limb darkening information from the data.

Session A-2 1355-Mon. CR1-42

PULSE AND TIME DOMAIN MEASUREMENTS

Co-Chairmen: R. A. Lawton, Electromagnetic Fields Division, National Bureau of Standards, Boulder, CO 80309; and T. K. Sarkar, Department of Electrical Engineering, Syracuse University, Syracuse, NY 13210

A2-1
1400

PULSE MEASUREMENTS IN THE FREQUENCY DOMAIN

Morris Engelson
Tektronix, Inc.
P.O. Box 500, Delivery Station 58-028
Beaverton, OR 97077

Pulse signal parameters can be completely described either in the time or frequency domain. These are uniquely related through the mathematics of the bilateral Fourier transform. It is intuitively obvious that it might be advantageous to measure and describe the frequency-related parameters in the frequency domain. It is also intuitively apparent that purely time-related factors, such as pulse width, should be measured in the time domain. However, this is not always so. It is sometimes easier, or more accurate, to measure in one domain and transform the results mathematically into the other domain.

This paper deals with the practical aspects of making measurements in the frequency domain and transforming results into the time domain as needed. The prime measurement tool is the modern calibrated spectrum analyzer. Topics covered include: practical measurement techniques, error analysis and reduction, signal acquisition, and advantages as well as disadvantages depending on signal parameter desired such as pulse width, amplitude, shape, carrier frequency, and on-off ratio. Mathematical formulas, specific procedures, references to the current state of the art literature, and examples are provided to help in the practical application of this theory.

A2-2
1420

A NANOSECOND TRANSIENT CHARACTERIZATION SYSTEM WITH SUBMILLIVOLT PRECISION

Steven R.Hessel
Hewlett-Packard
19447 Pruneridge Ave. MS 47U7
Cupertino, CA 95014

A measurement system is described which provides very high measurement accuracy at times close to large perturbations of the measured voltage. The system is intended principally to provide time domain data on pulses, such as the outputs of digital to analog converters. Time resolution of 50 ps and amplitude resolution of a few microvolts are clearly practical. Errors as small as 10^{-5} times a transition amplitude may be achieved 10 ns after the transition in some cases. The system is based upon time domain sampling oscillography. It employs algorithms which overcome the effects which normally limit the accuracy of averages and several measurement limitiations.

A2-3
1440

TIME DOMAIN RESPONSE OF M.I.C. SLOW-WAVE COPLANAR WAVEGUIDE

- C. SEGUINOT, M. EL KADIRI, P. PRIBETICH, P. KENNIS
  Université de LILLE I, Bât. P 4
- C.H.S. L.A. C.N.R.S. n° 287
  59655 Villeneuve d'Ascq - France
- J.P. VILOTTE, M. AUBOURG
  L.C.O.M. Limoges, France

Results are presented on the measurements in time domain of a M.I.S. coplanar waveguide propagating a slow wave mode. Two lines of different lengths have been characterized by this technic in order to obtain the reflection and transmission behaviours. Furthermore, theoretical analysis of such structure have been performed by using the classical Spectral Domain Approach, taking into account the different conductivities of each layer (M. AUBOURG, P. KENNIS, IEEE MTT-S Proc., 393-396, June 83).

The experimental results point out the peculiar behaviour of such a slow wave mode : a low characteristic impedance involving a high voltage reflection ; and attenuation of high frequencies leading to a decrease of the rise time of the transmitted voltage.

The satisfying agreement between theory and experiment will allow us to extend this study to the time domain behaviour of Schottky contact coplanar line.

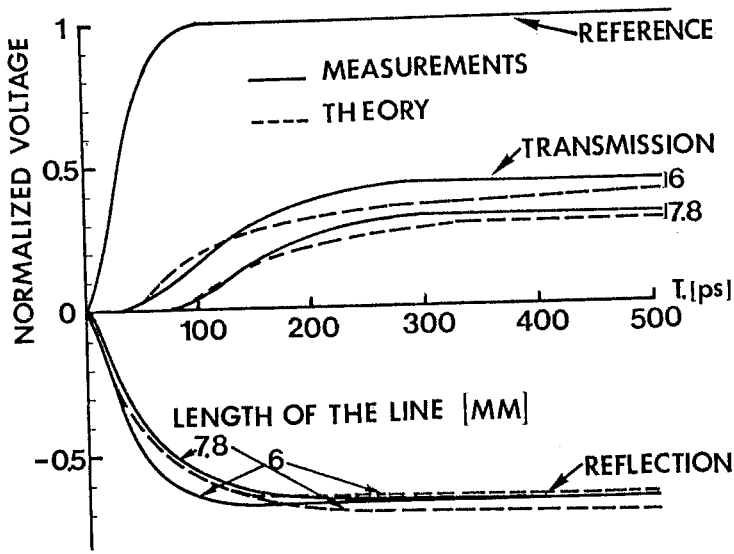

A2-4
1520

THE "ANALYTIC SIGNAL", ONE-DIMENSIONAL HOLOGRAPHY, AND RECOVERING THE TIME OF REFLECTION FROM A PULSED MEASUREMENT

W. Ross Stone
IRT Corporation
1446 Vista Claridad
La Jolla, CA 92037

Time domain measurements to guage the distance to an object, its dimensions, or, more generally, its shape, are quite common. Often this involves scattering a pulsed wave off the object and measuring the time between reflections off the object, as determined by the time delay between peaks or other features in the waveform. The signal processing associated with radar, sonar, ultrasonic inspection, and time-domain reflectometry often reduces to such measurements. Usually, features of the simple, real signal are employed. D. Gabor (J. Inst. Ele. Engrs. (London), Vol. 93, pp. 429-457, 1946) defined an "analytic signal" by replacing the usual real expression for a time-domain signal with a complex form. It has recently been shown that use of this analytic signal often makes processing easier and provides better resolution than using the real signal (see P.M. Gammell, Ultrasonics, Vol. 19, pp. 73-76, 1981, and references therein).

This paper reviews these results, and demonstrates the nature of the improvements with experimental results. It is shown that there is a simple relationship between the analytic signal and holography. This leads to an improved understanding of why the above advantages result, and identifies additional improvements which should be observed. For the case of measuring the distance between two interfaces using time-domain reflectometry, the accuracy of the measurement can be quite dependent on the wave being incident normally to the interface(s). The effect of employing the analytic signal in this case is investigated.

A2-5
1540

EXPERIMENTAL DETERMINATION OF THE IMPULSE OF A CONDUCTING SPHERE

Fung I. Tseng
Department of Electrical Engineering
Rochester Institute of Technology
Rochester, New York 14623

Tapan K. Sarkar
Department of Electrical Engineering
Syracuse University
Syracuse, New York 13210

A new experimental technique for determining the impulse response of a conducting sphere has been presented. A new method of exciting and recording transient waveforms scattered from conducting spheres of various sizes has been described and extensively tested. A modified conjugate-gradient method has been applied to the transient waveforms to determine the impulse response of the objects. It is shown that by proper weighting in computing the residual in the conjugate-gradient method the oscillation due to noise could be reduced. A recently developed data-processing technique has been applied to these impulse responses to obtain their spectra, which yield accurately the resonant frequencies of the objects.

A2-6 1600 POLARIZATION EFFECTS IN ELECTROMAGNETIC INVERSE SCATTERING OF DIELECTRIC CYLINDER

Tah-Hsiung Chu
RCA Laboratories
Room 3-231
Route 1
Princeton, NJ 08540

and

Nabil H. Farhat
Moore School of EE
University of Pennsylvania
200 South 33rd Street
Philadelphia, PA 19104

In this paper a theoretical vector development of the backscattered field of an infinitely long dielectric cylinder illuminated by a right-hand circularly polarized (RHCP) planewave is derived. The eigenfunction solution of the RHCP and LHCP components of the scattered far field can be separated into terms interpretable as arising from specular, axial, glory, and stationary rays determined from the modified geometrical-optics approach in the high frequency regime (R. Kouyoumjian, L. Peters, Jr., D. T. Thomas, Trans. IEEE, AP-11, 690-703, 1963). The magnitude and phase of the scattered field of each ray component in different polarization contain the information of cylinder dielectric constant and radius. Therefore, a Fourier analysis of the scattered LHCP and RHCP components with respect to the wavenumber k gives a range profile of the illuminated cylinder. The peaks in the profile represent the contribution from each ray component.

An automated microwave imaging system employing frequency, polarization and angular diversity is utilized to verify the theoretical results. By measuring the backscattered field RHCP and LHCP components over (6-17) GHz of a long solid plexiglass cylinder ($\varepsilon_r = 2.56$), and presenting them in polar format where the radial distance represents frequency, one can obtain a slice in the Fourier space of the object (N. H. Farhat, C. L. Werner, T. H. Chu, Radio Science, 19, 5, 1347-1355, 1984). Fourier inversion of the slice data would yield a projection image of the scattering centers of the object on a plane parallel to the plane of the Fourier slice. The analytical and experimental results obtained are shown to be in good agreement.

The images reconstructed from the scattered far field of each polarization give different features of the scattering object, from which one can identify the illuminated cylinder size and dielectric constant. Polarization effects of multi-layer cylinders are also discussed in this paper.

A2-7 Discussion
1620

Session B-2 1355-Mon. CR2-28
WAVES NEAR AN INTERFACE
Chairman: E. K. Miller, Lawrence Livermore National Laboratory, Livermore, CA 94550

B2-1
1400 SCATTERING FROM AN ARRAY OF NARROW CONDUCTING STRIPS ON A TWO-MEDIA INTERFACE

Chalmers M. Butler and Anthony Q. Martin
Department of Electrical and Computer Engineering
Clemson University
Clemson, South Carolina 29634-0915

The problem of determining the far-zone field scattered by an array of narrow conducting strips which reside on a two-media interface is investigated by a method which is essentially analytical. The strips are narrow relative to the wavelength in either medium, they are parallel, their axes are parallel to the interface, and they may be of different widths. The excitation is restricted to be transverse magnetic to, and invariant along, the strip axes. The current induced on such an array of strips has been determined by solving a set of coupled integral equations by a pseudo-analytical method (Butler, C.M., and A.Q. Martin, "Analysis of an array of narrow conducting strips on a two-media interface," 1984 IEEE International Symposium on Antennas and Propagation/National Radio Science Meeting, Boston, MA, June, 1984). The strip currents are represented as power series augmented with the correct edge condition, and the corresponding far-zone electric field is determined from these currents. Steps are outlined by means of which one first determines the far-zone field due to a line source at the interface between the two media and subsequently determines the total far-zone field from that of the line source weighted with the strip currents. Representative data are presented by means of which one may better understand the behavior of the field scattered by the array of narrow strips on the interface between two half spaces.

B2-2
1420

MOMENT-METHOD ANALYSIS OF WIRE ANTENNAS LOCATED OVER LAYERED GROUNDS USING SOMMERFELD THEORY

G. J. Burke and E. K. Miller
P.O. Box 5504, L-153
Lawrence Livermore National Laboratory
Livermore, CA 94550

A mode for wire objects of arbitrary geometry located near to, or penetrating, a planar interface was described previously (see for example, G. J. Burke and E. K. Miller, IEEE Trans. Antennas Propagat., vol AP-32, 1040-1049, 1984). The electric-field integral equation with Sommerfeld integrals to account for the effect of the interface is solved numerically using the Method of Moments. Model-based parameter estimation is used to reduce the computer time needed to evaluate the Sommerfeld portion of the integral-equation kernel. The total computer time is 4-8 times that required for the same object located in free space to be solved with comparable numerical accuracy.

The homogeneous, half-space model can provide a starting point in developing an approach for more general ground problems where various kinds of lateral and vertical inhomogeneities can occur. In this paper, we describe an extension of the above procedure to handle wire objects located above a layered half space. The extension is reasonably straightforward, with the Sommerfeld fields above ground now involving transmission-line-like terms for multiple-interface reflections. Once these fields have been obtained, the approach follows that previously used for the single interface. Results are shown for several layered-half-space problems, including the case where there is a salt-water half space at a variable depth beheath the ground-air interface, to study the effect of tidal change on the behavior of low-frequency antennas sited near a sea coast. Also discussed is generalization of the basic model to antennas penetrating into, or buried, in a layered half space.

B2-3 1440

A COMPARISON OF METHOD OF MOMENTS AND FINITE DIFFERENCES FOR THE DETECTION OF A BURIED OBJECT IN A LOSSY MEDIUM*

J. K. Breakall, M. J. Barth, and K. S. Kunz
Lawrence Livermore National Laboratories, Livermore, CA

A comparison of the Method of Moments integral equation computer program NEC (Numerical Electromagnetic Code) in the frequency domain and the Finite Differences differential equation computer program G3DXL3 (Generalized 3-Dimensional, Expandable, Lawrence Livermore Laboratory) in the time domain for detecting a buried metal object in various lossy mediums is given in this paper. This problem has had considerable interest in geophysical and remote sensing work here at Livermore and elsewhere. The object of interest is a perfectly conducting cylinder 6 meters in length and .25 meters in diameter. For the Finite Differences code the cylinder is approximated by a line of cubic cells .25 meters on a side. The metal bar is buried in an infinite lossy half-space 1.125 meters below the free space - lossy media boundary. The frequency range of interest is over the 2 to 30 MHz band. Continuous wave (CW) excitation is used at discrete frequencies in this range for the NEC frequency domain code. Pulse excitation of the form, $E(t) = e^{-\alpha t} \sin \beta t$, is used in the G3DXL3 time domain code with the constants chosen to have most of the energy in the above frequency band. The excitation is that of a plane wave incident on the medium and is polarized parallel to the boundary and aligned along the axis of the buried cylinder to give maximum coupling of current in the bar. Results have been determined for both scattered and total field at test points directly above the center and end of the bar at distances of 0 to 3 meters above the interface. These have been compared to those results without the bar present and differences are calculated giving the absolute level of detection for this case. Also, the current induced in the bar from the passing wave will be presented from calculations of both codes. It has been found that the bar is detectable with both codes, however, the perturbation effects at the above test points in the field are small. This paper will conclude with a discussion of further comparative experiments which need to be performed to test where each method is valid and advantageous in solving various electromagnetic problems most effectively.

* Work performed under the auspices of the U. S. Department of Energy by the Lawrence Livermore National Laboratory under Contract W-7405-Eng-48.

B2-4 1500 **SCATTERING FROM COATED PLANAR SURFACES FROM THE POINT OF VIEW OF TRAVELING-WAVE ANTENNA THEORY**

J. L. Karty, McDonnell Douglas Astronautics Company
L. W. Pearson, McDonnell Douglas Research Laboratories
P. O. Box 516
St. Louis, MO 63166

The scattering of a plane wave from a coated planar structure may be viewed in terms of traveling-wave antenna theory by interpreting departures from an infinite-extent planar geometry (e.g. edges, inhomogeneities, etc.) as secondary sources. These secondary sources are excited by an incident plane wave and excite in turn the spectrum of the multilayer slab waveguide made up of the coating materials.

This fact is illustrated by the simple canonical geometry of a perfectly conducting filament residing at the top face of a multilayer dielectric region backed by a perfect conductor. The current induced in the conductor may be approximated and the scattered fields computed asymptotically. The influence of the proper surface wave spectrum and the leaky wave spectrum upon the scattered field may be interpreted from this analogous problem. It is observed that a leaky-wave pole contributes a radiation lobe directly through the radiation leakage mechanism, while a proper surface wave must encounter a second discontinuity in order to radiate.

It is not presently practical to apply the spectral point of view to compute fields scattered from finite-extent coated planar structures because of the difficulties associated with treating realistic edge configurations as secondary sources. However, the spectral analog is helpful in understanding the way that material profiles influence the features that appear in scattered field patterns.

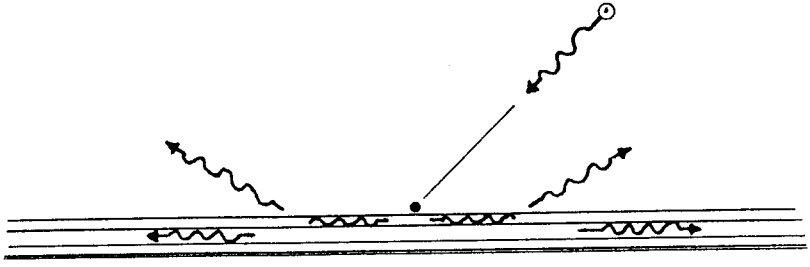

Session B-3 1535-Mon. CR2-28

ANTENNAS - I

Chairman: A. T. Adams, Syracuse University, Syracuse, NY 13210

B3-1
1540 NON-UNIFORM SAMPLING TECHNIQUES FOR ANTENNA APPLICATIONS: Y. Rahmat-Samii and R. Cheung, Jet Propulsion Laboratory, California Institute of Technology, Pasadena, CA 91109

Recent investigations have demonstrated that uniform sampling techniques can be effectively applied for reconstruction of far-field patterns of antennas. There are, however, many circumstances where it may not be practical to directly utilize uniform sampling techniques. For example, when performing antenna measurements it may not be possible to control the antenna movements to the desired locations. A recent example is the proposed measurement concept of large antennas aboard the Space Shuttle where it would be almost impractical to accurately control the movement of the Shuttle with respect to the RF source in prescribed directions in order to generate uniform (U, V) sampled points.

This paper presents a two-dimensional sampling technique which can utilize irregularly (non-uniformly) spaced samples in order to generate the complete far-field patterns. This technique implements a matrix inversion algorithm which only depends on the non-uniform sampled data point locations and not on the actual field values at these points. Once the matrix inversion is performed, it can be used repeatedly for the determination of the co-polar and cross-polar fields at any desired location, using the field values at the non-uniform sampled points. A powerful simulation algorithm is discussed for real-life simulation of many reflector/feed configurations to determine the usefulness of the non-uniform sampling technique for both the co-polar and cross-polar patterns. Additionally, an error simulation model is presented to identify the stability of the technique for recovering the field data among the non-uniform sampled data.

Numerical results are tailored for pattern reconstruction of an offset reflector antenna with a diameter of 20 meters operating at L-band. Both on-axis and off-axis beams are considered and many different non-uniform sampled data points are investigated. Results, so far, indicate that the technique is very powerful and could be used very advantageously for a variety of antenna pattern reconstructions from a limited number of non-uniform and sparse sampled points.

B3-2 The Application of a New Integration Algorithm to the Numerical
1600 Analysis of Reflector Antennas

Robin S. Lyons, Steven L. Dvorak
and
Ronald J. Pogorzelski
TRW Electronics and Defense
One Space Park
Redondo Beach, CA 90278

The electromagnetic behavior of reflector antennas is typically studied numerically by means of the physical optics approximation. This necessitates calculation of the integral of the currents multiplied by the free space Green's function, where the currents are obtained from the well known physical optics result, $2\hat{n}\times\vec{H}$. These integrals can be quite difficult to compute owing to the oscillatory nature of the integrand. For the past fifteen years the standard general method has been the so-called Ludwig algorithm which involves linear approximation of the amplitude and phase of the integrand over subregions of the two dimensional integration aperture. (A.C. Ludwig, IEEE Trans. AP-16, Nov. 1968, pp. 767-769) In special cases, such as a nearly focussed paraboloid, very efficient special purpose algorithms such as the Jacobi-Bessel series have been developed. (R. Mittra and V. Galindo-Israel, IEEE Trans. AP-25, Sept.1977, pp. 631-641.) However, for the general case which includes hyperboloidal subreflectors and shaped and/or highly defocussed paraboloids, the Ludwig algorithm has remained the method of choice.

Recently, a new algorithm was developed which is particularly effective in treating one dimensional integrals involving highly oscillatory integrands. (R.J. Pogorzelski and D. Mallery, IEEE Trans. AP-33, June 1985, pp. 800-804.) Subsequently, the algorithm was generalized to the two dimensional case. (R.J. Pogorzelski, 1985 North American Radio Science Meeting, Vancouver, B.C.) This new two dimensional approximation algorithm which involves polynominal approximation of the phase and Chebyshev approximation of the integrand, has been applied to the analysis of reflector antennas. This affords the first opportunity to compare the performance of this algorithm to that of the long standing Ludwig algorithm in the context of the practical electromagnetics application.

The performance of both the new algorithm and the Ludwig algorithm will be presented when applied to the hyperboloidal and defocussed paraboloidal cases. The computer implementation using the two algorithms is identical except for the integration routine. This results in a valid, direct comparison of efficiency and accuracy in a very practical context.

B3-3
1620

SYNTHESIS OF FREQUENCY INDEPENDENT CIRCULAR ARRAY PATTERNS

Hans Steyskal
Electromagnetic Sciences Division
Rome Air Development Center
Hanscom Air Force Base, MA 01731, USA

An attractive feature of a circular array antenna is that it can generate a radiation pattern, whose main beam and sidelobe structure are essentially independent of frequency. This is due to the fact that the far field pattern for an N element array can be represented in terms of N orthogonal phase modes (modes of unit amplitude/linear phase azimuth variation) and, so long as the relative amplitudes of these modes are controlled to be constant, the entire pattern is constant with frequency. The only frequency dependence found in this case, is in the amplitude relation between each far field phase mode and the corresponding cylinder current phase mode. However, by using an array feed network consisting of an NxN Fourier transformer, e.g., a Butler matrix or its digital equivalent, each phase mode can be individully accessed via one of the transformer input ports (B. Sheleg, Proc. IEEE, 56, Nov. 1968, p. 2016) and, with suitable filers at these points, the aforementioned frequency dependence can be removed. A desired pattern can thus be conveniently synthesized by driving the filter input ports with a desired set of complex amplitudes.

Although circular arrays have seen considerable theoretical and experimental development (A. Rudge, K. Milne, A. Olver, P. Knight (ed.): The Handbook of Antenna Design, Vol. 2, 298-329, Peregrinus Ltd., London, 1983), this approach to frequency independent pattern synthesis appears not to have been pursued and interesting questions remain. One relates to superdirectivity, since a beam of fixed angular widths is to be generated by an equivalent aperture that varies in terms of wavelength. Another concerns the residual pattern error caused by the excitation of the phase modes being discrete rather than continuous.

The paper discusses this pattern synthesis technique and presents results from a computer study of circular arrays containing in the order of 100 elements.

envisioned realization

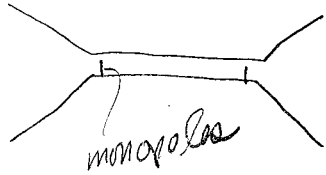

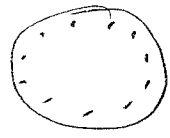

No show

B3-4
1640

REFLECTOR-TYPE WIRE-GRID POLARIZER

Devi Chadha
Department of Electrical Engineering
Indian Institute of Technology Delhi
Hauz Khas, New Delhi 110016, India
and
Rajendra K. Arora
Department of Electrical and Computer Engineering
Clemson University
Clemson, SC 29634-0915

A unidirectionally conducting (UC) screen, etched on a metal-backed dielectric sheet, can be used as a reflector-type broadband polarizer. The paper examines the reflection properties of such a structure for an incident plane wave of arbitrary polarization and angle of incidence. The direction of conduction of the UC screen is assumed to make an arbitrary angle (α) with the plane of incidence. The reflected wave is, in general, elliptically polarized. Numerical results are presented for the state of polarization (described in terms of the inclination and ellipticity of the polarization ellipse) for a range of parameters, including frequency, angle of incidence, and α. A number of such polarizers in tandem can be used to provide 90-degree rotation and very broadband characteristics. Also examined is surface-wave propagation on such a structure.

WAVEGUIDES

Chairman: Allan Q. Howard, Jr., Schlumberger Well Services, Houston, TX 77252

B4-1
1400

NUMERICAL SOLUTION OF INTEGRAL-OPERATOR EQUATION FOR INTEGRATED DIELECTRIC WAVEGUIDES

B.C. Drachman, Department of Mathematics and
D.P. Nyquist, Department of Electrical Engineering
Michigan State University
East Lansing, MI 48824

An integral-operator description for graded-index integrated dielectric waveguides provides a conceptually-exact description for surface-wave modes supported by guiding regions of arbitrary cross-section shape. The guiding region is immersed in a layered surround consisting of a film layer of refractive index n_f and thickness "t" deposited on a substrate of index n_s and covered by an overlay of index n_c. Contrast of the transversely-graded guiding region against the uniform cover layer is described by $\delta n^2(\vec{\rho})=n^2(\vec{\rho})-n_c^2$, where $\vec{\rho}$ is the 2-d transverse position vector. Eigenmode field $\vec{e}_m(\vec{\rho})$ of the m'th discrete surface-wave mode satisfies the 2-d EFIE

$$\vec{e}_m(\vec{\rho}) - (n_c^2k_0^2 + \nabla\nabla\cdot)\int_{CS} \frac{\delta n^2(\vec{\rho}')}{n_c^2} \overleftrightarrow{g}_\zeta(\vec{\rho}|\vec{\rho}')\cdot\vec{e}_m(\vec{\rho}')dS' = 0$$

... for all $\vec{\rho}\varepsilon CS$

where ζ is the axial transform variable, $\nabla = \nabla_t + zj\zeta$, and $\overleftrightarrow{g}_\zeta$ is a 2-d hertzian potential Green's dyad which depends upon ζ. Non-trivial solutions exist only for discrete propagation eigenvalues ζ_m. Physical parameters of the layered substrate/film/cover surround are embedded in $\overleftrightarrow{g}_\zeta$.

Elements of $\overleftrightarrow{g}_\zeta$ are typified by the Sommerfeld-type integral representation

$$g_{\zeta,\alpha\nu}(\vec{\rho}|\vec{\rho}') = \int_{-\infty}^{\infty} e^{j\xi(x-x')}\left[\frac{\delta_{\alpha\nu}e^{-p_c|y-y'|} + W_{\alpha\nu}(\xi)e^{-p_c(y+y')}}{4\pi p_c}\right]d\xi$$

which permits closed-form spatial integration. Numerical MoM surface-wave solutions are obtained for those $\zeta=\zeta_m$ leading to a vanishing MoM-matrix determinant. Integral representations of the latter matrix elements are evaluated by both real-axis integration and equivalent branch-cut integrals (where a simple stopping-point criterion for convergence is identified) augmented by surface-wave residues contributed by the layered surround. The latter representation leads to identification of the regimes of purely-guided and leaky surface waves. Implementation of the numerical solution is carried out on a CDC CYBER 205 super computer making extensive use of vector processing. Efficient numerical methods are identified, subsequent to which surface-wave modes of practical structures are quantified effectively.

B4-2
1420

THE STEP-WIDTH DISCONTINUITY IN A DIELECTRIC SLAB WAVEGUIDE

Edward F. Kuester and Fazle S. Quazi
Electromagnetics Laboratory
Department of Electrical and Computer Engineering
University of Colorado
Campus Box 425
Boulder, CO 80309

In a previous paper (Kuester and Quazi, 1985 North American Radio Science Meeting, Vancouver, Canada, p. 213) we used a bivariational formulation to obtain the reflection coefficient of a surface wave from the truncated end of a dielectric slab waveguide. This formulation, based on the polarization-current integral equation for the slab, needs only a free-space Green's function and does not require the separate determination of all higher-order modes of the structure.

In this paper, we extend this technique to treat the junction between two dielectric slabs of different widths. The crucial aspect of this work is that a variational expression for the transmission coefficient as well as for the reflection coefficient is obtained. Once this is done, the use of a simple trial function in the variational formula can be used to obtain very accurate results. Comparison to a rigorous numerical analysis (Rozzi, IEEE Trans. MTT, 26, 738-746, 1978) shows excellent agreement.

The formalism can now be easily extended to treat a very arbitrary junction between dielectric waveguides. The method has the potential not only to generate analytical formulas, but also to form the basis for more purely numerical attacks on this class of problems.

B4-3
1440 ELECTRIC DYADIC GREEN'S FUNCTIONS FOR INTEGRATED OPTICAL AND ELECTRONIC CIRCUITS

Jonathan S. Bagby, Dept. of Electrical Engineering
Univ. of Texas at Arlington; Arlington, TX 76019
Dennis P. Nyquist, Dept. of Electrical Engineering
Michigan State Univ.; East Lansing, MI 48824

Structures such as that below are common in integrated optical and electronic circuits, where sources radiate in a layered dielectric background. In optical circuits the substrate is semiconductor; for electronics it is often a ground plane. In both cases, prediction of device behavior requires evaluation of the electric field in the system.

Differential formulations are rendered ineffective by the inseperability of boundary conditions at device boundaries, and approximations based on these formulations neglect important radiative phenomina. Alternative formulations rely on integral equations to describe the behavior of the device. The field of the system is given by an integral of the current dotted into an electric dyadic Green's function; boundary conditions are incorporated in full generality in the Green's function for the system.

We present a unified formulation for electric Green's dyads for layered background structures of integrated optical and electronic circuits. They given in terms of Hertzian potential Green's dyads; the latter are developed by generalization of Sommerfeld's method. Incidently, the boundary conditions for electric Hertzian potential are utilized; these boundary conditions, which have been a source of confusion in the research community, are developed in full generality. Examples of the use of the Green's dyads in the analysis of integrated optical waveguides and microstrip transmission lines are presented.

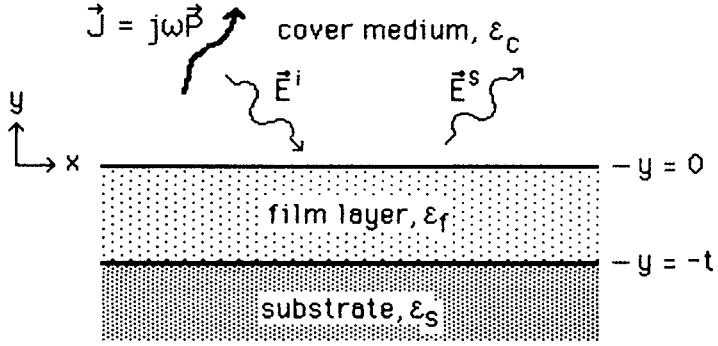

B4-4
1500

A DUAL–SERIES SOLUTION TO SCATTERING FROM A CIRCULAR IRIS IN A CIRCULAR METALLIC WAVEGUIDE*

S. L. Ray and R. W. Ziolkowski
Electronics Engineering Department
Lawrence Livermore National Laboratory
P.O. Box 5504, L-156, Livermore, CA 94550

The generalized dual–series approach (Ziolkowski, *SIAM J. Math. Anal.*, 16, 358–378) has been applied to the problem of a circular iris in a circular metallic waveguide. In this method, the fields on either side of the iris are written in terms of the normal waveguide modes. Dual–series equations are derived by enforcing the continuity of the tangential fields on the aperture/iris plane. The dual–series solution technique reduces these expressions to a matrix equation which indirectly yields the modal coefficients. Although this matrix equation must be solved numerically, it is very well behaved, having a relatively low order and being diagonally dominant. This is due primarily to the analytical extraction of the singular field behavior at the iris edge, a key feature of the technique.

The Riemann–Hilbert approach has provided an elegant solution to the dual–series equations in previous applications of this technique to EM aperture coupling problems. The Bessel function expansions required in the present problem have, to date, precluded the use of this approach. Instead, more traditional solution techniques (Sneddon, *Mixed Boundary Value Problems in Potential Theory*, Wiley, 1966) have been used.

Results are presented for the case of TE polarization. The technique is applicable to both single–moded and multi–moded guides and to any aperture size. A simple change of variables allows treatment of a cavity–backed iris. As the method generates the modal coefficients, field, current, and power distributions are obtained readily allowing detailed aperture coupling studies. Convergence of the solution is examined and is seen to be very good. The relationship between the dual–series, mode–matching, and moment methods is discussed in detail.

* Work performed under the auspices of the U.S. Department of Energy by the Lawrence Livermore National Laboratory under contract number W–7405–ENG–48

B4-5
1520

INFLUENCES OF OBLIQUE INCIDENCE AND MATERIAL LOSS ON CREEPING WAVE PROPAGATION ON COATED CONDUCTING CYLINDERS

L. Wilson Pearson
McDonnell Douglas Research Laboratories
P. O. Box 516
Saint Louis, MO 63166

The propagation of energy into the deep shadow region on an electrically large conducting cylinder coated with a lossless dielectric has been treated by a number of workers (R. S. Elliott, Jour. Appl. Phys., 26, 368-376, 1955; C. W. Helstrom, in Electromagnetic Theory and Antennas, E. C. Jordan (ed.), 1963; J. R. J. Paknys and N. Wang, North American Radio Science Meeting, June, 1985). All of these treatments are two-dimensional and are therefore scalar in character. Deep-shadow propagation for impedance surfaces has been treated in a counterpart fashion (c.f. W. Franz and P. Beckmann, IRE Trans. Antennas and Propag., AP-4, 203-208, 1956). When the field is incident obliquely upon the cylinder, or when the coating is slightly lossy, the above-cited formulations must be extended. A construction of a solution that takes these additional features into account has been given recently (L. W. Pearson, North American Radio Science Meeting, June, 1985). (This broader formulation is able to treat multiple layers also.)

In the present study, we explore the influence of moderate loss and of oblique incidence on propagation of fields into the deep shadow region. The propagation features are carried by the location of poles in the wavenumber plane associated with angular propagation in the same way that creeping wave poles or whispering gallery poles carry the behavior of those respective wave types. The study of these propagation features becomes one of numerical pole tracking under parameter variation and is computationally difficult because of the appearance of Hankel functions of complex order and complex argument in the field formulation.

Because the influence of material loss affects the azimuthal propagation in a qualitatively predictable fashion, these results are discussed only briefly. The influence of oblique incidence is somewhat more subtle, and some results associated therewith are presented and are interpreted in terms of an "effective contrast" concept. Numerical aspects of this class of problems have apparently not been discussed by previous workers, and we provide some data indicating the computation times that arise.

Session C-1 1355-Mon. CR1-40

MODULATION AND CODING FOR MAGNETIC RECORDING

Chairman: J. K. Wolf, University of California at San Diego, La Jolla, CA 92093

C1-1
1400

MODULATION AND CODING FOR MAGNETIC RECORDING:

J. K. Wolf, Center for Magnetic Recording Research, University of California - San Diego, La Jolla, CA 92093

The recording of digital data on magnetic media makes use of a number of different coding strategies. The first, modulation coding, insures that the data written on the media has a maximum and a minimum spacing between transitions. The second, error detection and error correction coding, insures that errors are detected and corrected in the read processing.

In this talk a short survey of these coding strategies will be presented. Some recent results on new strategies will also be discussed.

C1-2
1440

A FAMILY OF ERROR-CORRECTING CODES FOR MAGNETIC TAPES: Mario Blaum, IBM Research Laboratory, San Jose, CA 95193

We present a family of codes suitable for error-correction in multi-track magnetic tapes, the M(n,k)-codes. An M(n,k) code has rate k/n and can correct any n-k erased tracks (i.e, the tracks that have failed are known, but the information in them is lost). This error-correction capability is the same as the error-correction capability of maximum distance separable (MDS) block-codes, like Reed-Solomon or B(n,m)-codes. M(n,k)-codes, however, are convolutional. Their construction is very simple and does not involve operations on finite fields. In particular, the M(18,14)-code can be favorably compared to the AXP-code implemented in the IBM 3480 tape machines. We finally give a decoding algorithm for M(18,12) that can correct up to six track-erasures. The general case is an easy generalization.

C1-3 1600 NARROW TRACK LONGITUDINAL RECORDING AT TWO GIGABITS/SECOND: Leighton A. Meeks, Honeywell, Inc., Test Instruments Division, Denver, CO 80217

The paper describes longitudinal magnetic tape recording technologies which may be applied to very high rate digital recording or to large storage data bases. These technologies include use of narrow track heads, high accuracy tape guiding, precision head positioning, VLSI electronics, parallel structured system design including error correction strategies to achieve terabit capacities at gigabit rates.

C1-4
1640

ACHIEVABLE RATES FOR GAUSSIAN CHANNELS WITH TWO LEVEL INPUTS

L.H. Ozarow
AT&T Bell Laboratories
Room 2C-359
Murray Hill, NJ 07974
A.D. Wyner
AT&T Bell Laboratories
J. Ziv
Technion-Israel Institute of Technology

Magnetic storate media are often modelled as channels in which a two-valued "transmitted" signal is differentiated, filtered, and added to wideband Gaussian noise.

The capacity of this class of channels is unknown. In this paper we establish that this channel is identical in an information theoretic sense to the peak-limited channel, and we find achievable rates for some special cases.

Session F-1 1355-Mon. CR1-9

TROPOSPHERIC PROPAGATION AND ATMOSPHERIC REMOTE SENSING

Chairman: Kenneth S. Gage, Aeronomy Laboratories, ERL/NOAA, Boulder, CO 80303

F1-1 1400 THE TEMPORAL STRUCTURE OF A SIGNAL ATTENUATED BY RAIN: R. K. Crane and R. W. Cavanaugh, Thayer School of Engineering, Dartmouth College, Hanover, NH 03755

Attenuation by rain has been recognized as an important cause of reduced link reliability on terrestrial or earth-space communication links operating at frequencies above 10 GHz. A number of schemes have been proposed to mitigate the deleterious effects of rain. These include site diversity, uplink or downlink power control, switching a higher gain antenna to the link affected by rain, and coding for error correction. Each of these schemes needs more than a predicted or measured signal level distribution to optimize the design. Information is now required on the spatial and temporal structure of the attenuated signal. A procedure for the simulation of an expected signal level time series is needed by system designers.

Recent work at the Thayer School has included the study of the temporal structure of point rainfall rate and the spatial structure of rainfall rate as derived from radar measurements. A number of the current rain attenuation prediction models start with the assumption that the logarithm of the rain rate is normally distributed. Observations tend to support this assumption except in the high rain rate tail of the distribution. The temporal variation of the logarithm of 30-second averaged point rainfall rate was explored. Data from Boston and from West Germany produced consistent results. The power spectrum of the logarithm of rainfall rate has a power law shape identical to the shape observed for velocity or temperature variations produced by atmospheric turbulence. The outer scale corresponds to a period of about 30 minutes. The radar data also produced a power law power spectrum with a -5/3 (turbulence-like) slope. It had an outer scale on the order of 20 km. The radar and rain gauge results are consistent if one assumes a translation velocity of about 10 m/s.

The logarithm of specific attenuation is linearly proportional to the logarithm of rain rate. The -5/3 power law spectral shape requires the use of a linear filter with a number of poles to synthesize a signal with the requisite temporal structure. The signal level time series for a propagation path through rain may be simulated by passing normally distributed white noise through an eight pole linear filter, scaling the time series to represent the specific attenuation at the frequency of interest, non-linearly transforming the logarithm of specific attenuation to specific attenuation and passing the resultant signal through a moving average filter to simulate the integration of specific attenuation along the path.

F1-2
1420

UHF PROPAGATION MEASUREMENTS

Brent L. Bedford
NTIA/ITS
U. S. Department of Commerce
Boulder, CO 80303

Measurements of radio wave propagation in the UHF spectrum were conducted. The experiment consisted of a fixed transmitter and a mobile receiver. The receiver traveled along selected paths which involved varying distances from the transmitter.

Samples of the measurements which have been compiled and graphed, will be presented. A comparison of the measured data and the predicted data, generated by the Institute for Telecommunication Science Irregular Terrain Model, will be discussed along with comments on the validity of the latter.

F1-3
1440

USE OF DOPPLER RADAR AND RADIOMETER TO DETERMINE CAUSES OF MOISTURE CHANGE IN THE LOWER ATMOSPHERE

D.S. Zrnic' and R. Rabin
National Severe Storms Laboratory
1313 Halley Circle
Norman, OK 73069
J. Snider
Wave Propagation Laboratory
Boulder, CO

In the Spring of 1983 the Wave Propagation Laboratory and the National Severe Storms Laboratory conducted an experiment in the planetary boundary layer to explore the possibilities of combined radiometer-radar remote sensing of water vapor. The two channel microwave radiometer was pointed vertically to measure integrated vapor and liquid water, while radar data was collected on velocity azimuth display (VAD) scans to directly estimate mass convergence. From these two sensors and surface conditions we budget the moisture change into convergence, evaporation and advection. Also a relationship between radar reflectivity and moisture fluctuation is examined. It is found that reflectivity near the ground increases in time with evaporation.

Looking for moisture as a predictor of potential storm regions.
There will be 150 doppler radars in use

F1-4 1540 THE EFFECTS OF A BACKGROUND WIND AND AN EXTENDED BEAM ON OBSERVATION OF GRAVITY WAVE SPECTRA IN THE ATMOSPHERE BY MST RADARS

A. O. Scheffler and C. H. Liu
Department of Electrical and Computer Engineering, University of Illinois, Urbana-Champaign, IL 61801

Gravity wave spectra have been recently proposed as a cause for the observed mesoscale wind fluctuations in the atmosphere. In order to obtain the wave spectrum from the radar measured spectrum of wind fluctuation, it is important to apply the correct relationship between the two spectra. This relation has been derived using the dispersion and polarization equations for gravity waves for different observational configurations. When a high background wind is present, the resulting Doppler shift is shown to affect this relationship. In addition, it will be shown that the extended radar beam can also complicate the observed spectra by smearing the polarization of the observed wave components. Examples will be presented on how the theoretical results of these two problems affect the interpretation of observational data as well as the derived parameters for the model wave spectrum.

F1-5 1600 REMOTE SENSING INTEGRATED INTO AN ADVANCED WEATHER FORECASTING SYSTEM

P. A. Mandics, Environmental Research Laboratories, National Oceanic and Atmospheric Administration, Boulder, CO 80303

The Program for Regional Observing and Forecasting Services (PROFS) was established to improve short-range weather forecasting and to transfer the results to operational users. PROFS has created a computer facility to develop, test, and assess new forecasting techniques and technologies. The PROFS system ingests and analyzes practically all pertinent meteorological data and displays the results on an advanced workstation for the forecaster. Data from remote atmospheric sensors such as satellites, Doppler radar, and profilers form an important part of our effort. PROFS has conducted a number of exercises by operating the entire system in a real-time mode for several months. During the exercises, significantly better forecasts were produced due to the availability of remote sensor data, timely data presentation, and the superior data-integration capabilities of the PROFS workstation. We will show samples of workstation display products including remote sensor data and explain their role in producing improved forecasts.

As part of the technology transfer process, PROFS has initiated a number of joint projects with operational organizations such as the National Weather Service, Federal Aviation Agency, and U.S. Air Force Air Weather Service. All three agencies are interested in incorporating PROFS-developed techniques into their new, or upgraded weather service systems.

Session G-2/H-2 1355-Mon. CR2-26

NONLINEAR INTERACTION OF HIGH POWER RADIO WAVES - II

Chairman: Frank T. Djuth, Space Services Laboratory, The Aerospace Corp., El Segundo, CA 90245

G2/H2-1 1400 SATURATION OF PARAMETRIC INSTABILITIES IN IONOSPHERIC HEATING

J.A.Fejer
Department of Electrical Engineering
University of California at San Diego

Recent experimental work, using the chirp technique, by Hagfors et. al.(1985) combined with recent theoretical work on the formation of localized depressions of the plasma density near the reflection height of a powerful radio wave by several groups, has led to the tentative reinterpretation of previous observations on the relative heights of the neutral and enhanced plasma lines(Muldrew, D.B. and R.L.Showen, J.Geophys. Res.,82,4793,1977),on the changes in the plasma line spectrum during the first 10 m.s. after switching on the pump(Showen, R.L. and D.M. Kim,J.Geophys. Res.,83,623,1978),on changes of the spectral shape on change of pump power(Fejer, et al.,J.Atm.Terr. Phys,in press, 1985), and on the abscence of the decay lines in plasma line observations with the 46.8 MHz radar(Fejer et al. ,J.Geophys. Res.,88,2083,1983). Further experimental and theoretical work is required to check the new interpretation.

G2/H2-2
1440

OBSERVATIONS OF THE NATURAL AND THE ENHANCED PLASMA LINES IN ARECIBO HEATING EXPERIMENTS

T. Hagfors and W. Birkmayer
National Astronomy and Ionosphere Center
Cornell University
Ithaca, NY 14853
W. Kofman
CEPHAG
Domaine Universitaire
BP 46
St. Martin d'Heres 38402, France

Incoherent scatter observations at 430 MHz of the plasma line at the Arecibo Observatory have been made by means of a scheme which involves the linear frequency modulation of the transmitter and the demodulation (dechirping) of the received signals. This method of observation allows both the heater-enhanced and the photoelectron-enhanced plasma lines to be observed simultaneously.

The amplitude of the heater-induced striations, which is highly variable, can be derived directly from the observations. The relative amplitude of the plasma density fluctuations, when they are observed in these experiments are typically a few tenths of one per cent.

It is also shown that the HF heater wave, which is used in the ionospheric modification, creates a plasma depletion instantly on the time scale of the one second integration time used. The amount of depletion for a plasma frequency of 5.1 MHz, for a plasma frequency gradient of 50 kHz/km and for a free space heater power density input of $8*10^{-5}$ W/m^2 amounted to from 3 to 5 per cent.

These observations provide strong indications that the heater-induced plasma lines originate from plasma waves trapped in plasma cavities.

G2/H2-3
1500

NONLINEAR STRUCTURING OF IONOSPHERIC PLASMA BY HIGH POWER RADIO WAVES

J. P. Sheerin, D. R. Nicholson, and G. L. Payne
Department of Physics and Astronomy
The University of Iowa
Iowa City, IA 52242-1479

L. M. Duncan
M.S.466
Los Alamos National Laboratory
Los Alamos, NM 87545

Observations of the nonlinear structuring of the ionospheric plasma by high power radio waves may be broadly classified by their characteristic temporal and spatial scales. On small scales (periods less than a second and distances less than a kilometer), observations of an ion line overshoot developing simultaneously with the plasma line overshoot provide evidence of self-consistent structuring (soliton formation and collapse) of ionospheric plasma due to ponderomotive effects (L. M. Duncan and J. P. Sheerin, J. Geophys. Res., 90, 8371, 1985). On much larger scales, direct evidence of the deformation and structuring of the ionospheric profile is presented and analyzed within the context of theories of filamentation and self-focusing due to nonlinear thermal effects.

G2/H2-4 1520 GENERATION OF ELECTROSTATIC SIDEBANDS BY BUMP-IN-TAIL INSTABILITY DURING IONOSPHERIC MODIFICATION EXPERIMENTS*

Merit Shoucri, G.J. Morales, and J.E. Maggs
Department of Physics
University of California, Los Angeles
Los Angeles, CA 90024

The nonlinear modification of the background electron distribution function by resonant electrostatic fields generated during ionospheric HF heating experiments is calculated. It is found that the fields produced in the F region by present-day facilities can exceed the thresholds for bump formation and secondary sideband generation. A continuous spectrum of sideband frequencies centered around the frequency of the HF heater wave can be excited. Growth rates are calculated and relevance of the phenomenon to experimental observations is considered.

*Work supported by ONR.

G2/H2-5
1540

SCINTILLATIONS INDUCED BY HF HEATING AT MIDDLE AND SUB-AURORAL LATITUDES

Santimay Basu
Ionospheric Physics Division
Air Force Geophysics Laboratory
Hanscom AFB MA 01731

Measurements of radio-star and satellite scintillations in the VHF/UHF range induced by high power HF heating at Arecibo, Puerto Rico and Tromso, Norway have provided information on the growth, decay and spatial confinement of artificial irregularities in the sub-km range. Coordinated scintillation and plasma line measurements at Arecibo reveal the increased spatial discreteness of irregularity distribution at decimeter scales. Both the Tromso and Arecibo scintillation measurements indicate that a fairly bandlimited range of irregularity scales are excited by the heating. Results of more recent observations at Tromso with orbitting and near-geostationary satellites will be discussed.

G2/H2-6
1600 IONOSPHERIC MODIFICATION EFFECTS ON LONG WAVE REFLECTION COEFFICIENTS: Francis J. Kelly, Naval Research Laboratory, E. O. Hulburt Center for Space Research, Space Science Division, Ionospheric Effects Branch, Washington, DC 20375

Powerful HF ionospheric modification transmitters readily alter the properties of short wavelength waves, which are thus used to diagnose changes in the ionospheric plasma. Some studies suggest that ionospheric modification may not have a very significant effect on the propagation of long wavelength waves. However, an experiment in September 1980 demonstrated that the local reflection coefficient of low frequency (123.7 kHz) radio waves can be changed by as much as 10 dB by the Arecibo heater facility. Reasons for this effect will be discussed.

G2/H2-7
1620

IONOSPHERIC MODIFICATION WITH OBLIQUE INCIDENT RADIO WAVES

Gary S. Sales, Bodo W. Reinisch and
Claude G. Dozois
University of Lowell Center for
Atmospheric Research
Edward C. Field, Jr. and Chris R. Warber
Pacific Sierra Corporation
Raymond J. Cormier
Rome Air Development Command

On the basis of several published papers in the Soviet literature a combined theoretical and experimental program was undertaken to investigate the potential for ionospheric modification using high power obliquely incident HF radio waves. This particular project attempted to produce an interaction region in the ionosphere some 1300 km from a moderately strong experimental transmitter with an effective radiated power of about 20 MW.

Using oblique propagation, this interaction cannot take advantage of the resonance phenomena that makes vertical incidence heating such an effective process. Theoretical analysis shows that electron heating is the most likely mechanism for producing changes in the remote ionosphere. Strong electric fields are predicted in the caustic region near the reflection point. These intense fields are responsible for the ionospheric heating and when combined with heat conduction can produce a modified region of sufficient size to affect other radio waves incident on this region.

The experiment, which ran for one week in May 1984, used the Rome Air Development Center transmitter at Ava, NY for the oblique heating and a Digisonde 256 for vertical ionospheric sounding at the projected interaction point. It was recognized at the beginning of this experiment, based on the theoretical studies, that the transmitted power levels were below what would likely be required to achieve a detectable effect. The results of this experiment are presented.

G2/H2-8
1640

REVIEW OF SHORT SCALE STRIATION EXPERIMENTS AT ARECIBO*

A. J. Coster, M. I. T. Lincoln Laboratory, L-148, Lexington, MA 02173
R. J. Jost, Lyndon B. Johnson Space Center, NASA
F. T. Djuth, Space Sciences Laboratory, The Aerospace Corporation
W. E. Gordon, Dept. of Space Physics, Rice University

Short scale striations are among the phenomena that occur when the ionosphere is heated by high frequency (HF) radio waves with ordinary mode polarization. These striations are electron density irregularities aligned along the magnetic field lines in and near the heated region of the ionosphere. Experiments were performed at Arecibo, Puerto Rico from 1977 to 1983 to study these striations. During these experiments, the velocities of the short scale striations were observed, their rise and decay times were measured, and their associated cross sections were calculated. The results of these experiments will be reviewed. First, the velocities of the F-region striations were found to be well correlated with F-region ionization drifts, although on two occasions dramatic changes in the striations' velocities were observed shortly after ionospheric sunset. Second, the striations' rise times were found to vary inversely with the HF electric field. The E region data suggests this dependence is nonlinear. Third, the threshold component of the HF electric field perpendicular to the geomagnetic field is calculated to be 0.09 V/m in the F region and 0.37 V/m in the E region. Fourth, both the E and F region data verify theoretical predictions that the striations' decay times are directly proportional to the electron diffusion across the magnetic field lines. Suggestions for future areas of investigation will be given.

*This work was sponsored by the Department of the US Air Force with the support of the department under contract F19628-85-C-0002. The views expressed are those of the author and do not reflect the official policy or position of the U. S. Government.

G2/H2-9 1700 TECHNIQUES FOR CALCULATING THE ELECTRIC FIELD NEAR THE REFLECTION LAYER IN A PERTURBED IONOSPHERE*

J.D. Hansen and G.J. Morales
Department of Physics
University of California, Los Angeles
Los Angeles, CA 90024

Two methods (Langer's method and a Green's function technique) for calculating the electric field near the reflection layer for electromagnetic wave propagation along the magnetic field in a perturbed polar ionosphere ($\vec{k} \| \vec{B}_o \| \nabla n_o$) are compared. Perturbations on the zero order density profile are modelled by localized Gaussians whose depth and extent along the geomagnetic field can be varied. The Green's function technique is found to be useful when short scale length perturbations are present, but is limited by its domain of convergence and numerical efficiency. Comparison to the convergent Green's function technique shows inaccuracies in the Langer method for perturbations whose spatial extent is much smaller than the first lobe of the unperturbed Airy pattern. Two applications of the techniques are discussed. Results are presented of phase shifts due to short scale density cavities, as may arise from ponderomotive forces due to electrostatic waves. These results delineate the sensitivity required by experiments that use phase shift measurements as a diagnostic tool for identification and investigation of short scale phenomena. Secondly, the Langer method is used to calculate the electric field for long-scale cavities typical of ohmic heating modifications.

*Work supported by ONR.

Session G-3 1355-Mon. CR0-30

RADIO PROPAGATION

Chairman: A. K. Paul, Naval Ocean Systems Center, San Diego, CA 92152

G3-1
1400

IONOSPHERIC TILT MEASUREMENTS

Bodo W. Reinisch, Claude G. Dozois, Gary S. Sales and Klaus Bibl
University of Lowell Center for Atmospheric Research

For two days in March and April 1985 continuous 24 hour measurements of ionospheric tilt were made at Erie, Colorado using an ULCAR Digisonde 256. By measuring the F-region reflections at two frequencies we can identify separate reflection regions with a 10 second revisit time. The discrete Fourier spectra (phase and amplitude) of the signals received on each of the four receiving antennas are recorded on magnetic tape and then processed to determine the location of the reflecting sources in the ionosphere.

In daytime these sources were found to remain relatively fixed in a particular area of the "sky" and for each cluster of points a five minute average tilt angle, measured from overhead and a tilt bearing, measured east from magnetic north was produced for the 24 hour periods.

Special smoothing techniques were developed to estimate the degree of clustering of the source points and a significant difference between day and night became apparent. The diurnal variation of the tilt parameters are compared to the predicted tilts using the IONCAP ionospheric model.

G3-2
1420

MODELING THE EFFECT OF IONOSPHERIC GRADIENTS IN HF PROPAGATION PREDICTION PROGRAMS

Frank G. Stewart
National Telecommunications and Information Administration, Institute for Telecommunication Sciences, U.S. Department of Commerce, Boulder, CO 80303

Most HF propagation prediction programs currently in use assume that the ionosphere is either flat or concentric and that the electron distribution is constant about the reflection point of a radio wave. In recent papers (K. Davies and C. M. Rush, Radio Sci, 20, No. 1, 95-110, 1985 and K. Davies and C. M. Rush, Radio Sci, 20, No. 3, 303-309, 1985), a model was presented that accounted for horizontal gradients in the ionosphere and their effect on high frequency radio propagation. This model provides a reasonably simple approach to computing the effects of gradients and requires considerably less computation than the more complex raytracing programs. In this paper, the application of the model to specific HF propagation circuits will be addressed. Results will be presented that illustrate the magnitude of the errors in the calculated angle of arrival and circuit distance when the gradients in the electron density distribution are ignored in HF propagation prediction programs.

G3-3
1440

MONITORING OF INTENTIONAL HARMFUL INTERFERENCE TO THE HF BROADCASTING SERVICE I: OVERVIEW

Charles M. Rush, Mary W. Sowers, and Gregory R. Hand
National Telecommunications and Information Administration, Institute for Telecommunication Sciences, U. S. Department of Commerce, Boulder, CO 80303

An international program is underway to monitor the intentional harmful interference to the HF Broadcast Service. This program is being directed by the International Telecommunication Union's International Frequency Registration Board. As part of this effort, selected Administrations throughout the world have undertaken a highly coordinated observing program. This observing program has resulted in the detection of the location of over 80 different facilities used to create intentional harmful interference to the services provided by international broadcasters such as Radio Free Europe, Voice of America, British Broadcasting Corporation, and Deutsche Welle. In addition, it has been observed that there appears to be a preference for specific broadcasters and broadcast languages to be subjected to intentional harmful interference. In this paper, we will present the major findings that have been obtained from the monitoring program.

G3-4
1500 MONITORING OF INTENTIONAL HARMFUL INTERFERENCE TO THE HF BROADCASTING SERVICE II: PROPAGATION CONSIDERATIONS

Mary W. Sowers, Charles M. Rush, and Gregory R. Hand
National Telecommunications and Information Administration, Institute for Telecommunication Sciences, U.S. Department of Commerce, Boulder, CO 80303

Detailed studies have been undertaken to relate the results obtained as part of the International Telecommunication Union program of monitoring intentional harmful interference to specific radio propagation effects. The propagation studies involve using HF simulation programs (such as IONCAP and HFBC84) in conjunction with observed monitoring data. The results of the simulations are used to seek consistency between observed intentional harmful interference and that expected on the basis of actual broadcast operations. Particular emphasis is placed upon simulating the likelihood that emitters located great distances from the broadcast service area could be effective in creating intentional harmful interference to specific broadcast programs. The results of these studies indicate that the observed intentional harmful interference is consistent with basic HF propagation considerations.

G3-5
1540

BEHAVIOR OF ORDINARY MODE EXCITED ELECTROMAGNETIC WAVE FIELDS AT THE REFLECTION HEIGHT NEAR THE CRITICAL COUPLING ANGLE

T. A. Seliga and B. Abali*
Communications and Space Sciences Laboratory
Electrical Engineering Department
The Pennsylvania State University
University Park, PA 16802

In order to improve our understanding of the response of the ionospheric plasma to intense high frequency (HF) radio waves, numerical full wave solutions of the ordinary mode near the reflection height (X=1) are performed. These solutions reveal the structure and intensity of the electromagnetic wave fields for various model ionospheres and propagation conditions. Significant swelling of these fields occurs when the electron density gradients are large and when propagation of the HF wave is launched near the critical angles which occur in the magnetic meridian. In the latter case, the swelling of the field intensities is related to ordinary to extraordinary mode coupling and the subsequent deposition of the wave's energy into the plasma at the plasma resonance level which is just below the X=1 level. Example full wave solution fields are presented to demonstrate this behavior.

*With the Electrical Engineering Department, Ohio State University

G3-6
1600

VARIATION OF THE ORDINARY WAVE REFLECTION COEFFICIENT IN THE VICINITY OF THE CRITICAL COUPLING ANGLE

B. Abali*, T. A. Seliga and K. Aydin
Communications and Space Sciences Laboratory
Electrical Engineering Department
The Pennsylvania State University
University Park, PA 16802

The coupling of ordinary (O) to extraordinary (X) mode energy in the vicinity of the critical coupling angle may be studied by examining the variation of the O-mode reflection coefficient. The latter is derived from numerical full wave solutions of high frequency radiowaves propagating in a horizontally stratified magnetoionic medium. Generally, under low power excitation, the width of this coupling region is narrow (around 1°), but depends strongly on the electron density gradient at the O-mode reflection height (X=1). Computations for waves launched in directions slightly outside the magnetic meridian from the critical angle indicate that the coupling region is nearly circular in angular extent. A ground-based oblique sounding experiment is suggested to study the phenomenon which may be of central importance to ionospheric radiowave heating experiments.

*With the Electrical Engineering Department, Ohio State University

G3-7
1620

CONSEQUENCES OF AN "AC" THUNDERSTORM GENERATOR AND GLOBAL CIRCUIT

Leslie C. Hale
Communications and Space Sciences Laboratory
Department of Electrical Engineering
The Pennsylvania State University
University Park, PA 16802

Measurements and subsequent modelling of the electrical output of thunderstorms have shown that they may be regarded as simple broadband AC current generators with an average power output much greater than that due to electromagnetic radiation. In contrast to the DC generator, whose energy is dissipated in and whose currents are controlled by the lower atmosphere, much of this AC energy is "capacitively" coupled to the middle atmosphere, the ionosphere, and the magnetosphere. The AC current paths are controlled by these upper regions, tending to flow to the magnetically conjugate hemisphere along field lines and to spread globally in the E-region of the ionosphere. The AC energy dissipates by Joule heating in the middle atmosphere in a manner which is highly sensitive to the local conductivity profile and may be concentrated in the auroral zones. The frequency content of the AC generator is primarily in the ULF, ELF, and possibly extending into the VLF regions. The atmospheric noise produced by this mechanism is primarily "electrostatic" in nature and is strongly influenced by the middle atmosphere conductivity profile at the receiving location. Horizontal gradients in this profile could result in a highly variable magnetic field, which may help explain some puzzling Schumann resonance data. The total AC energy is comparable to the power in the aurora, with order of magnitude uncertainty. The coupling of substantial amounts of energy to the ionosphere and magnetosphere would depend on non-linear mechanisms such as rectification or the excitation of instabilities. Reverse coupling from the global circuit to thunderstorms would be enhanced by the much greater "aperture" of the thunderstorm for AC as compared to DC.

G3-8
1640

BALL LIGHTNING

John B. Smyth
Smyth Research Associates
San Diego, CA 92123

Lightning is an electromagnetic phenomenon, whose observables are described by Maxwell' s equations. An exact solution (Smyth, J. B. and D. C. Smyth, Radio Science , 11 , 977-984, 1976) provides the electromagnetic field of an electrical conduction current input to an infinitesimally thin, perfectly conducting filament. The solution describes the transformation of electric displacement into electrical conduction current, as well as the opposite transformation of electrical conduction current into electric displacement. This latter provides a description of an electromagnetic phenomenon known as ball lightning. It is shown how these luminous balls propagate through dielectrics such as glass window panes and cockpit windows of airplanes in flight. Characteristics such as the relaxation time and size of these electric displacement blobs are described by an appropriate solution of the heat conduction equation (Landau, L. D. and E. M. Lifshitz, Fluid Mechanics, Pergamon Press, 192-195, 1959).

Session J-2 1355-Mon. CR2-6
THE MICROWAVE BACKGROUND RADIATION
Chairman: S. Gulkis, JPL, Pasadena, CA 91103

J2-1
1400 LONG-WAVELENGTH MEASUREMENTS OF THE COSMIC BACKGROUND RADIATION SPECTRUM

C. Witebsky, G. F. Smoot, S. Levin, G. De Amici*
Lawrence Berkeley Laboratory and Space Sciences Laboratory
University of California Berkeley, CA 94720

We have measured the cosmic background radiation (CBR) temperature at five wavelengths (12, 6.3, 0.91, and 0.33 cm) in collaboration with research groups from Milano, Bologna, and Haverford, as reported by G. F. Smoot *et al.* (*Ap. J.*, **291**, L23–L27, 1985) and by G. De Amici *et al.* (*Ap. J.*, **298**, in press, 1985). The weighted mean of the five measurements is 2.72 ± 0.04 K. In combination with recent CBR measurements in the Wien region reported by other groups (J. B. Peterson, P. L. Richards, and T. Timusk, *Phys. Rev. Lett.*, **55**, 332–335; D. M. Meyer, and M. Jura, *Ap. J.*, **297**, in press, 1985), these values set new, stringent limits on distortions to the CBR spectrum arising from energy transfer between matter and radiation in the early universe.

In addition to the fixed-wavelength instruments, we have built a pair of tunable radiometers that function as microwave spectrometers, covering the ranges from 1.7 to 3.8 cm and from 3.8 to 10 cm, and we are developing a tunable radiometer in the 15–30 cm band. With these instruments, we will be able to make still more sensitive measurements of the CBR Rayleigh-Jeans spectrum in order to more accurately determine the thermal history of the early universe.

*On leave from Istituto di Radioastronomia/CNR, Bologna, Italy

J2-2
1420 SPECTRUM OF THE COSMIC BACKGROUND RADIATION AT MILLIMETER WAVELENGTHS: J. B. Peterson, P. L. Richards, and P. Timusk, Department of Physics, University of California, Berkeley, CA 94720

J2-3
1440

BALLOON-BORNE 3 MM ANISOTROPY MEASUREMENT

T. Villela and P. Lubin
Space Sciences Laboratory and
Lawrence Berkeley Laboratory
University of California
Berkeley, CA 94720

A liquid helium cooled 90 GHz Schottky diode mixer and GaAs FET IF amplifier have been utilized in a balloon-borne radiometer to map the large scale anisotropy in the cosmic background radiation. The radiometer has a noise temperature of 125 K over a bandwidth of 600 MHz with a spot noise of 80 K for the mixer and IF. The beam switch consisted of a rotating polished aluminum plate phase locked to a crystal reference to rotate at 23 2/3 Hz. The offset due to the beam switch is 200 mK at the flight altitude of 30 Km corresponding to an emissivity of 0.0009 in good agreement with the theoretical emissivity. Gain stability of the radiometer is within 1% over the approximately two years of use. Calibration was performed in flight using a full beam target with a measured reflection of -25 db yielding a calibration accuracy potentially at the 1% level. Current work is on developing a 3 mm SIS radiometer to measure the anisotropy in the background radiation.

J2-4
1500

A NOVEL INTERFEROMETER TO SEARCH FOR ANISOTROPY IN THE 2.7 K BACKGROUND RADIATION

P. T. Timbie and D. T. Wilkinson
Joseph Henry Laboratories
Physics Department
Princeton University
Princeton, N. J. 08544

A novel type of interferometer has been developed to measure anisotropy of the 2.7 K background radiation at an angular scale of 2.2^{o} and a microwave frequency of 46 GHz. A detection of anisotropy or placement of a limit on $\Delta T/T$ would help constrain the spectrum of density fluctuations in the early universe at the time of decoupling of the radiation from matter. The interferometer compares the temperature of 2 spots on either side of the North Celestial Pole with the temperature at the pole itself. During one 24 hour rotation of the sky, a circle is scanned about the pole. The interferometer minimizes systematic effects from ground radiation and reduces the effect of atmospheric fluctuations on this ground based experiment. Two low noise superconductor-insulator-superconductor (SIS) tunnel junction mixers allow the interferometer to achieve a sensitivity of $\Delta T_{rms} = 7\ mK/\sqrt{Hz}$. Noise from the receiver and atmosphere integrates down over an hour to within a factor of 2 of the ideal limit for white noise. Should the noise continue to fall off as $1/\sqrt{\tau}$ for longer times τ, we can expect to measure $\Delta T/T \sim 2.0 \times 10^{-5}$ in 24 hours of observation at 2 independent sets of spots around the pole.

J2-5
1520

MICROWAVE BACKGROUND OBSERVATIONS AT OVRO

A. T. Moffet
Owens Valley Radio Observatory
California Institute of Technology
Pasadena, CA 91125

The OVRO 40-meter telescope is located in a high desert site and is equipped with a very sensitive maser radiometer working in the 18-24 GHz range. It has been used during a large part of the last several winter observing seasons for two programs connected with the cosmic microwave background.

A number of fields have been observed near the north celestial pole. In 1983-84 the pole was compared with an annulus 7.15 arcmin away. Our value for the difference between the sky temperature at the pole and the average over the annulus is 5 ± 20 μK. In 1984-85 eight regions at a declination of 99° were observed, and the rms fluctuation in brightness among these is less than 60 μK.

The Sunyaev-Zel'dovich effect has been observed in three clusters of galaxies, 0016+16, A665 and A2218 with amplitudes of -400 to -600 μK. Mapping in declination gives a measure of the angular extent of the scattering gas. VLA observations have been made to determine the flux of confusing sources in the fields.

The maser is used at 20.0 GHz, with a bandwidth of 350 MHz. The system noise at the zenith is about 40 K. The beam throw is 7.15 arcmin, and the two beams are carefully balanced in noise level and gain. A separate water-vapor radiometer, working at 21.0 GHz with a 15° beam, is used to monitor atmospheric transmission. When the sky temperature is less than 8° per air mass the radiometer output is usually limited by thermal noise.

Numerous colleagues are involved in both these programs, and the work is sponsored by the National Science Foundation.

J3-1
1600 TEXAS 5-M ANTENNA EFFICIENCY DOUBLED AT 230-290 GHZ WITH ERROR CORRECTING SECONDARY OPTICS

Charles E. Mayer
Electrical Engineering Research Laboratory
University of Texas at Austin
10100 Burnet Rd
Austin, TX 78758

The surface of the University of Texas 5-m millimeter wave telescope has been measured holographically many times before to assess the distortion due to thermal and gravitational loads (Mayer, et. al., IEEE Trans. Instrum. Meas., vol. IM-32, pp. 102-109, 1983) and for comparison with another surface measurement technique. We decided to use this information to increase the aperture efficiency by decreasing the phase coupling losses. The procedure chosen was to modify the geometric ray path length with a compensated secondary mirror whose deformation were the inverse of the primary deformations, thus maintaining a constant path length. The geometry chosen was a folded Gregorian (FG) arrangement, which was compatible with our prime focus receivers.

An analytic ellipse was machined on a computer controlled milling machine, with 0.1 mil accuracy, and installed on the telescope. The phase of the aperture plane fields through the FG system was measured holographically at a frequency of 117 GHz. A 5-dimensional (k_x, k_y, x, y, z of feed) feed position optimization program was run on the data to remove small experimental effects. From these phase measurements, a mill driving program was written and the error correcting secondary was machined.

The aperture efficiency of the FG system was measured using Jupiter and Venus as point sources, extended molecular sources, and a pattern range transmitter. Comparisons were made between the previous f/0.5 prime focus system, the FG system with an analytic ellipse, and the FG system with the error corrector. The error corrector redirected much of the energy in the scatter pattern into a well structured main lobe resulting in an aperture efficiency improvement by more than a factor of two.

+

J3-2
1620

MULTI-FREQUENCY APERTURE SYNTHESIS MAPPING OF CIRCUMSTELLAR MOLECULAR LINE EMISSION:

J.H. Bieging, Radio Astronomy Laboratory, University of California, Berkeley, CA 94720,
and
Nguyen-Q.-Rieu, Observatoire de Paris-Meudon, F-92195 Meudon, France

We have used the Berkeley mm-wavelength 3-element interferometer to map the molecular envelopes of two late-type evolved stars with high rates of mass loss. We have taken advantage of the spectral multiplexing capability of the Berkeley cross-correlation spectrometer to observe several molecular transitions in the 3 mm atmospheric window simultaneously. IRC+10216, a late-type carbon star, was observed in 11 transitions of 8 different molecular species with only 3 local oscillator settings. CRL2688 (the "Egg" Nebula) was observed in 10 transitions of 6 different species, also with 3 LO settings. Four configurations of the 3 antennas, or 12 baselines in total, were used in the aperture synthesis, yielding a beamsize of about 7".

The maps for IRC+10216 show that different molecular species tend to have different emission sizes which must reflect variations either in chemical abundances through the circumstellar envelope, or in excitation conditions. The data are compared with theoretical models of molecular excitation to obtain physical and chemical conditions in the envelope.

In contrast to the circularly symmetric emission from IRC+10216, CRL2688 is clearly elliptical in its molecular line maps. The emission in the HCN line peaks at the IR star position and is extended in the same direction as the optical dark lane. These results are consistent with the idea that the circumstellar material is predominantly in the form of a dense rotating disk.

0830-Tues. UMC Center Ballroom
PLENARY SESSION

0830 Introduction: R. K. Crane

1. 0840 Student Paper 1

2. 0900 Student Paper 2

3. 0920 Student Paper 3

PS-4 1000 SCIENCE IN SPACE WITH THE SPACE STATION: Peter M. Banks, STAR Laboratory, Stanford University, Stanford, CA.

PS-5
1045

THE NASA/JPL SHUTTLE IMAGING RADAR PROGRAM

Dr. Daniel N. Held
Jet Propulsion Laboratory
California Institute of Technology
Pasadena, CA 91109

In November 1981 the first of a series of L-band synthetic aperture radars (SAR's) was launch into orbit utilizing the Space Shuttle as a platform. Known as the Shuttle Imaging Radar - A (SIR-A), the instrument provided detailed radar images of large portions of the Earth's surface, including some exciting subsurface images acquired over the Sahara desert.

Three years later, in October 1984, SIR-B, an improved version of the previous instrument featuring higher resolution and an all-digital data collection and processing system, was successfully launched and subsequently generated many hundreds of high-quality images for analyses by a multi-disciplinary scientific team.

The SIR-B instrument is currently scheduled for a second flight in the Spring of 1987. It will be followed by the development of the SIR-C system which will add the capability to simultaneouly image at three frequencies (L, C, and X-bands) and at multiple polarizations. In addition, the SIR-C system will feature electronic beam steering at both L and C-band.

This new class of instrument will significantly increase the ability of earth scientists to image the earth and space at microwave frequencies. Some of the future capabilities of the SIR-C instrument have already been demonstrated by a airborne SAR flying on the NASA CV-990 aircraft. Data from this airborne instrument, as well as the previous two spaceborne instruments, will be presente and compared.

Session B-5 1355-Tues. CR2-28
ELECTROMAGNETIC THEORY

B5-1
1400 Chairman: R. J. King, Lawrence Livermore National Laboratory, Livermore, CA 94550

AN ANISOTROPIC LENS FOR LAUNCHING TEM WAVES ON A CONDUCTING CIRCULAR CONICAL SYSTEM

A. P. Stone
University of New Mexico
Mathematics Department
Albuquerque NM 87131

C. E. Baum
Air Force Weapons Laboratory
Kirtland AFB NM 87117-6008

Among several possible approaches to transient lens design is one which might be termed a differential-impedance-matching and transit-time conservation approach. In this approach it is desired to transition a TEM wave so that it is transmitted undistorted and unreflected from one transmission line to another one. Thus it is intuitively necessary that impedances should be matched between regions and also that the travel time for waves following different paths should be equal. These conditions lead to a system of ordinary differential equations which describe the geometry and physics (i.e. the shape and material) of the lens. It is this approach which is used in the design of an anisotropic lens for launching TEM waves from a small source, through the lens, and onto a conducting circular conical system. An exact solution to the resulting system ODES is obtained. In addition, an approximate solution, which would be applicable to a design procedure, is also given.

B5-2 A SIMPLE MODEL OF INTERIOR ELECTROMAGNETIC COUPLING*
1420

J.K. Breakall, K.S. Kunz and R.J. King
Lawrence Livermore National Laboratory
L-156
P.O. Box 808
Livermore, CA 94550

Broadband (0.045-18 GHz), wide dynamic range (80-90 dB) measurements on canonical interior coupling geometries were made at Livermore's EMPEROR EM test facility. For the 10:1 scale size employed they yield scaled responses from 4.5-1,800 MHz. The upper limit is much greater than the upper limit of conventional full scale simulators used for EM coupling studies. From these measurements a simple model that describes the general behavior of the current induced on interior wires has been developed.

This simple model consists of an envelope that reasonably bounds the resonant peaks and a characterization of the Q's associated with the resonances. The envelope is given by the product of a shielding effectiveness (S.E.) term, representing the shielding provided by the exterior hull with an aperture in it, and a coupling effectiveness (C.E.) term, representing the integrating effect of the interior wires behaving like antennas. The SE term acts like a high pass filter, it models the relatively unimpeded flow of energy into the interior above the aperture cutoff frequency where the aperture circumference is roughly equal to a wavelength. The CE term acts like an integrator, it imposes a $1/\omega$ trend to the wire current response. This envelope model, called SEXCE, has bounded the responses of a variety of geometries, typically to within 3-6 dB and at most to within 12 dB.

To complete the modeling of the responses the Q's of the resonances must be estimated. These estimates can be heuristic, based on observations of many diverse systems or they can be analytically derived using the field strengths for the wire resonances at the aperture.

---

* Work performed under the auspices of the U.S. Department of Energy by the Lawrence Livermore National Laboratory under contract number W-7405-ENG-48.

B5-3
1440

ANALYSIS OF TRANSMISSION LINE FIELD-TO-WIRE COUPLING AT HIGH FREQUENCIES

A.T. Adams, J. Perini, K. Heidary, M. Miyabayashi, and D. H. Shau
Department of Electrical and Computer Engineering
Syracuse University, Syracuse, NY 13210

As frequency increases, the analysis of field-to-wire coupling becomes increasingly intractable as line lengths, line separations, and, finally, wire diameters become large electrically. Higher-order modes may propagate and moment methods require a large number of unknowns.

Transmission line field-to-wire coupling has been investigated in the region where line lengths may be long, wire separations may be large, but wire diameters are not large electrically. Numerous typical problems involving field-to-wire coupling to uniform and non-uniform (spherical) transmission lines are treated. Some results are obtained also for multiconductor transmission lines. The results indicate that higher-order modes do not appear to be very important in the cases treated, even when transmission line wire separation is several wavelengths. The current distributions obtained can be explained in terms of simple standing and traveling wave forms.

For long transmission lines which cannot be treated by moment methods, bounds may be obtained for induced currents by considering the transmission line as a receiving antenna. Bounds may be obtained for the magnitude of the antenna impedance and for the open-circuit voltage of the equivalent circuit, thus yielding bounds for induced current.

B5-4
1500

LOSS CALCULATION IN UNSTABLE OPTICAL RESONATORS:

M. H. Rahnavard and J. Zare-Moodi, Electrical Engineering Department, Shiraz University, Shiraz, Iran

Unstable optical resonator is used in medium and high powered laser. In stable resonator, when Fresnel number is greater than 0.5 all of the energy is not absorbed by first mode but energy is absorbed in higher order modes. For absorbing maximum energy from the material we should operate in higher modes with higher power loss capability. In unstable resonator, with proper gain it is possible to have mode with lowest power loss. This mode will absorb most of the energy from the laser material and it is possible to have optical resonator with smaller length. For this reason power loss calculation is important in unstable optical resonators.

At first Fox and Li calculated power loss in infinite strip cylindrical and spherical resonators with circular aperture for Fresnel number greater than 10 by scalar theory of diffraction using iterative method {1}, {2}, {3}. By using geometrical optics Siegman calculated power loss in optical resonators for large Fresnel number {4}. Sanderson and Striefer calculated power loss by Gaussion and Cornu spiral methods {5}, {6}. In the first method the integral is converted to a matrix. Using QR-method, value and eigen vector of the matrix is evaluated. Eigen vectors are electric field modes and power loss in each mode is equal to one minus absolute value of the eigen value of that mode. Siegman and Miller found eigen values for spherical resonator with circular aperture with Fresnal number greater than 13 using Prony's method {7}. Santana and Felson calculated eigen values using waveguide theory {8}.

In evaluating the integral for the field or resulting eigen matrix, Fresnel number is important. As Fresnel number gets larger, resulting series from the integral has more elements. The number of elements in the series is usually between 6 to 10 times the Fresnel number {7}. So power loss evaluation in optical resonators with Fresnel number greater than 10 takes a long time. Except for Santana and Felson {8}, all of the works which have been done are based on scalar theory of diffraction {1}. In this paper physical optics in exact form and with Fresnel approximation, scalar theory of diffraction without approximation, geometrical theory of diffraction, and physical theory of diffraction are used in analyzing and power loss calculation of cylindrical infinite strip optical resonators. Electric field of incident wave of one volt perimeter and zero phase is used. It is assumed that the incident wave is either lane or steady state geometrical optic case, although the latter is most practical and important. The results are then compared with each other and with the results which are obtained by other investigators.

Session B-6 1535-Tues. CR2-28

PROPAGATION

Chairman: E. F. Kuester, University of Colorado, Boulder, CO 80309

B6-1 1540 AN ANTENNA MODEL FOR GROUND WAVE PROPAGATION (10 kHz-30 MHz)

N. DeMinco, NTIA/ITS.S4
U. S. Department of Commerce
Institute for Telecommunication Sciences
325 Broadway
Boulder, CO 80303

An automated antenna model has been developed for performance prediction of communication circuits that use the groundwave as the primary mode of propagation. The model is in the form of a computer program that uses lookup tables and simple algebraic algorithms. The program computes the performance of several antenna types as a function of the independent variables; antenna geometry, ground conductivity, ground dielectric constant, frequency, and azmuthal directional characteristics. The look up tables and algorithms were derived from extensive method of moments caculations using the Numerical Electromagnetics Code(NEC) - version 3. The resulting computer program allows fast prediction of antenna performance with the model, since, all complex and time consuming electromagnetic calculations have been previously performed "offline". The Numerical Electromagnetics Code (NEC) is used to determine the gain of a short dipole over lossy earth with respect to an isotropic radiator in free space for all ground conductivities, ground dielectric constants, and frequencies. A ratio called the relative communication efficiency is then calculated for each subject antenna referenced to a short dipole as a function of ground constants, frequency, and antenna geometry. The net result is the equivalent gain of the subject antenna over lossy earth with respect to an isotropic radiator in free space. An explanation of the model derivation and sample calculations will be presented.

B6-2 1600 Lateral Wave Propagation in a Wedge Shaped Region

John M. Dunn
Division 7553,
Sandia National Laboratories,
Albuquerque, New Mexico, 87185

Lateral wave propagation in a wedge shaped region is examined. The geometry consists of two media, the lower one of which is bounded from below by a conducting plate. The plate intersects the interface between the two media from below at an oblique angle. The transmitting antenna is an infinite, time harmonic, electric line source located close to the interface between the two media, and oriented to make the problem two dimensional. The wavenumber of the upper medium has a magnitude which is much greater than that of the lower medium. The lateral wave travels downward from the source into the second medium, along the interface, and back up to the point of observation in the first medium. The problem cannot be solved in closed form easily as separation of variables techniques are not possible. An approximate analytical method is therfore used in which the two media are separated from one another at each step of an iterative procedure using impedance boundary conditions. This allows the use of more powerful single medium techniques in each region. The lateral wave field is expresssed either as a modal series or image series depending on the angle the plate makes with the interface and on the location of the source and receiver. The decay of the wave in the direction parallel to the interface is shown to be algebraic, even in the presence of the plate. The results are valid subject to the restrictions that the source and receiver are close to the interface and are not too close to each other or the edge of the plate. There will be other waves present which are not considered in this paper if the upper region is not conducting, although the expression for the lateral wave is still valid.

B6-3
1620

SURFACE WAVE PERFORMANCE OF DISTRIBUTED-WIRE ANTENNAS OVER MIXED TERRAINS

R. M. Bevensee, G. J. Burke, and R. J. King
Lawrence Livermore National Laboratory
P.O. Box 5504, Livermore, CA 94550

Surface wave performance of an antenna radiating over nonuniform terrain is characterized by the "relative surface wave power" E^2_{surf}/P_{in}. This parameter varies with distance as d^{-4}. It may conveniently be computed as the product of Relative Communication Efficiency (or RCE; R. C. Fenwick and W. L. Weeks, IEEE Trans. Ant. Prop., AP-11, 296-305, 1963) and E^2_{surf}/P_{in} of a reference dipole propagating over nonuniform terrain. It is significant to note that the RCE is unchanged from flat homogeneous earth to nonuniform terrain because, once launched, the surface wave propagates the same for both test and reference antennas.

RCE computations by the Numerical Electromagnetics Code (NEC) are presented for various homogeneous grounds and different antenna types; e.g., loop, Beverage, vertical half-rhombic, and Yagi. An electrically short vertical dipole with insulated end touching the ground serves as the reference. Its relative surface wave power, measured by the perpendicular component of electric field is computed by the WAGNER code (R. H. Ott, Radio Science, 6, 429-435, 1971) for various nonuniform terrains; e.g., forest to clearing and vice versa, good ground to poor ground and vice versa, land-to-sea paths, and over hills.

By multiplying the RCE of a test antenna over a given flat homogeneous earth by the relative surface wave power of the reference dipole radiating over a nonuniform terrain one obtains E^2_{surf}/P_{in} of the test antenna over that nonuniform terrain.

B6-4
1640

VHF/UHF DIFFRACTION OVER IRREGULAR TERRAIN — CALCULATION BY NUMERICAL INTEGRATION

J. H. Whitteker,
Communications Research Centre, Department of Communications,
3701 Carling Ave., Box 11490, Station H,
Ottawa, CANADA K2H 8S2

Suppose that terrain elevations are given at various distances x_j measured horizontally from a transmitting antenna along a VHF or UHF transmission path. Between the given points, the surface of the ground is assumed to follow straight lines joining the points, and to be uniform perpendicular to the direction of propagation. On a smaller scale, the ground surface is assumed to be rough, so that reflections are important only near grazing incidence. By the repeated application of Huygens' principle, and using the Fresnel-Kirchhoff approximation, it is possible to calculate the diffraction attenuation on the path. For each x_j in turn, the wave field is found at ground level and at a number of points along a line extending upward from the ground.

Finding the field at some point at distance x_j from the transmitter involves performing an integration with respect to the vertical coordinate y at distance x_{j-1}. (In general, two integrations must be done, one for the direct wave, the other for the reflected wave.) The integral is of the form

$$\int A(y) \exp(i\phi(y))\, dy$$

where A is the wave amplitude at y, and ϕ is the phase of the wave at y plus the phase path between y and the field point. The integration is done by substituting for y a dimensionless variable t defined by $t^2 = \phi(y) - \phi_0$, where ϕ_0 is the minimum phase of the integrand. The resulting expression

$$\exp(i\phi_0) \int \frac{A(y)}{dt/dy} exp(it^2)\, dt$$

can be evaluated in terms of the Fresnel integral by choosing a polynomial representation of the factor $A(y)/(dt/dy)$.

The value of this sort of calculation is most evident for irregular terrain that is not easily represented by a small number of simple geometrical forms. Also, in contrast with most ray-theory calculations, the region of validity is not restricted to the far field of diffracting edges. The method is being tested for various path profiles. In the special case of featureless terrain with the earth's curvature (represented as a polygon), the calculated attenuations agree with those given by spherical diffraction theory to within a few decibels, in spite of the use of different boundary conditions.

Session B-7/E-2 1355-Tues. CR2-6

ELECTROMAGNETIC THEORY FOR INTERFACE PROBLEMS

Chairman: Carl Baum, Air Force Weapons Laboratory, NTAAB, Kirtland AFB, NM 87117

B7/E2-1
1400

Submicrosecond Structure of Lightning Return Stroke Fields

E. P. Krider[1], C. Leteinturier[2], and

J. C. Willett[3]

Abstract

An experiment to measure the electric field, E, dE/dt, and HF signatures that are radiated by lightning return strokes at known locations was conducted at the NASA Kennedy Space Center during the summer of 1984. Values of the maximum dE/dt during the initial, fast-rising portion of first strokes were found to have a mean and standard deviation of 45.4 ± 13.4 V/m/μsec, when range-normalized to 100 km, when HF at 5 MHz was used as the trigger signal. The full width at half-maximum of dE/dt was 97 ± 18 nsec. If these fields are produced by a single current pulse that propagates up a single channel at a typical velocity of 10^8 m/sec, then the above values of dE/dt imply that the mean maximum dI/dt at the lightning source is about 230 kA/μsec, a value that is substantially larger than most tower measurements.

---

1 University of Arizona, Tucson, AZ 85721

2 CNET MER/GER, 22301 Lannion, France

3 Naval Research Laboratory, Washington, D.C. 20375

B7/E2-2
1420

RETURN-STROKE TRANSMISSION-LINE MODEL*:

Louis Baker, Mission Research Corporation,
1720 Randolph Road, S.E., Albuquerque,
New Mexico, 87106

A simple transmission-line model is developed for the lightning return stroke. It is treated as a transmission-line surrounded by a corona discharge [1]. Hydrodynamic channel expansion, radiative losses, channel resistance, non-linear line capacitance are included in the model by means of a "two-zone" model which is an extension of those developed by Strawe [2] and by Braginskii [3]. The resulting equations are solved numerically using the AFWL CRAY-1, typical runs requiring only a few seconds of CPU time. Once channel geometry, etc. are specified there is only one ad hoc parameter, which is equivalent to specifying the wave speed along the transmission line.

The shape of the current pulse is shown to change substantially with propagation; simple models without channel resistance ("ideal transmission lines") can be misleading in this regard, as they predict current pulses that preserve shape as they propagate up the line. The fall-off in the radiation-zone fields is due to the decrease in I-dot at the front, which is caused by an increase in front rise time, before the current amplitude decreases substantially. In contrast, ideal transmission line models give radiation-zone fields of the same shape as the current pulse.

1. C. E. Baum and L. Baker, NEM 84 conference, p. 24.

2. D. F. Strawe, "Non-Linear Modeling of Lightning Return Strokes," preprint.

3. S. I. Braginskii, Soviet Physics-JETP, 34, 1068(1958).

---

*This work was performed under Air Force contract F29601-82-C-0027.

B7/E2-3
1440

CONCEPTS FOR MEASURING LIGHTNING FIELDS VIA AN AIRBORNE ELECTROMAGNETIC PLATFORM

D.V. Giri
Visiting Faculty, Dept. of EECS
University of California, Berkeley, CA
Pro-Tech, 125 University Avenue
Berkeley, CA 94710

Recently, an airborne electromagnetic platform has been designed, fabricated and applied in measuring the far magnetic field of a pulse radiating antenna. The radiated pulse simulates an EMP and is useful in measuring the response of an aircraft in flight for the incident simulated EMP environment. The theoretical considerations for this airborne magnetic field sensor have been reported in (D.V. Giri and C.E. Baum, Sensor and Simulation Note 184, May 1984), the design considerations in (D.V. Giri and S.H. Sands, EM Platform Memo 1, September 1983) and the successful results of measurement and comparison with computed radiated fields are under publication (Air Force Weapons Laboratory TR). The airborne platform is designed so that the electromagnetic (EM) field sensor measures the incident field while minimizing its response to fields scattered by the aircraft itself.

In this paper, certain measurement concepts for lightning generated EM fields and currents will be examined. The lightning currents and the aircraft response to lightning have been measured and reported extensively, for example in (F.L. Pitts, AIAA Paper 81-0083). The concepts examined here, have their basis in the practical implementation of the airborne platform described above. However, there are problems unique to lightning measurements and they will be discussed. It is noted that the discussion will be at a conceptual level, since detailed design considerations of any of these concepts for lightning application have not been carried out as yet.

B7/E2-4
1500

CALCULATED TEMPERATURE AND BRIGHTNESS OF A LIGHTNING DISCHARGE*

R. L. Gardner, A. H. Paxton, and L. Baker
Mission Research Corporation, 1720 Randolph Road, S.E., Albuquerque, New Mexico 87106

In order to develop techniques for remote sensing of lightning currents and other internal electrical parameters a detailed model of the energy balance of a lightning discharge has been constructed. We present here a detailed one-dimensional hydrodynamic model of a slice of unit length of a lightning channel.

The energy is input to the channel by joule heating. A known current is impressed on a channel whose resistance is calculated from a conductivity profile which is a function of the local gas temperature. Energy is distributed across the cross section of channel as if it were a set of parallel resistors. The current is assumed to vary slowly enough that the diffusion time is negligible.

Energy losses are more varied. The hot gas loses energy immediately through radiation. In this model radiation losses and redistribution of energy throughout the gas are calculated using multi-group diffusion. Eight frequency bands are chosen and for each a diffusion calculation is performed. The bands are chosen in such a way that the opacity varies by no more than a factor of two over a single band. Hydrodynamic expansions, including pseudo-viscous pressure for shocks is included to complete the energy balance. A complex equation of state for an idealized air molecule is used in the calculations.

This model is intended for use in remote sensing of lightning currents. For that purpose, the model must be experimentally verified. Experiments in which brightness and current are simultaneously measured are just becoming available. However, the model is compared to available experimental data.

---

*This work was performed under Air Force contract F29601-82-C-0027.

B7/E2-5 1540 ERROR BOUNDS FOR NATURAL FREQUENCY ESTIMATION:

Sung-won Park and J. T. Cordaro

A problem of practical interests in electromagnetics is that of estimating the natural frequencies or poles of a scatterer from transient surface current density measurements. When the measurements are noisy the estimated poles are random variables. Several investigators have compared pole extraction techniques by using simulation to find the variance of the estimated poles. We have two general results that provide lower bounds on the variance. Both results assume the noise is Gaussian and uncorrelated.

The first applies to the case of one pole-pair. We have lower bounds directly on the variance of the real and imaginary parts of the poles. No unbiased pole estimation technique can have lower variance.

The second result is a lower bound on the variance of the coefficients of the characteristic equation of the poles. This bound is very useful for comparing various pole extraction techniques against the ideal. Several applications of each bound are given.

B7/E2-6 1600 CHARACTERIZATION OF TRANSIENT TIME DOMAIN WAVEFORMS: J. P. Castillo, R & D Associates, Albuquerque, NM 87106; J. Lubell, Mission Research Corporation, Colorado Springs, CO 80919; and L. O. Marin, Dikewood Division, Kaman Sciences Corporation, Santa Monica, CA 90405

There is a growing interest in the characterization of transient time domain waveforms. Transient phenomenon occurs in lightning, nuclear electromagnetic pulse, and high power microwaves. It is important to understand the important aspects of the interaction of these transients with modern electronic systems. Permanent damage and upset can occur when this interaction process takes place. The purpose of this paper is to present a method for characterizing transients and transient responses so that the cause and effect are better understood and simpler to categorize. Of particular interest are norms which are specifically related to the response of diverse circuits. The norm quantities of interest include:

- o Peak Amplitude
- o Peak Derivative
- o Peak Impulse
- o Rectified Impulse
- o Action Integral

Examples of the applicability of these norm quantities will be given.

B7/E2-7
1620

SOME BOUNDS CONCERNING THE RESPONSE OF LINEAR SYSTEMS WITH A NONLINEAR ELEMENT

C. E. Baum
Air Force Weapons Laboratory
Kirtland AFB NM 87117-6008

This paper addresses the problem of nonlinear elements present in otherwise linear electromagnetic systems. What effect does such an element have on a linear analysis of such systems? Here we obtain some bounds on such effects. At a minimum these bounds can give some criteria as to under what conditions some nonlinearities can be neglected in the analysis of the system electromagnetic response.

B7/E2-8 1640 ON THE RESPONSE OF OVERHEAD POWER LINES TO TRANSIENT ELECTROMAGNETIC FIELD INTERFERENCE

F.M. Tesche
LuTech, Inc.
3742 Mt. Diablo Blvd.
Lafayette, CA, 94549

Abstract

The effect of lightning on power systems has long been regarded as a possible threat to the stability and continued operation of the power grid. Consequently, much work has been done to determine the levels of lightning-induced surges on power lines, how they propagate along the line, and how they affect components in the system.

With the advent of microprocessor controls in the power system, the possible effects of lightning on the system are more severe, due to the decreasing susceptibility of these components. Moreover, the emergence of the nuclear electromagnetic pulse (NEMP) as a possible threat to the power system requires additional consideration.

This paper discusses some of the calculational models which can be used to estimate the response of overhead power lines to transient electromagnetic (EM) excitation. For the case of lightning, both the direct-strike and near-strike cases are treated, and the calculational models are compared and contrasted with those suitable for determining the HEMP response of the line. For this latter case, the excitation EM field is essentially a plane wave providing a global excitation of the entire power grid, and consequently, the line response is different from that due to lightning. Sample numerical results for these different excitations will be discussed in this paper.

Another form of EM interference to power lines which is well known in the power community arises from geo-magnetic storms. A similar man-made environment could exist several seconds after a high altitude nuclear detonation, and is referred to as magnetohydrodynamic EMP. These two late-time EM environments and their effects on long power lines are also discussed in the paper.

Session C-2 1355-Tues. CR1-40

FAST ALGORITHMS FOR DIGITAL SIGNAL PROCESSING

Chairman: R. E. Blahut, IBM Corp., Oswego, NY

C2-1
1400

A SURVEY OF FAST ALGORITHMS FOR MULTIDIMENSIONAL FOURIER TRANSFORMS

Richard E. Blahut
IBM Corporation
Owego, NY 13827

There are now many fast algorithms known for computing multidimensional Fourier transforms in both the complex field and the real field. This talk will briefly survey some of them.

C2-2
1420

COMPUTING THE DISCRETE FOURIER TRANSFORM USING RESIDUE NUMBER SYSTEMS IN A RING OF ALGEBRAIC INTEGERS

John H. Cozzens
The Mitre Corporation
Bedford, Massachusetts 01730
Larry A. Finkelstein
Northeastern University
Boston, Massachusetts 02115

This talk describes a new method for computing an $N = R^m = 2^{vm}$ -point complex DFT which uses quantization within a dense ring of algebraic integers in conjunction with a residue number system over this ring. The algebraic and analytic foundations for the technique are derived and discussed. The architecture for a radix-R FFT algorithm using a residue number system over $Z[\omega]$, where ω is a primitive R-th root of nuity, is developed; and range and error estimates for this algorithm are derived.

C2-3
1440

FAST ALGORITHMS FOR MAGNETIC RESONANCE IMAGING

Ephraim Feig
IBM Research
Yorktown Heights, New York

Magnetic Resonance Imaging (MRI), as is commonly practiced, is a rather slow procedure, its lengthiest part by far being the scanning or data gathering routine. A designer of fast algorithms for MRI cannot merely consider the speedup of solving the various arithmetic problems that he is given. He must take the intiative and design new and more efficient scanning procedures which will be amenable to fast computation and which will yield pictures which are meaningful to the radiologist or the medical scientist. In this talk we briefly survey some new fast algorithms for MR imaging and in vivo spectroscopy.

C2-4
1540

HYPERBOLIC HOUSEHOLDER TRANSFORMATIONS AND THE SOLUTION OF LEAST-SQUARES PROBLEMS

Alan O. Steinhardt, Charles M. Rader
MIT Lincoln Labs
Lexington, Mass. 02173

A class of transformation matrices analogous to the Householder matrices is developed with a nonorthogonal property designed to permit the efficient deletion of data from least-squares problems. These matrices, which we term hyperbolic Householder, are shown to effect deletion, or simultaneous addition and deletion, of data with much less sensitivity to surrounding errors than for techniques based on normal equations. When the addition/deletion sets are large, this numerical robustness is obtained at the expense of only a modest increase in computations. However, when a relatively small fraction of the data set is modified, this numerical robustness is fortuitously accompanied by a decrease in required computations. Two applications to signal processing problems are considered.

C2-5
1600

BERLEKAMP'S ALGORITHM AND EUCLID'S ALGORITHM :A COMMON THREAD

Todd K. Citron
Space Communications Group
Hughes Aircraft
P. O. Box 92424
Los Angeles, CA 90009

A major step in the decoding of Reed-Solomon and BCH codes involves the solution of what Berlekamp called the key equation. Historically there have been two approaches to solving this equation. Berlekamp's algorithm and later Euclid's algorithm for computing GCD's. In this paper, with the intuitive aid of scattering theory, we derive Berlekamp's algorithm as a particular way of implementing Euclid's algorithm. In fact, there are many other ways to implement Euclid's algorithm. Depending on the hardware environment, one or another may be optimal. This has led to the development of a new high speed VLSI decoder for Reed-Solomon and BCH codes.

C2-6 1620 SOME ASPECTS OF PARALLEL PROCESSING AS APPLIED TO SIGNAL PROCESSING: J. E. Hershey, BDM Corp., Boulder, CO 80301

Session G-4 1355-Tues. CR0-30
HIGH LATITUDE IONOSPHERE
Chairman: E. J. Fremouw, Physical Dynamics, Inc.,
Bellevue, WA 98009

G4-1
1400

ON THE ANISOTROPY OF SCINTILLATION-PRODUCING IRREGULARITIES AT HIGH LATITUDES

E.J. Fremouw
Physical Dynamics, Inc.
Bellevue, WA 98009 USA

Anisotropic irregularities produce enhanced scintillation of radio waves when the line of sight grazes an elongation axis. For axially symmetric irregularities aligned along the magnetic field, such enhancement occurs in a region near the magnetic zenith of a ground-based receiver. For irregularities also displaying cross-field anisotropy, the region is extended along a line through the magnetic zenith. For instance, scintillations observed by means of the Wideband Satellite at Poker Flat, AK, at night showed clear enhancement when the line of sight grazed within a few degrees of the L-shell through the receiver. Geometrical enhancements often are quite prominent in scintillation records from individual passes of a low-orbiting satellite. At times, however, they can be obscurred by patchiness of scintillation-producing irregularities. Presumably, the effects of patchiness will average out of a large data base, leaving geometrical enhancement as its most prominent feature. We have organized intensity and phase scintillation measurements made at Tromso, Norway and Sondre Stromfjord, Greenland by means of the HiLat Satellite through all of 1984 into a grid of off-L-shell and off-magnetic-meridian angle as a way of identifying geometrical enhancement. Results are that such enhancement is not as prominent at either station as it was at Poker Flat in 1976-79. Nighttime data from Tromso, however, do show evidence of both along-field and crossfield anisotropy, as seen at Poker Flat. Daytime data from Tromso and both daytime and nighttime data from Sondre Stromfjord show evidence of elongation along the magnetic field but no evidence of cross-field anisotropy.

G4-2
1420

THE SPATIAL WAVENUMBER SPECTRUM OF HIGH-LATITUDE F-REGION IRREGULARITIES INFERRED FROM HILAT SATELLITE PHASE SCINTILLATION DATA

C.L.Rino and T.M. Dabbs
Radio Physics Laboratory
SRI International
Menlo Park, CA 94025

Ionospheric irregularities with spatial scales from a few hundred meters to several tens of kilometers typically are characterized by the distribution of the intensity of their spatial fourier components. We have developed a multi-component power-law curve fitting procedure that optimally determines the number of power-law segments, their break-points, and the power-law index and strength for each segment. HILAT phase scintillation data acquired from stations at Sondre Stromfjord, Greenland and Tromso, Norway over a 15-month period from November 1983 through March 1984 have been analyzed.

In more than 68 percent of the measured phase spectra, there is a well defined intermediate scale segment corresponding to an average one-dimensional in-situ spectral index of $1.7 \pm .2$. The characteristics of the intermediate scale segment (other than its strength) show no significant seasonal, diurnal, nor latitudinal variations. Indeed, the structure is virtually identical to the corresponding intermediate scale F-region irregularities we have measured in situ near the geomagnetic equator. This suggests a source mechanism that produces sharp gradients as do convective instabilities.

At larger scale sizes (> 10 km), however, pronounced steepening of the spectrum is observed in 30 to 40 percent of the HILAT passes. Preliminary identification of these structures suggest that they result directly from magnetospheric sources, possibly "stirring" by large scale shears in the convection velocity field.

G4-3
1440

SOURCE MECHANISMS OF HIGH LATITUDE IONOSPHERIC IRREGULARITIES

M.C. Lee
Research Laboratory of Electronics
Massachusetts Institute of Technology
Cambridge, Massachusetts 02139
J. Buchau, H.C. Carlson, Jr., J.A. Klobuchar,
E.J. Weber
Ionospheric Physics Division
Air Force Geophysics Laboratory
Hanscom Air Force Base, Massachusetts 01731
S.P. Kuo
Polytechnic Institute of New York, Long Island Center
Farmingdale, New York 11735

The high latitude ionosphere can be significantly perturbed by the precipitating particles, intense quasi-DC electric field, electrojets,and field-aligned currents etc. that form the potential sources of various plasma instabilities creating ionospheric irregularities in the E and F regions. Coordinated experiments using optical and radio waves and in situ measurements have provided extensive information about the large scale structures and dynamics of the high latitude ionosphere, and the relations of these to the occurrence of ionospheric irregularities. Several plasma instabilities will be examined as possible source mechanisms for exciting ionospheric irregularities. Factors such as precipitating electrons, horizontal transport, and relative ion-neutral velocities within ionospheric structures will be considered. In particular, various thermal effects that can contribute to the generation of irregularities in the high latitude ionosphere will be discussed.

G4-4
1500 KELVIN-HELMHOLTZ INSTABILITY AND ASSOCIATED SMALL SCALE STRUCTURES IN THE HIGH LATITUDE IONOSPHERE*

P. Satyanarayana,** H. Mitchell,** M. Keskinen,
J. Fedder, S. Zalesak, and J. Huba
Geophysical and Plasma Dynamics Branch
Naval Research Laboratory
Washington, DC 20375-5000

Numerical and analyical studies of the nonlinear evolution of the Kelvin-Helmholtz velocity shear instability and associated small scale structures in the high latitude ionosphere are presented. In our numerical simulations we solve a simple set of plasma fluid equations in the electrostatic approximation under a variety of initial conditions. We attempt to include the effects of density gradients and particle collisions in our analysis. In the nonlinear regime we compute numerically the power spectrum of velocity and density fluctuations and compare with theoretical estimates. Finally, we compare our results with experimental observations.

* Work supported by DNA, NASA, and ONR.
**Science Applications International Corporation, McLean, VA 22102

G4-5 1520 A Statistical Survey of Results from the Goose Bay HF-Radar

R. A. GREENWALD
K. B. BAKER (The Johns Hopkins University Applied Physics Laboratory, Laurel, Maryland 20707)
R. A. HEELIS (University of Texas at Dallas, Richardson, Texas 75080)

We have analyzed a random sampling of data from the APL HF-Radar experiment in Goose Bay, Labrador. The results of this survey cover a one-year period from July 1, 1984 to June 30, 1985. Overall, the probability of observing backscattered power sometime within a randomly selected hour is greater than 50% and the probability within the midnight local time sector is around 80%. When scatter is observed, it is usually either ionospheric or a combination of ionospheric scatter and ground scatter. In only about 12% of the cases is the observed scatter purely ground scatter. The Doppler velocity spectra show significant variations as a function of both local time and radar range. Spectra from ranges close to the radar are predominantly from the E-region and tend to be narrower than the spectra observed at larger ranges where the backscatter comes predominantly from the F-region. The spectra observed around local noon are often significantly wider than the spectra observed at other times.

G4-6
1540

COMPARISON OF SPACED RECEIVER DRIFT MEASUREMENTS AT HIGH LATITUDES WITH CONVECTION PATTERNS DERIVED FROM DE-2

Sunanda Basu and Emanoel Costa
Emmanuel College
Boston MA 02115
Santimay Basu and Paul Fougere
Air Force Geophysics Laboratory
Hanscom AFB MA 01731
W.R. Coley and R.A. Heelis
University of Texas at Dallas
Richardson TX 75080

Spaced receiver scintillation measurements at Thule, Greenland and Goose Bay, Labrador conducted with quasi-stationary polar beacons at 250 MHz have been utilized to determine anisotropy and drift measurements of high latitude irregularities in the polar cap and auroral oval during some days in January and March, 1982. Simultaneous measurements of ion drift velocity from DE-2 have been used for comparison with the spaced receiver measurements. The day-to-day variability of convection velocities is highlighted and the effect that such variable drifts have on scintillation spectra and decorrelation times are discussed.

G4-7
1600

CALCULATED AND OBSERVED WINTERTIME NMAX(F2) VALUES AT THULE

D.N. Anderson, J. Buchau, E.J. Weber and H.C. Carlson, Jr.
Air Force Geophysics Laboratory
Hanscom AFB MA 01731

Extensive observations of the diurnal variation in polar cap ionospheric densities at Thule, Greenland have been made during winter months from solar cycle maximum to solar minimum periods. Experimental evidence strongly suggests that the daytime plasma densities in the ionospheric F-region originate equatorward of the dayside cusp region and are produced primarily by solar ultraviolet radiation rather than by precipitating low energy electrons. To study the process in more detail, the time-dependent ion continuity equation is solved numerically including the effects of production by solar radiation and precipitating particles, loss through charge exchange with N_2 and O_2 and transport by ambipolar diffusion, neutral wind and high latitude E x B convection drift velocity. Calculated electron density values as a function of local time at Thule are compared with recent observations during a period of declining sunspot activity. The relative contributions from solar production and precipitating particle production are discussed for various E x B plasma convection patterns.

G4-8
1620

HIGH-LATITUDE IONOSPHERIC CONVECTION PATTERNS DEDUCED FROM COMBINED INCOHERENT-SCATTER AND MAGNETIC VARIATION DATA

A.D. Richmond
High Altitude Observatory
National Center for Atmospheric Research
P.O. Box 3000
Boulder, CO 80307

Y. Kamide, Kyoto Sangyo University, Japan
O. de la Beaujardiere, SRI International, USA
J.C. Foster, MIT Haystack Observatory, USA
C. Senior, CRPE, France

By using combined information on ionospheric electric fields measured by incoherent-scatter radar and on ionospheric currents inferred from magnetic variations, maps of time-varying high-latitude ionospheric convection patterns can be produced. This talk presents the analytic technique together with examples for some active periods.

G4-9
1640

THE MORPHOLOGY OF TOTAL ELECTRON CONTENT IN THE POLAR CAP

R.C. Livingston, N.B. Walker, M.A. McCready, J.F. Vickrey
Radio Physics Laboratory
SRI International
Menlo Park, CA 94025

Total electron content (TEC) in the polar cap has been measured since late 1983 using the coherent beacon onboard the HILAT satellite. Season-to-season variations show that the overall distribution in TEC is controlled by a combination of solar production and large-scale convective processes. In the noon sector, for example, convection of plasma from the low latitude afternoon sector produces a large morning/afternoon asymmetry in TEC levels. Year-to-year comparisons of the same season show similar distribution patterns, but a large decrease in TEC level from 1983 to 1984. The change is larger than that expected from decreasing solar flux, and is discussed in terms of Sondrestrom radar data taken during the same period.

Session H-3 1355-Tues. CR2-26

WAVE INJECTION IN SPACE PLASMAS BY LIGHTNING AND BY GROUND OR SPACE BASED VLF AND HF TRANSMITTERS

Chairman: D. L. Carpenter, STAR Laboratory, Stanford University, Stanford, CA 94305

H3-1
1400

VLF WAVE-INJECTION EXPERIMENTS FROM SIPLE, ANTARCTICA

R. A. Helliwell, U. S. Inan, T. F. Bell, and D. L. Carpenter
Space, Telecommunications, and Radioscience Laboratory
Stanford University
Stanford, CA 94305

Active probing of the magnetospheric plasma through the injection of VLF waves has proved to be a useful tool for quantitative investigation of wave-particle interaction processes. Recent results from the Siple/Roberval conjugate experiments include an input power threshold for wave amplification and emission triggering, suppression of growth and generation of sidebands, and simulation of magnetospheric hiss. Observations of the injected signals on the DE-1, ISEE-1 and ISIS-2 satellites have led to the observations of sidebands generated by nonducted signals, a hybrid mode of propagation, the spectral broadening phenomenon, and a new type of triggered VLF emission. An overview of these and other recent results will be presented.

H3-2
1440

QUASI STEADY STATE SIMULATIONS OF WHISTLER-MODE WAVE GROWTH

C. R. Carlson, R. A. Helliwell, U. S. Inan
Space, Telecommunications, and Radioscience Laboratory
Stanford University
Stanford, Ca. 94305

Cyclotron resonant interactions of energetic electrons with monochromatic waves near L=4 in the magnetosphere are simulated using a test particle model. The nonlinear trajectories of a large number of test particles are computed in order to estimate the phase bunched currents and the resulting stimulated radiation. Beam-like distribution functions are considered which cover a full range of pitch angles ($0° - 90°$) and a relatively narrow range of parallel velocities (few percent) and centered at the resonant velocity. Regions of the electron distribution in velocity space are identified in terms of their contribution to the stimulated wave field.

Two types of wave growth behaviour are simulated. The first concerns waves which have grown to a saturated steady state and self-consistent steady-state profiles of the spatial currents and stimulated radiation are obtained. The second concerns waves whose growth and saturation are associated with increasing frequency and are based on a quasi-steady-state two-port feedback model. Using selected beams, the space-time evolution of the current and wave field profiles are calculated for the wave growth phase of the interaction. The simulation results are compared with experimental data in order to determine the beam characteristics which would be consistent with observations including growth rate, saturation, and wave-phase evolution. The simulations produce features similar to those observed including wave growth, saturation, and phase advance. However, while the observations reveal that wave growth is exclusively associated with an advance in phase, the simulations produce phase retardation as well as phase advance.

H3-3
1520 WHISTLER MODE ELECTRON RESONANCES IN THE TOPSIDE IONOSPHERE

T. Neubert and T. Bell
Space, Telecommunications and
Radioscience (STAR) Laboratory
Durand 331A
Stanford University
Stanford, CA 94305

Landau resonance and cyclotron resonance of whistler waves and electrons are explored for magnetoplasmas with appreciable gradients in the plasma density and magnetic field. It is shown that, in the topside ionosphere, the gradients along a magnetic field line may match in a way which enhances the interaction between the waves and electrons with certain energies and pitch angles. This matching can lead to enhanced energetic electron precipitation. The fast Trimpi effect and the influence of ground based transmitters on electrons in the magnetosphere are discussed in this context.

H3-4
1540

ANALYSIS OF GROUND TRANSMITTER SIGNALS RECEIVED ON A SATELLITE

Vikas S. Sonwalkar
Space, Telecommunications, and Radioscience Laboratory
Stanford University
Stanford, CA 94305

This research concerns the analysis and interpretation of a ground transmitter siganl received on a spacecraft in the earth's magnetosphere. We present a systematic theoretical investigation of the relation between the wave structure to be measured and the actual voltages developed across the antennae terminals on a spinning spacecraft. The formalism explicitly takes into account the constraints resulting from the linear and spin motion of the spacecraft and the known physics of the medium. It is shown that the method of analysis developed can be used (1) to deduce the wave structure present, (2) to measure the *in situ* antenna response function and (3) to measure *in situ* medium properties such as electron density. We provide the application of the formalism to find the wave normal direction of the Siple station transmitter signals observed on the ISEE-1 and DE-1 satellites. We show that the effective length of an electric dipole receiving antenna in a magnetoplasma is the same as its physical length i.e. about twice the conventional value.

H3-5 1600 PLASMA INSTABILITIES STIMULATED BY HF TRANSMITTERS IN SPACE: PAST, PRESENT AND FUTURE

Robert F. Benson and Adolfo F. Vinas,
Laboratory for Extraterrestrial Physics,
Goddard Space Flight Center, Greenbelt,
MD 20771

Diffuse incoherent signal returns are often observed on topside ionograms in addition to the coherent echoes involving both electromagnetic waves (over distances covering hundreds to thousands of kilometers below the spacecraft) and electrostatic waves (over distances covering tens to thousands of meters from the spacecraft). These diffuse signals, which at times can be the dominant features on topside ionograms, have been attributed to sounder-induced temperature anisotropies which drive the Harris instability (H. Oya, Phys. Fluids, 14, 2487, 1971; R. F. Benson, Phys. Fluids, 17, 1032, 1974; Y. Kiwamoto, J. Geophys. Res., 84, 462, 1979; Y. Kiwamoto and R. F. Benson, J. Geophys. Res., 84, 4165, 1979). These investigations were all based on the electrostatic approximation to the dispersion equation. The present paper will present calculations indicating that when the electromagnetic terms are retained in the dispersion equation the whistler-mode has a greater temporal growth-rate than the electron cyclotron harmonic waves central to these investigations. Conventional sounder operations, however, are not well suited to detect such wave growth because the receiver and the transmitter sweep together in frequency. Alouette 2 topside sounder observations indicate that the sounder-induced plasma heating is greatest under certain ambient plasma conditions and that the most dominant signal returns are present at frequencies above the ambient electron cyclotron frequency f_H (Benson, Radio Sci., 17, 1637, 1982). Thus if large whistler-mode signals ($f<f_H$) can be stimulated by sounder-induced plasma turbulence when the sounder is tuned to frequencies greater than f_H, they would not be detected. The highly flexible sounder designed for the waves in space plasmas (WISP) portion of space plasma lab, scheduled for a 1990 shuttle flight, will be ideal for such investigations.

Session B-8 0835-Weds. CR2-28
SCATTERING - II

B8-1 0840 Chairman: L. Wilson Pearson, McDonnell Douglas Research Laboratories, St. Louis, MO 63166

SCATTERING AT SKEW INCIDENCE BY AN IMPERFECT RIGHT-ANGLED WEDGE

T.B.A. Senior and J. L. Volakis
Radiation Laboratory
Dept. of Electrical Engineering and Computer Science
The University of Michigan
Ann Arbor, MI 48109

A case of particular interest in edge diffraction is an imperfectly conducting wedge of non-zero included angle illuminated by a plane wave at skew incidence, i.e., not in a plane perpendicular to the edge. A method has recently been developed based on the use of Maliuzhinets' technique (Sov. Phys. Dokl. 3, 752-755, 1959) in conjunction with a modified form of the impedance boundary conditions that makes possible the solution for a class of wedge geometries. One such geometry is a right-angled wedge with its upper face imperfectly conducting and the other perfectly conducting, and this is the problem considered.

When Maliuzhinets' technique is applied, it is found that the difference equations for the spectra appearing in the Sommerfeld integral representation for the axial field components can be decoupled by introducing subsidiary spectra. The expressions for these spectra involve three constants which must be chosen to eliminate certain poles whose contribution would otherwise violate the radiation condition. These constants are determined and their dependence on the angle of incidence and the impedance are displayed. The optics components and the edge-diffracted field are then obtained, and the nature of any surface wave contribution that may exist is also discussed. As a final step, the total field is expressed in a uniform form according to the UAT ansatz.

Computed patterns are presented to show the dependence of the diffracted and total fields on the angles of incidence and scattering. The dependence on the surface impedance, complex as well as real, is also examined.

B8-2
0900

DIFFRACTION BY A DOUBLE WEDGE IN THE PRESENCE OF A CIRCULAR CYLINDER

A. Z. Elsherbeni and M. Hamid
Antenna laboratory
Department of Electrical Engineering
University of Manitoba
Winnipeg, Canada, R3T 2N2

ABSTRACT

A simple technique for solving the problem of an E-polarized plane wave scattered by three objects consisting of two wedges with sharp edges and a circular conducting or dielectric cylinder is presented. The method is based on an extension of the authors solution for the diffraction by a double wedge (Elsherbeni and Hamid, IEEE Trans. Ant. and Propag., AP-32, No. 11 , pp. 1262-5, 1984), and is applied here to investigate the transmission coefficient through the aperture of a wide double wedge in the presence of a circular cylinder whose axis is parallel to the edges of the two wedges. An improvement in the transmission coefficient is observed in the presence of a dielectric cylinder, whereas a conducting cylinder yields a lower transmission coefficient relative to the case when the cylinder is absent.

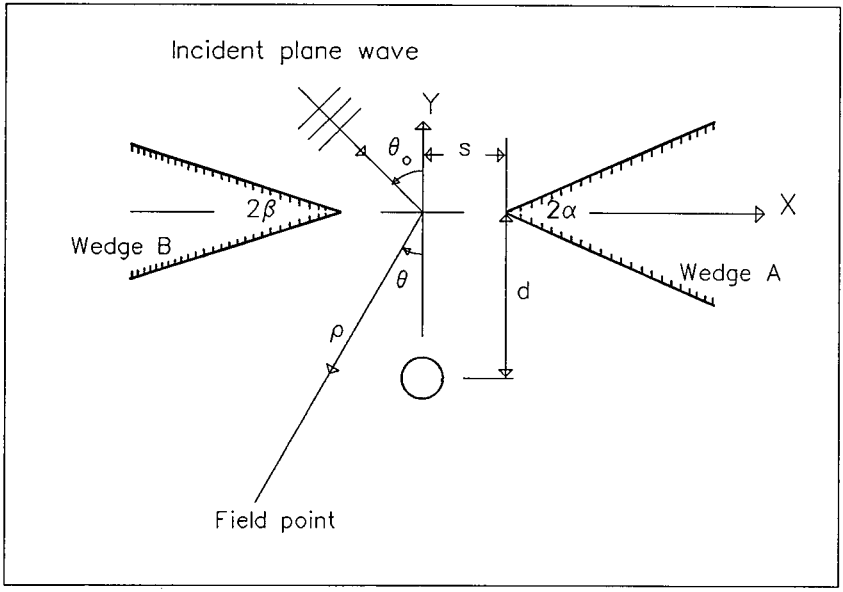

Geometry of the problem

B8-3
0920

CYLINDRICAL HARMONIC EXPANSION OF THE EDGE-GUIDED WAVE SUPPORTED BY A PERFECTLY CONDUCTING WEDGE

L. Wilson Pearson
McDonnell Douglas Research Laboratories
P. O. Box 516
St. Louis, MO 63166

Recent work (Kouyoumjian and Buyukdura, URSI EM Wave Symposium, 1984; Buyukdura, Ph.D. dissertation, Ohio State University, 1984) has computed the field of a point source radiating near edge of a perfectly conducting wedge. This work applies spherical harmonic expansion of the electric field dyadic Green's function for the wedge and identifies the asymptotic field contribution for observations points that are close to the edge but far removed from the source along the edge. The term "edge-guided wave" is associated with this asymptotic field. This term has arisen also in work by Sikta (Ph. D. dissertation, Ohio State University, 1981) and in the interpretation of measured data for a conducting disk in a paper by Senior (IEEE Trans. Antennas and Propag., AP-17, 751-756, 1969).

In the present work we explore the guidance interpretation by carrying out the same asymptotic field evaluation using a cylindrical harmonic expansion. The method of Levine and Schwinger (Comm. Pure and Appl. Math., III, 351-391, 1950) is used in the derivation of the Green's function. This method is operational, and lacks the rigor of the Hansen vector expansion used by Kouyoumjian and Buyukdura. However, their asymptotic form is recovered by the present method. The cylindrical harmonic expansion is in terms of an integration over the longitudinal wavenumber α and allows us to consider the edge-guidance aspect of this field in terms of singularities in complex α-plane.

It is shown that the singularity in the α-plane that makes the asymptotic contribution is a first order branch point at $\alpha = k$, where k is the wavenumber of the medium surrounding the wedge. The multivalued behavior at this branch point arises in the course of the separation of variables process--i.e. it arises by way of a scalar facet of the Green's function construction. It acts concomitantly with a factor $(\alpha - k)^{-1}$ that arises in the vector separation of Maxwell's equations. This latter factor, taken alone, is a pole, consistent with guided-wave interpretation. The combined effect of the branch point and this factor, however, leads to a fall-off in the field as it propagates along the edge--a behavior contradictory a guided wave interpretation.

B8-4
0940

CURRENT INDUCED ON A NARROW CONDUCTING STRIP: A COMPARISON OF AN ANALYTICAL APPROXIMATION AND A NUMERICAL SOLUTION

Anthony Q. Martin and Chalmers M. Butler
Department of Electrical and Computer Engineering
Clemson University
Clemson, SC 29634-0915

Analytical solutions are available to the approximate equations for the current induced on a narrow conducting strip illuminated by TM and TE excitation (IEEE Trans. Ant. and Propagat., Oct., 1985.). These approximate equations are valid for a strip which is narrow relative to wavelength. The purpose of this paper is to provide data which suggests the accuracy of the approximate analytical solutions by comparing them to numerical solutions of the exact equations for the strip current. Also, the far-zone scattered field due to an incident plane wave illumination, computed from analytical expressions and by numerical methods, is compared for different widths of the narrow strip. The analytical solutions are available in series form so due attention is given to the convergence properties of these series as well as of those for the far-zone field. In order to adequately account for the singular behavior of the current at the strip edges and yet not exceed a reasonable number of unknowns, the numerical solution method employs non-uniform sampling allowing the density of sampling to be greater near the edges than it is remote from them. With such a scheme high accuracy can be achieved with a modest expenditure of computer resource. From the data and the comparisons presented, one can judge the accuracy of the available analytical approximations for the strip current and the far-zone scattered field of a narrow conducting strip.

B8-5
1000 SCATTERING BY A THICK PERFECTLY CONDUCTING EDGE AND STRIP

J. L. Volakis and M. Ricoy
Radiation Laboratory
Dept. of Electrical Engineering and Computer Science
The University of Michigan
Ann Arbor, MI 48109

As an alternative to the Wiener-Hopf technique (S. W. Lee and R. Mittra, IEEE Trans. AP-16, 454-461, 1967), the angular spectrum method (P. C. Clemmow, Proc. Roy. Soc. 205A, 286-308, 1951) is employed to solve the problem of a plane wave incident on a thick perfectly conducting edge. Both polarizations are considered, and in contrast to the Wiener-Hopf technique, the method leads to a relatively simple derivation of equations for the surface current spectra. These are solved to give explicit expressions for the field diffracted by the edge as well as for the coupling, launching and reflection coefficients associated with each mode. The relative simplicity of the angular spectrum method gives hope that other geometries can be treated in the same manner.

Using models designed to isolate the edge scattering, several backscattering patterns have been measured for a thick edge and a step on a ground plane. These were found to be in good agreement with the theoretical results. In addition, calculations based on a self-consistent GTD analysis applicable to thicker edges (more than a half wavelength in thickness) are presented. The combination of the angular spectrum and GTD results then provides an efficient method for treating edges of arbitrary thickness. These same techniques are also applicable to thick strips and to steps in a ground plane.

B8-6
1020

THE VECTOR POTENTIAL INTEGRAL EQUATION APPROACH TO THE ELECTROMAGNETIC DIFFRACTION BY A PERFECTLY CONDUCTING HALF PLANE SCREEN

Alexander Pal* and L. Wilson Pearson
McDonnell Douglas Research Laboratories
P. O. Box 516
Saint Louis, Mo. 63166

Rahmat-Samii, Mittra et al. (Radio Science, 8, 869-875, 1973), and also, Wilton and Dunaway (Air Force Weapons Laboratory Interaction Note 214, 1974) applied the properties of the magnetic vector potential to the numerical solution of the thin plate EM diffraction problem. They pointed out that even though the vector potential on the plate satisfies a (two dimensional) inhomogeneous Helmholtz equation, this condition determines it only up to an unknown term which satisfies the homogeneous Helmholtz equation and is also irrotational. This term expresses the coupling of the two components of the current density $J(x,y)$ at the edge of the plate. The additional unknown term, a boundary distribution, provides the coupling between the formally decoupled integral equations for the respective components of currents.

In this paper it is demonstrated that this "vector potential integral equation" method is applicable in the theoretical analysis of some EM plate diffraction problems as well. In the case of diffraction of a plane wave by a perfectly conducting half plane, it is shown that the unknown homogeneous solution describes two spatially harmonic current waves propagating toward and away from the edge of the plate, respectively. Causality requires us to discard the current wave propagating toward the edge, allowing determination of the vector potential on the plate up to a single unknown constant. Considering that the current density vanishes on the complementary half plane, and the known relation between current density and vector potential, the problem is formulated in terms of a Wiener-Hopf problem for the x-Fourier transform of $A(x,y,0)$. The unknown constant is determined from the boundary condition that the normal component of J vanishes at the edge of the plate, easily translated into spectral variable form. The Meixner edge condition is then a simple corollary to this requirement. Solution of the Wiener-Hopf problem leads to a comprehensive form of the known classical solution (c.f. Principals of Optics, M. Born and E. Wolf (eds.), 1975) resulting in compact vector expressions for **J**, **A** and other field components. The result is applied to the discussion of grazing incidence, including the derivation of the the so-called edge-guided wave as a limiting case.

*On leave from Southern Illinois University of Edwardsville.

B8-7
1040

ELECTROMAGNETIC SCATTERING FROM A RECTANGULAR PLATE

by A.Q. Howard, Jr.
SCHLUMBERGER WELL SERVICES
HOUSTON, TEXAS 77252-2175

and J.W. Miles
RICE UNIVERSITY
HOUSTON, TEXAS 77001

A numerically efficient procedure is described to compute the scattered electromagnetic field from a thin perfectly conducting rectangular plate. The source is a magnetic dipole. The plate dimensions are required to be no more than a few wavelengths. The numerical results are for cases where both the source and observation points are on the order of a wavelength from the plate. The numerical method is based upon an E field integral equation. The integral equation is solved using the volume current method where the plate surface current is expanded in disc shaped subdomain functions. This choice enables both the integration and differentiation operations occuring in the integral equation to be performed analytically. The resulting matrix equation for the plate current amplitudes is full, complex symmetric. The matrix elements I_{nm} are seen to contain both a monopole and a quadrupole current interaction strength between the n^{th} and m^{th} surface patches. The matrix elements are Fourier Bessel numerical integrals. They are evaluated on the real axis but require a delicate numerical limiting process with respect to the plate thickness. The situation is similar to the thin wire antenna kernel function which requires that the observation point and secondary source point be separated by the wire radius.

An experimental program was conducted to confirm the theoretical predictions. A network analyzer controlled by a laboratory computer was configured to automate the amplitude and phase measurements of the RF signal. Measurements were taken at 900 through 1300 MHz in steps of 100 Mhz. Several rectangular copper plates were used with widths between 10 and 45 cm, heights between 1 and 12 cm and thickness on the order of .1 mm.

B8-8 1100 SCATTERING FROM A SLIT CYLINDER ENCLOSING AN OFF-SET IMPEDANCE SURFACE*

Richard W. Ziolkowski and Ronald F. Schmucker
Lawrence Livermore National Laboratory
Electronics Engineering Department
P.O. Box 5504, L-156
Livermore, California 94550

Canonical electromagnetic scattering problems are important from several points of view. They provide basic understanding of scattering processes which can be extrapolated to more general geometries. Moreover, they provide fundamental benchmarks for general purpose scattering codes.

The generalized dual series solution to the coupling of an H-polarized plane wave to a perfectly conducting infinite cylinder with an infinite axial slot enclosing a concentric impedance cylinder was given by Ziolkowski, Johnson and Casey [Radio Sci., vol. 19 (b), p. 1425-1431 (1984)]. This solution is extended to the case of an off-set interior impedance cylinder in this paper. With this solution one can study the effect of the location of an interior object on the electromagnetic coupling.

Results will be presented for the case where the interior object is a perfectly conducting wire. Frequency scans of the bistatic cross-section will be given for various locations and radii of the interior wire. These results are dominated by anti-resonance features whose characteristics reflect the variations in those parameters. The behavior of the currents on the slit cylinder as the frequency and the interior wire location and radius are varied will also be given.

* This work was performed by the Lawrence Livermore National Laboratory under the auspices of the U.S. Department of Energy under Contract W-7405-ENG-48.

B8-9 1120 SCATTERING FROM AN OPEN SPHERICAL SHELL HAVING A CIRCULAR APERTURE AND ENCLOSING A METALLIC OR DIELECTRIC SPHERE

Richard W. Ziolkowski and Diane Peplinski
Lawrence Livermore National Laboratory
Electronics Engineering Department
P.O. Box 5504, L-156
Livermore, California 94550

Louis F. Libelo
Harry Diamond Laboratories
2800 Power Mill Road
Adelphi, Maryland 20783

Canonical electromagnetic scattering problems are important from several points of view. They provide basic understanding of scattering processes which can be extrapolated to more general geometries. Moreover, they provide fundamental benchmarks for general purpose scattering codes. However, there are few fully three-dimensional scattering problems for which solutions have been found, especially when the scattering body includes an aperture.

The solution to the scattering of an arbitrary plane wave from a perfectly conducting spherical shell having a circular aperture was obtained recently by Ziolkowski and Johnson [submitted to J. Math. Phys., July, 1985]. It is based upon an essentially analytic solution of the coupled dual series equations for the TE and TM modal coefficients arising from the enforcement of the electromagnetic boundary conditions over the aperture and the shell. In this paper that solution is extended to the case where the open spherical shell encloses a concentric, perfectly conducting metallic sphere or a concentric homogeneous, lossless dielectric sphere.

Several results will be given for the case of normal incidence. These include the currents on the inner and outer metallic spheres, the energy captured by the open shell/interior body cavity, and various cross-sections. Frequency scans of these quantities demonstrate that they are dominated by anti-resonance features which depend on the characteristics of the interior sphere. It will be shown how these resonance features change as the radius and the dielectric constant of the interior sphere change. The effect these anti-resonance features have on the time domain scattered fields will also be discussed.

B8-10
1140

NON-SPECULAR SCATTERING FROM COUPLED THIN, FINITE WIRES

Terry L. Krohn and Louis Medgyesi-Mitschang
McDonnell Douglas Corporation
P.O.Box 516
St. Louis, Missouri 63166

Scattering from infinite sheets of perfectly and imperfectly conducting thin wires, arranged in parallel or grid orientation has been extensively investigated. (J.R.Wait, IEEE Trans. AP-25, 409-412, 1977; M.I.Kontorovich, Radio Eng. Electron. Phys.(USSR), 8, 1446-1454, 1963) These analyses yielded results primarily for specular reflection and transmission. For imperfectly conducting wires, the Schelkunoff approximation can be used. Arbitrary oblique illumination of a single infinite dielectric rod was treated by Wait. (J.R.Wait, Can.J.Phys., 33, 189-195, 1955).

In the present investigation, the effect of finiteness of the system of wires on the non-specular scattering is examined, as is the conductivity, particularly with respect to the traveling wave. An entire domain Galerkin expansion is used, allowing systems of electrically large scatterers to be treated with the Method of Moments. Inherent in this approach and solution is the flexibility of scatterer spacing, orientation, length, radius, and material properties. The formulation is illustrated for a number of finite planar configurations composed of wires spanning irregular boundaries. The computed cross sections are compared with experimental measurements for arbitrary illumination. Modal convergence of the Method of Moments solution is examined. Effect of the number of modes and the condition number of the resulting system matrix is given. The accuracy of the Schelkunoff approximation for imperfectly conducting wires is examined. Generalizations of this formulation to infinite strips of finite wires are also explicated.

Session C-3 0840-Weds. CR1-40

DIGITAL SIGNAL PROCESSING AND VLSI ARCHITECTURES

Chairman: A. J. Viterbi, QUALCOMM, Inc., San Diego, CA 92121

C3-1
0920

DIGITAL SIGNAL PROCESSING AND VLSI ARCHITECTURES ego,

Richard A. Roberts
Department of Electrical and Computer Engineering
University of Colorado
Campus Box 425
Boulder, CO 80309

Structures or algorithms for digital filters should be chosen based on the computational resource available for computing the input/output characteristic, e.g., the transfer function. In the case of VLSI, filter structures are desired which optimize criteria such as data throughput, complexity of the chip, finite-length register effects, and geometrical properties of the layout. These properties include such factors as the regularity of the design, the modularity of the design, the local conectivity of modules, and the placement of ground and power busses. This paper discusses a class of structures which fulfills many of these criteria. We shall also detail a generalized state variable description used in the description of this new class of filters.

C3-2
1040

A PARALLEL PROCESSING SPEECH RECOGNITION ARCHITECTURE ON THE BBN BUTTERFLY MULTIPROCESSOR:

Michael A. Krasner, Bolt Beranek & Newman Inc., Cambridge, MA 02238

Future speech recognition systems will require high accuracy performance for continuous speech input with a large vocabulary and natural language grammar. The computational requirements for the real-time implementation of such recognition systems have been estimated to exceed one billion instructions per second. These requirements necessitate the development of advanced multiprocessor architectures and of parallel processing techniques to utilize the capabilities of such multiprocessor systems.

The BBN Butterfly Multiprocessor is a shared-memory system composed of microprocessor-based processor nodes connected by a high bandwidth switch. The Butterfly has a real-time operating system and is programmed in a high-level language (C). Nearly linear performance improvements over a range of 1 to 256 processors have been achieved on a number of benchmark programs.

To explore techniques for real-time speech recognition utilizing highly parallel architectures, the BBN speech recognition system is being implemented on the Butterfly Multiprocessor. The focus of the implementation is the effective utilization of a large number of processors, with techniques that are extensible in principle to a much larger number of processors.

C3-3
1120 PROCESSOR ARCHITECTURES FOR NEAREST-NEIGHBOR SEARCHING IN VOICE COMPRESSION: Allen Gersho and Grant Davidson, Department of Electrical and Computer Engineering, University of California, Santa Barbara, CA 93106

Nearest-neighbor searching, or pattern matching, is a procedure for extracting the members of a set of pattern vectors which most closely approximates a given input vector. A distortion or dissimilarity measure serves as a basis for comparing a pattern vector with the input vector. The nearest-neighbor search produces an index identifying the pattern vector which minimizes this distortion metric.

Nearest-neighbor searching is the fundamental operation in Vector Quantization (VQ), a block source compression technique which computer simulations have shown is very powerful but also computationally demanding. The intensive but crucial search operation is particularly problematic when it must be performed in real-time.

Specialized processor architectures can greatly increase the capability of pattern matching systems. The architectures of some of today's programmable DSP chips, although fundamentally limited by their sequential nature of instruction execution, are suitable in certain applications. We can achieve even greater capability by designing architectures which exploit the repetitive and non-conditional nature of pattern matching calculations. Parallel and pipelined architectures are particularly well-suited for this task. Furthermore, systolic architectures which achieve orders of magnitude reduction in search time (compared to sequential architectures) can readily be designed.

In this presentation, we will first discuss the nearest-neighbor problem as it relates to voice compression with VQ. Next, we will describe several architectures which are appropriate for these applications and will present the search speed vs. hardware complexity tradeoffs inherent in each. Finally, we will describe specific examples of special-purpose VLSI architectures which we have designed, fabricated, and tested.

Session G-5 0835-Weds. CR0-30

INCOHERENT SCATTER

Chairman: W. L. Oliver, Northeast Radio Observatory Corp., Haystack Observatory, Westford, MA 01886

G5-1
0840 SOLAR CYCLE VARIABILITY OF EXOSPHERIC TEMPERATURE AT MILLSTONE HILL

M. E. Hagan
Department of Physics, Boston College, Chestnut Hill, MA 02167
W. L. Oliver
Massachusetts Institute of Technology, Haystack Observatory, Westford, MA 01886

Neutral exospheric temperatures from incoherent scatter measurements made between 1970 and 1980 at Millstone Hill (42° N) are examined for solar cycle variations during geomagnetically undisturbed times. Analysis reveals unexpectedly large diurnal temperature amplitudes during solar cycle 21 at moderate to high levels of solar activity ($150 \leq \bar{F}10.7 \leq 230$) pointing to the increased role of ion drag in the adiabatic compression of the thermosphere. A heuristic model assuming momentum balance between the pressure gradient and ion drag, and thermal balance between EUV heating, its vertical conduction and adiabatic compression serves to illustrate modulation of adiabatic cooling efficiency by enhanced ion drag effect. This effect is further illustrated in the interpretation of full-scale simulations of the thermosphere.

G5-2 0900 MAGNETIC STORM RESPONSE OF THE THERMOSPHERE AS OBSERVED FROM MILLSTONE HILL

J. M. Forbes
Department of Electrical, Computer, and Systems Engineering, Boston University, Boston, MA 02215
W. L. Oliver
Massachusetts Institute of Technology, Haystack Observatory, Westford, MA 01886

Neutral exospheric temperatures from incoherent scatter measurements at Millstone Hill during two geomagnetic storm events are analyzed. The two intervals, 17-24 September, 1984 (The "Equinox Transition Study (ETS)") and 21-22 March, 1979 (including the "CDAW-6 Interval"), are characterized by well-defined storm events preceded by periods of geomagnetic quiet. The quiet-time variations are extrapolated into the disturbed periods to isolate the storm effects, which are in excess of 150K for these events. The possible effects of Joule heating on the results are evaluated. Comparisons are made with predictions of the MSIS-83 empirical model. In addition, using the steerable capability of the Millstone Hill Radar, latitude variations of the amplitude and time delay of the response are investigated.

G5-3
0920

MAPPING THE F REGION ION VELOCITY FIELD AT ARECIBO

R.G. Burnside, M.P. Sulzer and
C.A. Tepley, Arecibo Observatory,
P.O. Box 995, Arecibo, Puerto Rico 00613

By using a multiple-frequency incoherent scatter technique, the precision of ion velocity measurements at Arecibo has been improved by almost a factor of three. A method of data analysis has been developed that allows velocity gradients in the plane of the magnetic meridian to be determined, if it is assumed that magnetic field lines are equipotential. A detailed comparison of F layer behavior has been made for a magnetically quiet and an active night in the summer of 1985. Horizontal advection of plasma is largely responsible for the maintenance of high electron densities on the disturbed night.

G5-4
0940 THE DIURNAL VARIATION OF MERIDIONAL WINDS IN THE THERMOSPHERE

K. L. Miller and D. G. Torr
Center for Atmospheric and Space Sciences,
Utah State University, Logan, Utah 84322-4145

We present the results of a method for deriving meridional wind speeds from measurements of the height of the F2 layer maximum electron density (h_{max}). This method uses an ionospheric model to determine the relationship between neutral wind and h_{max} at specified local time, location and solar conditions. The meridional wind is derived from a comparison of the modeled layer height with the measured height. Our results show good agreement when compared with coordinated Fabry-Perot interferometer and incoherent scatter radar experiments. This method is not limited to clear nighttime conditions, and can be used effectively to study the diurnal behavior of the winds in the F region. We present examples of diurnal meridional winds in the thermosphere above Millstone Hill as derived from measured electron density profiles.

G5-5
1000 GRAVITY WAVE OBSERVATION AT MILLSTONE HILL DURING THE WAGS CAMPAIGN: W. L. Oliver, Northeast Radio Observatory Corp., Haystack Observatory, Westford, MA 01886 et al

Session G-6 1020-Weds. CR0-30

GRAVITY WAVES AND TRAVELING DISTURBANCES IN THE IONOSPHERE

Chairman: R. D. Hunsucker, Geophysical Institute, University of Alaska, Fairbanks, AK 99701

G6-1
1020

THE WORLDWIDE ACOUSTIC GRAVITY WAVE STUDY (WAGS) - A SUMMARY

Paul E. Argo
Los Alamos National Laboratory
Earth and Space Sciences Division
Los Alamos, New Mexico 87545

The month of October 1985 has been selected as a period in which to conduct a worldwide study of acoustic gravity wave generation and propagation. The three days of October 15-18 were chosen to be an URSI sponsored three day World Day run, during which the Incoherent Scatter Radars will be operated as part of the larger study. There will be approximately nine countries, 24 organizations and one hundred researchers participating.

The campaign will have focused primarily on large scale waves, with wavelengths of thousands of kilometers and periods of one or more hours. Early estimates of the statistics of observations will be presented. Medium scale waves, which have a much smaller spatial coherence distance, will have been studied by sets of "clumped" experiments in the western and eastern USA, India, China, and Australia.

This paper will summarize the WAGS campaign, and give any preliminary results that are available at meeting time.

G6-2
1040

ACOUSTIC-GRAVITY WAVES IN THE THERMOSPHERE

A.D. Richmond
High Altitude Observatory
National Center for Atmospheric Research
P.O. Box 3000
Boulder, CO 80307

Acoustic-gravity waves are a prominent form of atmospheric motion in the thermosphere. Large amplitudes can be attained because of upward wave growth with decreasing atmospheric density, and because of strong sources existing at auroral latitudes. The waves can affect the thermosphere and ionosphere by producing fluctuations in density, temperature, and motions; by transporting momentum and energy; and by generating turbulence. They can also be very useful as diagnostics of wave sources and of background thermospheric temperatures and winds. This talk reviews some characteristics of thermospheric acoustic-gravity wave propagation, with particular reference to information the waves can give us about auroral sources.

G6-3
1100

OBSERVATIONS OF TID'S AT L ≃ 4.5 WITH A CLOSED-SPACED IONOSONDE TRIANGULATION NETWORK IN WESTERN QUEBEC

M.G. Morgan, Radiophysics Laboratory, Thayer School of Engineering
Dartmouth College
Hanover, NH 03755

A close-spaced triangulation network (approximately 50 km on a side) of rapid-run ionosondes was installed at Chibougamau, Quebec (at L ≃ 4.5), last winter and spring. By the time the stations were brought into satisfactory operation, summertime conditions had set in (increased absorption, low values of foF2, and the presence of F1) greatly impairing our technique for studying TID's (see Morgan et al., Radio Sci., 13, 729, 1978). The network resumed operation in early October, when this abstract was due, and results obtained since then will be presented. The network is augmented by an additional identical ionosonde 500 km to the north-northwest (at L = 6). It is also augmented by fan-beam riometers 130 km and 260 km to the south-southeast in the anticipated source region (see Morgan, Radio Sci., 18, 1066, 1983). The normal to the fan beams is north-northwest (or south-southeast).

G6-4
1120 SIMULTANEOUS OBSERVATIONS OF TID/AGW PHENOMENA AT SONDRESTROM, GREENLAND AND AT MIDDLE LATITUDES DURING THE "WAGS" CAMPAIGN

Robert D. Hunsucker and Donald D. Rice
Geophysical Institute, University of Alaska-Fairbanks
Fairbanks, AK 99775-0800

During the Worldwide Atmospheric Gravity wave Study (WAGS) in October 1985, the incoherent scatter radar (ISR) at Sondrestrom, Greenland (invariant latitude $\simeq 75^{\circ}$) was operated in a multiposition mode to obtain plasma densities, electric fields, temperatures and plasma drift velocities in the F-region. These observations of ionospheric dynamics and their relation to selected midlatitude ionospheric observations, including the Millstone Hill and Arecibo ISR's, will be discussed.

G6-5
1140 OBSERVATIONS OF GRAVITY WAVES IN THE THERMOSPHERE USING INCOHERENT SCATTER RADAR

D. R. Sheen and C. H. Liu
Department of Electrical and Computer Engineering, University of Illinois, Urbana-Champaign, IL 61801

In this paper the propagation of gravity waves in the ionosphere will be discussed. Theoretical aspects will be reviewed with the discussions of how parameters of individual waves and the spectrum of waves can be obtained from incoherent scatter radar data. The theory will be used to interpret data obtained with the incoherent scatter radar facility operated by SRI in Sondrestrom, Greenland. This radar offers a unique opportunity to observe gravity waves near the auroral source. It is important to examine the background gravity wave spectrum near the source in order to help determine how the waves are generated as well as how they propagate and dissipate energy. Data for ion velocity along the magnetic field line, gathered at Sondrestrom, was analyzed to yield the gravity wave spectrum as well as special individual wave events. These experimental results will be presented and interpreted.

G6-6 1200 ELECTRON DENSITY PROFILES AND F-REGION VARIABILITY

Adolf K. Paul
Naval Ocean Systems Center
Ocean and Atmospheric Sciences Division
Code 544
San Diego, CA 92152-5000

Computation of electron density profiles from ionograms assumes that the ionosphere is horizontally stratified and that the maximum of a layer has a parabolic shape. Ionograms recorded with high temporal resolution (six ionograms per hour or more) show that the F-region in all its parameters is frequently very variable with periodicities of ten minutes or longer. If angle of arrivals are recorded at the same time, deviations from vertical propagation are often observed changing in direction and magnitude with frequency. These observations indicate deviations of the F-layer from horizontal stratification and deformation of the layer shape which can cause relatively large errors of the extrapolated peak parameters, e.g. height of maximum, thickness parameter and also critical frequency. In simple cases, error estimates can be obtained by ray tracing model studies, while in general the quality of electron density profiles has to be judged by the degree of the F-region variability and the angle of arrival measurements.

Session H-4 0835-Weds. CR2-26
WAVE INJECTION BY PARTICLE INJECTION - I
Chairman: W. J. Raitt, Center for Atmospheric and Space Sciences, Utah State University, Logan, UT 84322

H4-1
0840

PROGRESS IN UNDERSTANDING ELF WAVE PRODUCTION BY AN ELECTRON BEAM IN THE IONOSPHERE BY ANALYSIS OF ASSOCIATED ELECTRIC FIELDS AND THERMAL ION DRIFTS

K. N. Erickson, Y. Abe, and J. R. Winckler
School of Physics and Astronomy
University of Minnesota
Minneapolis, MN 55455

The spinning Plasma Diagnostic Package (PDP), which separated from the ECHO 6 accelerator payload, surveyed the hot plasma, the vector electric wave fields and the thermal ion spectra in the region out to 110m perpendicular from the field lines on which the electron beams were injected. The hot plasma was established in a time of the order of a msec following beam turn-on out to the largest distance observed. We have found that the electric wave fields for the same beam energy and current show dramatically different wave production characteristics that depend on the pitch angle of the injected beam:

1. With beam injections transverse to B, the hot plasma appears to distances of 60m transverse and the quasi-DC associated electric fields are directed radially inward toward the axis of this column of hot plasma and are only detected when the PDP is in the hot plasma region. These fields are observed to decay with a time constant of about 10msec following gun turn-off showing that they are associated with the radial structure of the hot plasma region and not with the vehicle or beam potentials. By a study of the ram direction of ionospheric thermal ions using a low energy ion spectrometer rotating its view direction with the PDP, we have established that the normal ion ram associated with the ionospheric $\vec{E} + \vec{V}\times\vec{B}$ electric field changes such that the ions circulate around the hot plasma region in the drift direction corresponding to the radial inward electric field produced by the injection. When this occurs, low frequency waves of approximately 50 Hz in the range of the oxygen ion cyclotron resonance are observed in the electric field. These regular oscillations are not observed outside the central hot plasma region. It seems highly probable that the low frequency ion waves are of electrostatic nature and are produced by a drift instability in the circulating plasma surrounding the system.

2. In contrast, when the beam is injected upwards parallel to B, the equilibrium hot plasma region does not extend to the region surveyed by the PDP and the associated quasi-DC electric fields are very small. Nevertheless, a spectrum of waves is excited extending from 200 Hz up to the Nyquist limit of the system at 1250 Hz. The proton gyro resonance near 800 Hz is consistently excited and observed under these circumstances. If the plasma has been heated by a transverse injection, the proton resonance appears only when the plasma has cooled. In contrast to the drift mechanism responsible for the low frequency waves, the proton and lower hybrid range frequencies seem produced more directly by the instabilities associated with the parallel beam plasma interaction.

3. The most powerful phenomena observed are transients occurring across the wave spectrum with beam turn-on in which large pulses of electric field, hot plasma production and photometric luminosity are observed out to the largest distances surveyed.

H4-2
0900

VLF WAVE STIMULATION BY ELECTRON INJECTION: RESULTS FROM STS-3

E.G.D. Reeves, A.C. Fraser-Smith,
T. Neubert, and P.M. Banks
STAR Laboratory
Durand 202
Stanford University
Stanford, CA 94305

Analysis of data from Space Shuttle flight STS-3 of March 22 to 30 of 1982 has revealed many interesting results. In this paper we present the findings from the VLF (radio frequency) beam-plasma experiment in which and electron beam from the Fast Pulsed Electron Generator (FPEG) was pulsed at a frequency of several kilohertz and the plasma response was measured with the electric and magnetic antennae on the Plasma Diagnostics Package (PDP).

Harmonics of the fundamental frequency were detected and were determined to be electromagnetic. The spectral structure of the waveform was found to vary considerably from one firing to another.

In addition, 'satellite lines' were frequently seen around the primary spectral lines. These lines appear in a variety of ways including one slightly higher frequency, higher and lower frequency, and complex multi-banded structures. They appear to be electromagnetic and are seen even when the PDP is far from the beam column on the Remote Manipulator arm.

The same instruments were flown again on Spacelab-2 in July 1985. Results of this flight will be compared to results and predictions from the earlier mission.

H4-3
0920

LOW FREQUENCY ELECTROMAGNETIC FIELD PHENOMENA ASSOCIATED WITH PULSED ELECTRON BEAMS ON STS-3

A.C. Fraser-Smith, P.M. Banks, T. Neubert,
K.J. Harker, and E.G.D. Reeves
STAR Laboratory, Stanford University
Stanford, CA 94305
D.A. Gurnett, W.S. Kurth, G.B. Murphy, and
J.S. Pickett
Department of Physics and Astronomy
The University of Iowa
Iowa City, Iowa 52242
S.D. Shawhan
NASA Headquarters
Washington, D.C. 20546

An electron beam generator was flown on a Space Shuttle orbiter for the first time during the March 1982 flight of the Columbia, or STS-3. A large number of active electron beam experiments were conducted during the flight, which was notable for its particularly complete instrumentation for plasma and electromagnetic field diagnostic measurements. In this presentation we discuss some of the results of experiments in which the electron beam (beam energy 1 keV; beam current 100 mA) was pulsed at frequencies in the sub-LF range, i.e., at frequencies less than 30 kHz.

During many of the experiments the measurements made by the electric and magnetic field sensors located on the Plasma Diagnostics Package (PDP) near the electron beam generator showed little evidence for the occurrence of beam/plasma interactions. However, there were a number of occasions when anomalous electric and magnetic field phenomena where observed, suggesting that such interactions could occur when the conditions were favorable. These phenomena included the generation of noise bands, extra harmonics, and a variety of side frequencies.

We have found that the harmonic structure of the electromagnetic fields produced during sub-LF modulation of the electron beam appears to be a particularly sensitive indicator of these anomalous effects. The harmonics, in the absence of interactions, have a particularly well-defined and predictable structure covering a broad range of frequencies, and peculiarities in the fields show up comparatively conspicuously against such a background. Deviations from the expected harmonic structure can vary from strong changes, such as those listed above, to small changes in the relative amplitudes of the harmonics. It is often interesting to attempt to reconstruct the shape of the electron beam pulses from the field measurements, and such reconstructions may ultimately provide useful diagnostic information about the beam.

H4-4
0940

WAVE GENERATION IN SEPAC PARTICLE BEAM INJECTION:
T. Obayashi, N. Kawashima, K. Kuriki, S. Sasaki, and M. Yanagisawa, The Institute of Space and Astronautical Science; W. T. Roberts and D. L. Reasoner, NASA Marshall Space Flight Center; W. W. L. Taylor, TRW Space and Technology Group; P. R. Williamson and P. M. Banks, Stanford University; and J. L. Burch, Southwest Research Institute.

Various kinds of VLF and HF wave emissions were observed when an electron beam, plasma beam, and gas plume were injected in SEPAC Spacelab-1 experiment in 1983. Electron beams up to 5 kV 300 mA, 10^{19} pairs of electron and ion, and 10^{23} nitrogen molecules were repeatedly injected from the orbiter at the altitude of 250 km. Three types of VLF spectrum depending on the orbiter charging potential have been identified in the electron beam experiments. A broadband emission around lower hybrid frequency was detected at and after the plasma injection. At the joint injection of electron and plasma beams, a suppression of VLF waves and an enhancement of broadband HF emission below electron cyclotron frequency were detected. During the nitrogen gas injection, a broadband VLF emission was observed, which strongly depended on the flight configuration of the orbiter with respect to the velocity vector.

H4-5
1020

WAVE EMISSIONS FROM THE SL-2 ELECTRON BEAM: SIMILARITIES TO THE AURORA

D. A. Gurnett, W. S. Kurth, J. T. Steinberg
Dept. of Physics and Astronomy
The University of Iowa
Iowa City, IA 52242

T. Neubert, R. Bush and P. Banks
Dept. of Electrical Engineering
Space, Telecommunications and Radioscience Laboratory
Stanford University
Stanford, CA 94305

During the Spacelab 2 mission the Plasma Diagnostics Package (PDP) performed a fly-around of the Shuttle at a distance of up to 300 meters while an electron beam was being ejected from the Shuttle. At several points during the fly-around the PDP crossed through the magnetic flux tube connecting the PDP and the Shuttle. This paper discussed one particular flux tube crossing which occurred while the electron gun was being operated in a steady (DC) mode. During this crossing the plasma wave instrument on the PDP detected a radio emission spectrum remarkably similar to the radio emission spectrum from the natural aurora, as detected for example by the Dynamics Explorer 1 spacecraft. The similarities include: a funnel-shaped "auroral hiss" emission, narrowband electron cyclotron waves near the electron cyclotron frequency, a broadband of electrostatic noise at frequencies below a few kHz, and a strong static electric field.

The funnel-shaped emission has been analyzed in detail and is believed to be due to short wavelength whistler-mode waves generated by the beam. The shape of the funnel is caused by the frequency dependent propagation of whistler mode waves near the resonance cone, with the higher frequencies propagating at a larger angle to the magnetic field. The observations show that the radiation is produced by a Landau, $\omega/k_{\parallel} = v_b$, interaction, since both the waves and the beam are propagating in the same direction.

H4-6
1040

OBSERVATIONS OF WAVE STIMULATION BY PULSED ELECTRON BEAM EXPERIMENTS ON SPACELAB-2

R.I. Bush, P.M. Banks, T. Neubert, K.J. Harker
Space, Telecommunications,
and Radioscience Laboratory,
Stanford University
Stanford, CA 94305
W.J. Raitt
Center for Atmospheric and Space Sciences
Utah State University, Logan, UT 84322
D.A. Gurnett, W.S. Kurth
Dept. of Physics and Astronomy
University of Iowa, Iowa City, IA 52242

Important, new observations of plasma waves stimulated by a pulsed electron beam were made in July, 1985 during the flight of Spacelab-2. The experiments were part of a cooperative activity between the Vehicle Charging and Potential (VCAP) experiment from Stanford University and Utah State University and the Plasma Diagnostic Package (PDP) experiment from the University of Iowa. During a six hour period the Space Shuttle Orbiter moved in a roughly circular orbit around the PDP at distances varying between 200 and 300 meters. An important aspect of the designed trajectory targeted the Orbiter to intersect the magnetic field line passing through the PDP twice per orbit. At selected times, the VCAP electron generator on the Orbter emitted a 1 keV electron beam pulsed at frequencies between 10 Hz and 20 kHz in an attempt to stimulate plasma waves. The observations to be reported on were made by plasma wave receivers on the PDP. During one of the magnetic field conjunctions between the Orbiter and the PDP, strong signals were measured in both the electric and magnetic field antennas while the electron beam was pulsing at 1.2 kHz. The strength of the emissions dropped rapidly as the PDP separated from the core of the electron beam but were observed out to separation distances of about 60 meters.

H4-7
1100

VELOCITY DISTRIBUTIONS OF PLASMAS ASSOCIATED WITH ELECTRON BEAM INJECTIONS DURING THE SL-2 MISSION

L. A. Frank and W. R. Paterson
Department of Physics and Astronomy
The University of Iowa
Iowa City, IA 52242

P. M. Banks and R. I. Bush
Space, Telecommunications and Radioscience Laboratory
Stanford University
Stanford, CA 94305

W. J. Raitt
Center for Atmospheric and Space Sciences
Utah State University
Logan, UT 84322

A quadrispherical LEPEDEA is employed on the Plasma Diagnostic Package (PDP) to measure the three-dimensional velocity distributions of ions and electrons within the energy-per-unit charge range 2 V to 40 kV. The magnetic flux tubes that were carrying the electron beam injected from the shuttle were approached twice by the PDP spacecraft. The direct signature of electron beam injection at distances of several hundred meters from the shuttle is observed at distances from the flux tube considerably larger than the gyroradius for the injected electrons. In addition the electron velocity distribution is no longer monoenergetic at these positions and ion heating is observed at distances of closest approach to the magnetic flux tube.

A search is currently underway in order to attempt identification of hot ion velocity distributions associated with ion pick-up via photoionization and charge exchange of neutral molecules, in particular water molecules released from the shuttle. These ions are believed to be associated with the broadband electrostatic emissions that are detected with the plasma wave instrumentation on the PDP spacecraft. The preliminary results of this survey will be reported.

Session J-4 0835-Weds. CR2-6

PROPAGATION EFFECTS IN RADIO ASTRONOMY - I: TROPOSPHERE AND IONOSPHERE

Chairman: William J. Welch, Radio Astronomy Laboratory, University of California, Berkeley, CA 94720

J4-1
0840

NEW WATER VAPOR RADIOMETERS FOR TROPOSHERIC PATH DELAY MEASUREMENT

M. A. Janssen - 183-301
Jet Propulsion Laboratory
4800 Oak Grove Drive
Pasadena, CA 91109

T. A. Clark
G. M. Lundquist
Goddard Space Flight Center
Greenbelt, MD 20771

The unpredictable component of path delay due to tropospheric water vapor is known to be a limiting source of error in geodetic baseline measurements using very-long-baseline interferometry (VLBI) or Global Positioning System (GPS) techniques. In 1983 the NASA Crustal Dynamics Program began a project to develop water vapor radiometers (WVR's) to provide wet path delay corrections, with the goal of providing operational systems sufficient to meet their needs for the foreseeable future. Several theoretical analyses using realistic instrumental error models have shown that path delay corrections with errors less than 0.5 cm in the vertical are achievable under a wide variety of weather and climatic conditions. Results are presented from two prototype WVR models which have been tested in the field since November 1984, and March 1985, respectively, and demonstrate that this level of error may indeed be reached with a practical system.

J4-2
0900

THE ACCURACY OF WATER-VAPOR RADIOMETERS

J.L. Davis, T.A. Herring, I.I. Shapiro
Harvard-Smithsonian Center for Astrophysics
60 Garden Street
Cambridge, MA 02138

The use of water-vapor radiometers (WVR's) to monitor the microwave emission of tropospheric water vapor, and to infer from these measurements the line-of-sight wet path delay at radio frequencies, has for some time been considered the most promising alternative to relying on models of this delay based on surface meteorology. Such models fail to describe fully the spatial and temporal variability of tropospheric water vapor, and the errors in these models are thought to be the dominating error source in the estimates of the vertical coordinate of site position from very-long-baseline interferometry (VLBI) data, introducing as much as 6 cm scatter into these estimates.

We have used VLBI data to assess the accuracy of WVR's. The process involves comparing estimates of the wet path delay inferred from WVR data to estimates of the wet path delay obtained from a Kalman filter analysis of VLBI data. The estimates of the wet delay from the Kalman filter are independent from the corresponding estimates from the WVR data. Several of these comparisons will be presented. We will also discuss the uses of the WVR and the Kalman filter in analyzing VLBI data.

J4-3
0920

CORRELATED MEASUREMENTS OF ATMOSPHERIC FLUCTUATIONS AT 10, 33 AND 90 GHZ

S. Levin, G. De Amici*, G. Smoot, and C. Witebsky
Lawrence Berkeley Laboratory and Space Sciences Laboratory
University of California Berkeley, CA 94720

Between summer 1983 and summer 1984 a set of measurements have been made of atmospheric stability and fluctuations at microwave frequencies (10, 31.5, 33 and 90 GHz). The radiometers had sensitivity of 46, 100, 84 and 120 mK/$\sqrt{\text{Hz}}$. Data were collected over different kinds of weather and for periods of (typically) 1024 seconds. The data suggest a strong correlation of the fluctuations, which can be described by a simple parameterization. The results are in good agreement with the hypothesis that fluctuations in water vapor content dominate the atmospheric fluctuations. The data also suggest that the Kolmogorov turbulence theory can be used to predict the temporal and spatial spectra of atmospheric scintillation and emission variation.

*On leave from Istituto di Radioastronomia/CNR, Bologna, Italy

J4-4
0940

RADIO ASTRONOMICAL SEEING

R.A. Sramek
National Radio Astronomy Observatory
P. O. Box O
Socorro, NM 87801

Measurements have been made of the atmospheric phase structure function at the National Radio Astronomy Observatory's Very Large Array (VLA) in New Mexico. Weekly measurements have been made between December 1983 and December 1985 at 6 cm and 2 cm wavelengths. Statistics of phase stability and thus radio astronomical seeing are compared with surface meteorological parameters, time of day, season of year, etc.

J4-5 1020 PRELIMINARY RESULTS OF APPLYING ARIMA MODELING AND KALMAN FILTERING TO VLA IMAGE PROCESSING

Yi Zheng and John P. Basart
Department of Electrical Engineerging
and Computer Engineering
Iowa State University
Ames, IA 50011

Atmospherically induced phase variations can cause severe problems in producing quality images in radio astronomy. The problem is particularly severe for long baselines and high observing frequencies. We are modeling the phase variations by the Box-Jenkins method and then using these models in Kalman filters to reduce the phase variation. A bank of filters is run for each time series of phase for each pair of antennas.

The phase variations caused by the atmosphere are highly correlated in time. Because of this correlation, the variations can be represented by ARIMA processes. The model parameters can be placed in a state variable format as required for the Kalman filter algorithm. Four state variables were used to describe each filter and 351 filters were used to process the data from 27 antennas.

Three types of tests have been completed. In the first type of test, noise was added to a single time series of VLA data. The process was modeled and filtered. In the second type of test, noise was added to actual data (with a high signal-to-noise ratio) from 27 VLA antennas. The usual mapping, cleaning, and self-calibration were completed for the original data, the artificially corrupted data, and the filtered output of the corrupted data. The latter map was essentially the same as the first one indicating that the Kalman filter effectively removed all of the added noise. The third type of test was to model and filter data from a point source which had a very large amount of atmospheric noise. Two thirds of the 351 correlator outputs had an rms noise above 24°. The worst case was 43°. The usual methods of mapping, cleaning, and self-calibration were completed on the filtered and nonfiltered data. By Kalman filtering, the dynamic range increased from 362 to 657.

J4-6
1040

IONOSPHERIC REFRACTION BELOW 100 MHZ

W. Erickson*, M. Mahoney*, A. Szabo*, and J. Dodoo**

* Clark Lake Radio Observatory
University of Maryland
College Park, MD 20742
** Department of Natural Science
University of Maryland Eastern Shore
Princess Anne, MD 21853

The Clark Lake telescope operates in the 15 to 125 MHz frequency range and ionospheric refraction measurements have been made for several years in connection with radio source observations. Most of the data has resulted from calibration source observations that have been included in most observing programs. These calibration observations are usually spaced at intervals of an hour or two. Under stable ionospheric conditions nighttime refraction is found to have an RMS amplitude in each coordinate of three arc-minutes in the 50 MHz range and it is usually stable to within an arc-minute over periods of several hours. The magnitude of these ionospheric postional offsets, when scaled in frequency, agree with those measured at Westerbork.

The field of view of the system is several degrees wide and, in almost every field, sources may be found whose positions have been accurately determined at higher frequencies. When source positions are compared within a single field, they agree within measurement accuracy of a few tenths of an arc-minute. No differential refaction within a single field has yet been found.

Since June, 1985, special runs to monitor ionospheric refraction effects have been carried out on a regular basis. During these runs the telescope switches between several sources in different parts of the sky every few seconds. This provides data concerning dynamic ionospheric phenomena such as traveling ionospheric disturbances (TID's). Results from these measurements will be presented.

J4-7
1100 SUDDEN, INTENSE IONOSPHERIC DISTURBANCES DETECTED BY VERY LONG BASELINE INTERFEROMETRY

D. B. Shaffer
Interferometrics Inc.
8150 Leesburg Pike
Vienna, Virginia 22180
and
J. E. Salah and A. E. E. Rogers
Massachusetts Institute of Technology
Haystack Observatory
Westford, Massachusetts 01886

The Gilmore Creek Very Long Baseline Interferometry (VLBI) antenna, near Fairbanks, Alaska, is situated under the northern hemisphere auroral belt. Dual-frequency VLBI observations at 2.3 and 8.4 GHz, made for NASA's Crustal Dynamics Project during the summers of 1984 and 1985, show occasional large, rapid phase changes in the signal received at Gilmore Creek from cosmic radio sources. The phase variations are proportionally larger at the lower frequency, as expected from variations in the total electron content (TEC) of the ionosphere, and opposite the signature of equipment problems.

More than 4 turns of S-band phase occurred in as little as 15 seconds starting at 0948 UT on 30 August, 1984, corresponding to a sudden increase in TEC of $\sim 7 \times 10^{12}$ cm^{-2}. This implies an approximate doubling of the TEC in a few seconds. Earth surface magnetic fields and currents measured at Fairbanks show large variations nearly simultaneous with this and another large event discovered by VLBI.

In 1984, the observations most affected by what appear to be auroral events occur between 0900 and 1500 UT. Local midnight at Fairbanks is about 1000 UT. The number and intensity of the events seem to be less in 1985, perhaps correlated with lower solar activity.

These propagation events could limit the accuracy of differential position measurements made at high latitudes with the Global Positioning System (GPS), which transmits on the lower frequencies of 1227.6 and 1575.42 MHz. The sudden variations in phase must be taken into account in a GPS solution for position, particularly for those receivers which rely on sequential sampling of several satellites.

J4-8
1120 IONOSPHERIC CORRECTIONS FOR RADIO INTERFEROMETRY: Carl R. Gwinn, Center for Astrophysics, Cambridge, MA 02138

J4-9
1140

PROPAGATION OF KILOMETER-WAVE RADIO RADIATION FROM BEHIND THE SUN

G.A. Dulk[1], J.L. Steinberg[2], A. Lecacheux[3], S. Hoang[2], and R. MacDowall[2,4]

[1] Department of Astrophysics, CB 391, University of Colorado, Boulder, CO 80309, USA
[2] DESPA, Observatoire de Paris, 92190 Meudon, France
[3] DASOP, Observatoire de Paris, 92190 Meudon, France
[4] Department of Physics and Astronomy, University of Maryland, College Park, MD 20742, USA

Solar radio bursts in the range of about 100 kHz to 1 MHz are observable with a sensitive radio receiver (as on the ISEE-3 spacecraft) irrespective of the location of the radiating source, whether it is in front of or behind the Sun. More than 95% of type III bursts observed by the Voyager spacecraft when they were in the solar hemisphere opposite Earth were also recorded by ISEE-3. In addition, 10 of 21 bursts known to have originated between Sun an Earth were also recorded on the far side of the Sun by Voyager, sometimes with a flux density (scaled to 1 AU) larger than was recorded on the near side by ISEE-3.

Because these bursts originate where the plasma frequency is at or near the observing frequency, the radiation is subjected to a very high degree of ducting an scattering by interplanetary irregularities of many scales. Large scale, considerably overdense structures such as sector boundaries and stream-stream interaction regions are probably of special importance, playing a role as scattering screens and allowing the radio radiation to diffuse around the Sun without large attenuation.

Session B-9 1355-Weds. CR2-28
NUMERICAL METHOD
Chairman: T. K. Sarkar, Syracuse University, Syracuse, NY 13210

B9-1
1400

A CONJUGATE GRADIENT METHOD UTILIZING A HYBRID ERROR CRITERIA

Tapan K. Sarkar
Department of Electrical Engineering
Syracuse University
Syracuse, New York 13210

ABSTRACT: The objective of this presentation is to present a version of the conjugate gradient method which minimizes a hybrid error criterion. The hybrid error is a combination of the errors of the sum of the squared residuals plus the squared of the error between the solutions. The presentation would include development of this new error criterion along with numerical examples. Comparison would also be made with existing methods.

B9-2
1420

TM SCATTERING FROM MULTIPLE CONDUCTING AND LOSSY DIELECTRIC CYLINDERS OF ARBITRARY CROSS SECTION.

Ercument Arvas, Tapan K.sarkar and S.M.Rao,
EE Dept., Rochester Institute of Technology,
Rochester, NY 14623.

A simple moment solution is given for the problem of electromagnetic scattering from multiple perfectly conducting and lossy dielectric cylinders of arbitrary cross section. The conductors may be in the form of strips , they may partially be inside dielectrics, and the dielectrics may be of the form of shells. The system of multiple conducting and dielectric cylinders is excited by an electromagnetic wave polarized transverse magnetic to the axis of the cylinders. The equivalence principle is used to replace the conductors by surface electric currents radiating in an unbounded homogeneous medium. Similarly dielectrics are replaced by equivalent electric and magnetic surface currents. A set of coupled integral equations are obtained by enforcing the boundary conditions on the tangential components of the fields. The method of moments is used to solve these integral equations. A point-matching technique is used with pulse expansion functions for the unknown currents. E-field, H-field and the combined field methods are used and a comparison of the performance of these methods is given. Computed results include the current densities on the surface of the cyliders, the scattered fields on on the surface of the cylinders, the scattered far field and the radar cross section.The agreement with available published data is excellent.

The system shown below (a conducting strip of width 1.1λ extending between the centers of two circular lossy dielectric cylinders of radii 0.1λ) is just one of the examples considered.

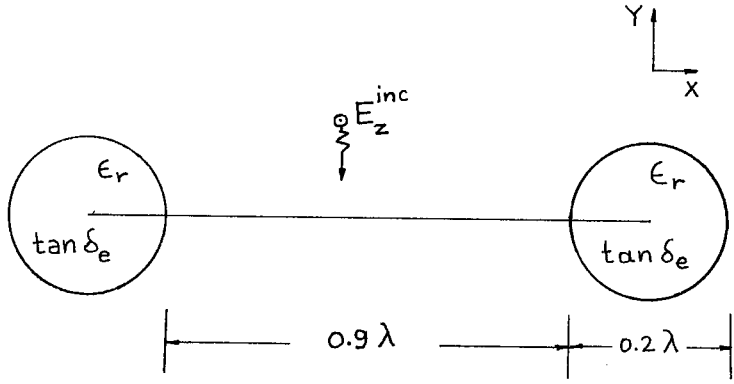

B9-3
1440

MIXED DOMAIN GALERKIN EXPANSIONS IN ELECTROMAGNETIC PROBLEMS

J. M. Bornholdt
McDonnell Aircraft Company
L. Medgyesi-Mitschang
McDonnell Douglas Research Laboratories
Saint Louis, MO 63166

Entire domain Galerkin expansions provide a computationally efficient representation in method of moment solutions for electrically extended surfaces forming a part of a separable coordinate geometry. For surfaces not conforming to such geometries, such as those with discontinuities, subdomain representations have been used. For many classes of scattering and radiating bodies, a mixed domain Galerkin expansion is shown to lead to a computationally efficient formulation. Electromagnetic scattering solutions are developed for classes of electrically large two-dimensional scatterers having localized discontinuities. Convergence of the solution is illustrated with choice of mixed domain expansions as a function of surface discontinuity. The computed results are given for both TM and TE polarizations and are compared with published results. Extension to surfaces with material discontinuities is discussed. Generalization of the approach to rotationally symmetric bodies is outlined.

B9-4
1500

GEM3D – A TIME DOMAIN, THREE DIMENSIONAL, LINEAR FINITE ELEMENT MODELING CODE*

J. B. GRANT and N. K. MADSEN
Electronics Engineering Department
Lawrence Livermore National Laboratory
P.O. Box 5504, L–156, Livermore, CA 94550

Codes for time domain modeling of electromagnetic scattering and radiation can be divided into two groups: general purpose and special purpose. For the general purpose codes the usual approach is to use finite differences or finite elements. With the finite difference technique, geometries are usually restricted to rectilinear grids and are able to utilize fast algorithms. On the other hand, finite elements are able to conform to arbitrarily shaped boundaries, but the technique requires more computational effort, and more information (memory), than does the finite difference technique. Until recently, 3D codes have been restricted to finite differencing due to the complexity and large memory requirements of finite elements. GEM3D overcomes these problems while maintaining all of the nice features of the finite element technique.

GEM3D, a *G*eneral *E*lectromagnetics *M*odeling code in *3D*, is a time domain finite element code utilizing an approximate diagonalization of the mass matrix. Consequently, little computational effort is required for matrix solutions. Additionally, most geometry quantities are easily recomputed as needed. This avoids storage of large arrays which, for three dimensional problems, is prohibitive. To compensate for this added computational effort, major portions of the code are written in a vectorizable fashion. On a million word machine, models with 25,000 elements can be solved without buffering to disk.

The utility of the GEM3D code is shown here by applying it to a truely three dimensional model. Meshes are generated by a versatile mesh generator and the GEM3D output can be examined as contour plots on three dimensional surfaces or with simple plots.

* Work performed under the auspices of the U.S. Department of Energy by the Lawrence Livermore National Laboratory under contract number W-7405-ENG-48

B9-5
1540

THEORETICAL AND EXPERIMENTAL DETERMINATION OF THE NATURAL FREQUENCIES OF A THIN WIRE ELLIPTICAL LOOP

E. Rothwell, D.P. Nyquist, K.M. Chen and
N. Gharsallah
Department of Electrical Engineering
and Systems Science
Michigan State University, East Lansing, MI 48824

Electromagnetic scatterers of simple geometry provide the opportunity to test both the validity of a natural mode representation of the late-time scattered field waveform and the usefulness of the singularity expansion method (SEM). A thin wire formed into an elliptical loop is particularly interesting in that the natural frequencies for its two limiting cases -- a circular loop and a nonradiating transmission line -- are well known.

Unlike other simple targets, such a straight wire or a sphere, the elliptical loop allows a simple method for performing measurements above a conducting ground screen at multiple aspects. Assuming a natural resonance expansion of the late-time portion of the scattered field, the natural frequencies of the loop can be determined from the measurements by using a variety of methods. If the natural resonance expansion is indeed valid, the natural frequencies thus determined should be independent of target aspect.

The natural frequencies of the elliptical loop can also be determined theoretically by solving the homogeneous transform domain electric field integral equation. This approach is based on the SEM assumption of a natural resonance expansion of the late-time scattered field. Thus, agreement of the experimental and theoretical frequencies provides additional validation of the natural mode representation.

B9-6
1600

IDENTIFICATION OF THE NATURAL FREQUENCIES OF A TARGET FROM A MEASURED RESPONSE USING E-PULSE TECHNIQUES

E. Rothwell, D.P. Nyquist, K.M. Chen and W.M. Sun
Department of Electrical Engineering
and Systems Science
Michigan State University, East Lansing, MI 48824

The late-time portion ($t > T_L$) of a measured transient response, r(t), of a conducting object is held to consist of a pure finite sum of natural oscillation modes. An E-pulse, e(t), is a waveform of finite duration T_e which when convolved with the measured response yields a null result:

$$q(t) = \int_0^{T_e} e(t')r(t - t')dt' = 0 \qquad t > T_L + T_e$$

If the natural frequencies in r(t) are known, e(t) is easily constructed by forcing E(s), the Laplace spectrum of e(t), to be zero at these frequencies. If the frequencies in r(t) are unknown, they can be identified by taking either of the following two approaches.

The integral equation given by q(t) = 0 can be solved by expanding e(t) in a set of basis functions and applying the method of moments. With e(t) determined, the natural frequencies in r(t) can be identified by solving for the roots to E(s) = 0. Through the use of appropriate basis functions, the zeroes can be found quite easily.

Alternatively, the integral equation can be solved by minimizing $q^2(t)$. If this minimization is carried out with respect to the complex frequencies used to construct e(t), then the natural frequencies in r(t) are taken to be the complex frequencies used to construct e(t) at the minimum point.

In contrast to Prony's method and its derivatives, these techniques have been found to be relatively insensitive to noise and to the number of natural modes assumed present in r(t).

B9-7
1620

ASPECT-INDEPENDENT TARGET DISCRIMINATION USING DISCRIMINANT SIGNALS

K.M. Chen, D.P. Nyquist, E. Rothwell, W.M. Sun, N. Gharsallah and B. Drachman*
Department of Electrical Engineering and Systems Science, and Department of Mathematics*
Michigan State University, East Lansing, MI 48824

A new radar target discrimination scheme using aspect-independent discriminant signals, called Extinction-pulse (E-pulse) and single-mode extraction signals, is being developed.

When the discriminant signals for an expected target are convolved with the late-time radar return of that target, the convolved outputs are zero or single-mode responses. On the other hand, when the discriminant signals for the expected target are convolved with the radar return of a different target, the convolved outputs will be significantly different from the expected zero or single-mode responses. Thus, the different targets can be discriminated.

Discriminant signals for simple and complex targets, which include bent wires and aircraft models, were synthesized on the basis of their natural resonant frequencies that were extracted from measured pulse responses or the induced currents on the targets using a Continuation method.

Recently we have experimentally proved the aspect-independency of our scheme. The E-pulse of a target was convolved with the pulse responses of that target measured at various aspect angles. The convolved outputs give small (nearly zero) late-time responses for all the aspect angles. When this E-pulse was convolved with the pulse responses of other targets measured at various aspect angles, the convolved outputs consisted of large late-time responses for all the aspect angles.

Session C-4 1355-Weds. CR1-40

METEOR SCATTER AND VHF COMMUNICATIONS

Chairman: P. A. Kossey, RADC Hanscom AFB, MA 01731

C4-1
1400

INFORMATION TRANSFER IN OPERATIONAL MB SYSTEMS

Harold N. Ritland, Consultant
Meteor Communications Corporation
22415 72nd Avenue South
Kent, WAsh;ington 98031

A review will be given of current operational civil meteor burst communciations systems in the United States, Alaska, Canada, and various foreign countries. Emphasis will be placed on the functions served by these systems, the information transfer requirements, the system hardware configurations, and the protocols and message structures utilized.

C4-2
1420

AN OVERVIEW OF THE METEOR BURST COMMUNICATION CHANNEL

Jay A. Weitzen
SIGNATRON, Incorporated
12 Hartwell Avenue
Lexington, MA 02173

This paper reviews the properties of the meteor burst communication channel using information from the literature supplemented with data from recent experimental programs.

The model for the channel is developed in terms of the basic elements of meteor burst modeling: the statistics of the arrival of meteor trails, the location, intensity and migration of "hot spots" of meteor activity within the antenna pattern, the distribution of trail durations and signal levels, and the multipath and Doppler profiles of the channel. The effect of high latitude propagation phenomenon including auroral propagation and sporadic-E propagation on the communication characteristics of the meteor channel is included in the model. Differences in the communication characteristics of the various types of meteor trails are presented.

Results from two RADC/EEPS sponsored high latitude meteor burst experiments including measurements of the multipath and Doppler profiles and the statistics of trail durations, arrival times, signal levels and number of arrivals are presented to support the development of the model. Improvements to current models based on recent experimental data are presented. The work was performed under US Air Force contract F19628-84-C-0117.

C4-3 1440 THE EFFECT OF ERRORS ON METEOR BURST THROUGHPUT:

John D. Oetting, Booz, Allen and Hamilton, Bethesda, MD 20814

Previous analyses of the throughput of point-to-point meteor burst systems (e.g., J. D. Oetting, IEEE Transactions on Comm, COM-28, 1591-1601, 1980) have either ignored the effect of errors or assumed that the error rate is fixed. In fact, the error rate of a meteor burst link varies dramatically both within a burst and from burst to burst. The purpose of this paper is to extend the results for a message broadcast system (J. R. Hampton, IEEE Military Communications Conference, Boston, MA, paper 32.2, 1985) to the case of a traditional point-to-point meteor burst system.

A simplified version of the underdense model for meteor burst signals is used to determine the time varying characteristics of the signal-to-noise ratio. The use of this model is justified by virtue of the fact that, in conventional meteor burst systems, most of the throughput is carried by underdense trails. The throughput is calculated as a function of the average interval between bursts and the average burst duration, assuming a packetized point-to-point meteor burst transmission system. The use of error correction coding is examined as a possible means of increasing the throughput. The throughput with coding is compared with the throughput without coding for various situations of interest and for various packet sizes and coding schemes.

C4-4
1540

A PERFORMANCE EVALUATION OF A PHYSICAL METEOR-BURST MODEL

D.W. Brown
Computer Sciences Corporation
6565 Arlington Boulevard
Falls Church, Virginia 22046

There is a great need for an accurate meteor-burst model to support the design and analysis of meteor-burst communication links and networks. Some success with modeling meteor-burst communications has been achieved using extrapolation according to physically based formulas from data measured on a reference meteor-burst link. The more similar the target link is to the reference link the more accurate the reference link technique is. Some of the shortcomings of a reference model can be overcome by incorporating a number of reference links in the model and choosing the one most similar to the target link. Data on high and low latitude links, on east-west and north-south paths, on vertical and horizontal polarization, on low and high frequencies etc., would be required to obtain the highest fidelity with this technique.

This paper describes an alternative approach - a physical meteor-burst model based upon physical models, and astronomical observations of meteors, particularly their orbits around the sun, their composition and mass distribution. Since the physical meteor-burst model described, incorporates all phenomena affecting a meteor-burst link, it should be accurate over the full range of meteor-burst circuit parameters. A comparison of the physical model results with a variety of experimental data is presented - this data includes: SHAPE Technical Centre data from meteor-burst trials in the 1960's at 40 and 100 MHz, Rome Air Development Center data from on-going trials in Greenland at 45, 65 and 104 MHz, and published southern hemisphere data.

C4-5
1600

CHARACTERISTICS OF HIGH LATITUDE METEOR SCATTER PROPAGATION PARAMETERS OVER THE 45 - 104 MHZ BAND

Michael J. Sowa, John M. Quinn, Paul A. Kossey, & John E. Rasmussen
Rome Air Development Center
Survivable Propagation Branch
Hanscom AFB, MA 01731-5000

This paper reviews the characteristics of polar meteor scatter propagation parameters using data acquired on an experimental test - bed located in northern Greenland. Emphasis will be focused on providing estimates of: the availability of useable meteor trails, the potential performance of candidate meteor scatter systems employing a variety of modulation schemes and signalling speeds, and the application of adaptive data rates to improved system performance. The use of the data to validate and expand propagation prediction techniques for the polar region is also discussed.

C4-6
1620 ON THE PERFORMANCE OF METEOR BURST COMMUNICATION SYSTEMS OVER VARIABLE PATH LENGTHS: T. Kaliszewski, The Mitre Corp., Bedford, MA

Many of the currently proposed applications of meteor burst communications imply either a mobile operation or a network that is composed of variable path length links. Experience with and performance data for such systems are meager or non-existent. To gain some insight into the performance of a meteor burst system over variable path lenghts we endeavor here to model a strawman circuit with a view of calculating its duty cycle as a function of path length. We also address the related problem of fixed-length message delays. Two frequencies, 41 and 70 MHz, path lengths from 200 to 2000 kilometers and data rates in the range of 1200 to 9600 bits/second are considered.

Session F-2 1355-Weds. CR1-9

EARTH AND OCEAN REMOTE SENSING

Chairman: R. K. Moore, Remote Sensing Laboratory, University of Kansas Center for Research, Inc., Lawrence, KS 60045

F2-1
1400 A MICROWAVE IMAGING SYSTEM FOR REMOTE SENSING OF SOIL PROPERTIES: G. De Amici, H. Dougherty, S. Levin, G. Smoot, and C. Witebsky, Lawrence Berkeley Laboratory and Space Sciences Laboratory, University of California, Berkeley, CA 94720

F2-2
1420

GROUND WAVE AUTOMATED PERFORMANCE ANALYSIS (GWAPA) FOR INHOMOGENEOUS SMOOTH AND IRREGULAR LOSSY EARTH

N. DeMinco, NTIA/ITS.S4
U.S. Department of Commerce
Institute for Telecommunication Sciences
325 Broadway
Boulder, CO 80303

An automated analysis model has been developed for systems performance prediction to aid in the estimation of performance of communications circuits using the ground wave as the primary mode of propagation. The computer program Ground Wave Automated Performance Analysis (GWAPA) is a structured set of a number of computer programs that predict propagation loss, electric field strength, received power, noise, received signal to noise ratio, and antenna factors for a variety of antennas. The computer program combines the propagation, system, and antenna models into a user friendly analysis model. The program contains three separate propagation models; a smooth earth model, a smooth earth mixed path model, and an irregular terrain model that includes forested and built-up terrain. The systems analysis models convert transmitter input power, receive and transmit antenna gain factors, and propagation losses into received power, received signal to noise ratio, and electric field strength. The antenna model contains simple lookup tables and algebraic algorithms to describe the performance of several antennas as a function of antenna geometry, ground conductivity, ground dielectric constant, frequency, and azmuthal direction. The computer model also provides the capability to calculate: the achievable distance given the required signal to noise ratio and reliability; and the achievable reliability given the required signal to noise ratio and distance. The irregular terrain propagation model accesses terrain files automatically given the appropiate LAT/LONG or manual terrain can be input by the user. An explanation of the model, its limitations, and some sample calculations will be presented.

F2-3
1440

ELECTROMAGNETIC WAVE PROPAGATION IN AN ASYMMETRICAL COAL SEAM

David A. Hill
Electromagnetic Fields Division
National Bureau of Standards
Boulder, Colorado 80303

During the 1970's, communication at MF (300 kHz - 3 MHz) was demonstrated in coal seams for horizontal ranges of several hundred meters. The dominant mode of propagation in coal seams at MF is transverse magnetic (TM), and it has usually been excited and received with loop antennas. More recently the dominant TM mode has been found useful in remote sensing of coal seams because its propagation constant depends on the coal seam parameters (thickness and electrical properties).

Previous theoretical models for coal seams have assumed a uniform coal layer bounded above and below by rock of higher conductivity (A.G. Emslie and R.L. Lagace, Radio Sci., 11, 253-261, 1976; J.R. Wait, Radio Sci., 11, 263-265, 1976). For simplicity, it was assumed that the floor and roof rock had the same electrical properties. Recent experimental work in coal mines has revealed that the roof rock is often not the same type of rock as the floor and hence has different electrical properties. In this talk we analyze an asymmetrical coal seam where the floor and roof have different electrical properties.

The mode equation is derived for an asymmetrical seam, and a simple expression for the propagation constant is obtained for the case where the floor and roof have high conductivity. For the general case, the mode equation is solved numerically. Numerical results for the attenuation rate and field distribution of the dominant are shown as a function of coal seam parameters. For the asymmetrical seam, the horizontal magnetic field and the vertical electric field are nearly constant within the coal seam, but the decay rate is different in the floor and roof. Thus the dominant mode can be efficiently excited or received by a horizontal magnetic dipole (small loop) or a vertical electric dipole located at any height within the coal seam.

F2-4
1540

INTERFACE EFFECTS ON HORIZONTAL WIRE OBJECTS LOCATED NEAR THE AIR-GROUND INTERFACE

R. J. Kane, E. K. Miller and G. J. Burke
P.O. Box 5504, L-153
Lawrence Livermore National Laboratory
Livermore, CA 94550

It has been demonstrated computationally that as a horizontal wire antenna is lowered towards the air-ground interface its power flow changes from being primarily into the air to primarily into the ground (G. J. Burke, et. al., Electromagnetics, 1, 29-29, 1981). The region over which this change occurs is generally less than one-tenth of the free-space wavelength in vertical extent. Accompanying this change in power flow is a smooth transition of the current wavelength on the wire from approximately that of free space to that of the ground, a change that occurs over an even smaller region only a few thousandths of a free-space wavelength in extent. It is important to have a quantitative understanding of both of these effects when designing horizontal antenna structures for operation near the air-ground interface.

In this paper, we summarize some results obtained from a computational study of these interface-induced phenomena. Two antenna configurations are examined, a single, straight, horizontal wire, and a horizontal, co-planar array of straight wires. The influence of length and feedpoint for the single wire, and of the spacing and number of elements for the array, are examined as a function of distance from the interface and ground permittivity and conductivity. We present results for the current distribution, upper- and lower-half-space radiation patterns (for the lossless ground), input impedance and upper-half-space radiation efficiency and gain. Also studied is the effect of a dielectric sheath to insulate the antenna from a lossy medium. Some concluding comments are addressed to the question of how the upper-half-space radiation characteristics of buried antennas might be improved.

F2-5
1600 ULF/ELF ELECTROMAGNETIC FIELDS GENERATED ALONG THE SEA FLOOR INTERFACE BY AN INFINITE CABLE: U. S. Inan, A. C. Fraser-Smith, and O. G. Villard, Jr., San Francisco State University, Division of Engineering, San Francisco, CA 94132

Propagation of ULF/ELF electromagnetic fields along the sea-floor interface (assumed to be a plane boundary separating two semi-infinite conducting media) is considered. Earlier expressions for the electromagnetic fields generated by a straight current source of infinite length are applied to the sea/sea-bed interface. The field components are calculated numerically and are compared to the field components in sea water of infinite extent. At the sea-floor boundary, the fields can propagate longer distances because of the lower sea-bed conductivities. The new horizontal component of the magnetic field generated as a result of the existence of the sea/sea-bed interface becomes larger than the vertical component of the magnetic field at large distances; it is also more sensitive to the conductivity of the sea bed at low frequencies. The results indicate that there is an optimal frequency at which two of the field components have a maximum field intensity at a certain distance from the source. Some practical applications are discussed.

F2-6
1620

A NEW POTENTIAL METHOD FOR MAPPING OCEAN MESOSCALE FEATURES USING AN ALTIMETER IN NON-REPEAT ORBIT

E. B. Dobson
The Johns Hopkins University
Applied Physics Laboratory
Johns Hopkins Road
Laurel, Maryland 20707

Satellite-borne altimeters measure the distance between the satellite and the ocean surface. This distance after correction for all error sources can be viewed as the combination of the earth's geopotential surface (GEOID), and the height of dynamic topography. When the height of the GEOID is known from other sources, this height can be removed from the altimeter measurement to yield dynamic height. Unfortunately, an accurate GEOID is not presently available over most of the world's oceans. Realizing this factor, researchers have investigated other techniques which yield variability of dynamic topography. While not as useful as an absolute measurement, these methods allow mapping and tracing of ocean features.

There are two methods that have been applied most frequently to obtain mesoscale variability. These are called "repeat orbit differencing" and "crossover differencing" techniques. The former requires a satellite in a repeat orbit on time scales comparable to mesoscale movement. The latter technique can be applied to any orbit.

The method of measuring variability to be discussed in this paper has the advantage over the other two in that it can be applied to a satellite in any orbit and provides a larger data base than the crossover technique, which is limited to those intersections of the satellite ascending and descending ground tracks. The method, to be referred to as a "variance technique", entails differencing of the variance of the altimeter signal over time. The principles of the technique will be discussed along with presentation of data which compares the three methods using altimeter data.

F2-7 1640 **WIND-PRODUCED SOLITONS IN OCEAN WAVE SURFACE GENERATION AND SCATTERING**

David Middleton, Consultant, and R.H.Mellen,
Planning Systems Inc., Marine Sciences Div.,
95 Trumbull Street, New London, Conn. 06320

Sonar and radar backscattering measurements indicate that the wind-driven sea surface does not behave according to linear theory at high wavenumbers. Moreover, backscatter strengths at high frequencies and small grazing angles are much greater than expected from classical wave models, and the scattering elements appear to move without the usual dispersion associated with "capillary waves". Theory shows that nonlinear effects of surface drift and wave-wind intermodulations can account for the shock--like properties of wave generation (D. Middleton and R.H.Mellen, IEEE J. Oceanic Eng., Vol. O-10, Oct., 1985).

Initially, periodic ripples develop coherent harmonics with increasing fetch. Then, subharmonic growth leads to rapid degener--ation and a continuous spectrum. Multiple intermodulations between wind and wave leads to chaotic behavior and redirection of energy to the lower wavenumbers. In the equilibrium stages, further development of longer gravity waves ceases as they out--run the source, incoming energy being balanced by high wavenumber dissipation.

It is inferred from the above model and from X-band and underwater acoustic measurements at high frequencies and small grazing angles (in "bubble-free" régimes) that the unstable dist--urbances thus produced on the underlying gravity-capillary wave surface degenerates into ensembles of solitons. Here these are "hydraulic bumps"-vis-à-vis "hydraulic jumps"-, or one-sided waves (analytically limiting solutions of the celebrated Korteweg-de Vries equation). They are propagated nondispersively on the thin wind-drift layer which rides on the gravity-capillary surface. The resultant soliton ensemble, with wavenumber spectrum $O(k^{-\gamma}), k \to \infty$) appears capable of accounting for the Doppler spreads, linear (mean) Doppler shifts, and backscatter crossections (which are O[10-- 20 dB] larger than conventional theoretical predictions), observed acoustically at high frequencies O(5-20kHz), small angles (θ[5-20°]), and medium wind speeds ($\bar{U}_{\lambda}$ = 10m/s), in "bubble-free" régimes (W.I.Roderick, J.B.Chester, and R.K.Dullea, Naval Underwater Systems Center Tech. Doc. 7183, July 12, 1984.)

Session F-3 1355-Weds. CR1-46

MILLIMETER AND SUBMILLIMETER WAVES - MOBILE COMMUNICATIONS

Chairman: Dusan Zrnic', National Severe Storms Laboratory, Norman, OK 73069

F3-1
1400 OBSERVATIONS OF THE SPECIFIC ATTENUATION OF MILLIMETER WAVES BY RAIN IN TWO CLIMATES

K. C. Allen, R. H. Espeland, and E. J. Violette
National Telecommunications and Information Administration, Institute for Telecommunication Sciences
Boulder, Colorado 80303

Measurements of the specific attenuation (dB/km) by rain at 28.8, 57.6, and 96.1 GHz made on short paths are described. The measurements were made near the northern California coast (Gasquet, California) from February through April and near the front range in central Colorado (Boulder, Colorado) during June and July.

Cumulative distributions of the rain rate and specific attenuations were computed. From these the specific attenuations were related to rain rate by relating the values corresponding to each percentage of time. Two significant results were found from the analysis.

One was that the aR^b relationship describing microwave attenuation as a function of rain rate held for these higher frequencies as well.

The other was that the specific attenuation rates were strikingly different for the two climates. For example, the 0.01 percent of time exceedance level for rain rate was 27 mm/hr in Gasquet and 55 mm/hr in Boulder. One would therefore expect more attenuation in Boulder at this exceedance level. However, the corresponding specific attenuations were 16 dB/km in Gasquet and 8.75 dB/km in Boulder at 96.1 GHz. These results indicate that the climatic dependence of specific attenuation (dropsize distribution) must be considered as well as the climatic dependence of rain rate in order to predict cumulative distributions of rain attenuation at these frequencies.

The values of a and b for the aR^b relationship were computed for the three frequencies and two climates and compared to the values computed for popular theoretical dropsize distributions.

F3-2
1420

MILLIMETER WAVE TELECOMMUNICATIONS IN AN URBAN ENVIRONMENT

K. C. Allen and E. J. Violette
National Telecommunications and Information Administration, Institute for Telecommunication Sciences
Boulder, Colorado 80303

In a computer model, the urban environment is idealized to consist of flat streets with uniform distance between buildings. The principal propagation paths between transmitting and receiving antennas within a few meters of the ground are described for this environment. The signal amplitude for each path is estimated from propagation losses including free space loss, clear air absorption, and loss during reflection from street and/or building surfaces (reflection coefficients). The delay time is computed from each path length. The angle of arrival at both antennas is computed for each path. Antenna gain patterns may be applied to compute the amplitudes of the various path components that comprise the received signal.

From the information computed for each ray path, telecommunication system performance may be described in a number of ways. For example, the impulse response may be predicted. In addition, the received signal level (RSL) may be found by adding the various signal components.

In actual urban environments the relative phases of the various path components cannot be readily predicted because of irregularities in the street and building surfaces. By assuming random uniformly distributed phase for the path components a cumulative distribution of RSL is predicted for an ensemble of urban environments. The distribution is modeled as Nakagami-Rice and approximated using the Weibull distribution.

Model predictions are compared to data measured in downtown Denver, Colorado.

F3-3
1440

ANALYSIS OF SOME RECENT MILLIMETER-WAVE RAIN ATTENUATION DATA

E. J. Dutton
National Telecommunications and Information Administration
Institute for Telecommunication Sciences
325 Broadway
Boulder, CO 80303

The Institute for Telecommunication Sciences has been continuously recording rain attenuation data on short ($\approx$ 1 km) links at various locations around the United States of America at three frequencies of 28.8, 57.6, and 96.1 GHz since mid-1984. Some of these data have been analyzed by two different methods oriented toward fade-margin design of millimeter-wave links.

First, power-law fitting techniques are discussed and compared. Results are obtained for Boulder, Colorado data taken in the summer of 1984, and for the far larger sample of data taken at Gasquet, California, in early 1985. The large variability associated with these power-law fits leads to the conclusion that they are more useful as a trend indicator than for engineering-design purposes.

Next, a model for the prediction of annual "worst-case" specific rain attenuation is evolved to more directly aid in engineering design. This model is derived from a sample of daily specific rain attenuation distributions at Gasquet, California. These worst-case results are then compared with some more recent data from Gasquet, California.

F3-4
1500

MOVING SPOT ILLUMINATED SEMICONDUCTOR PANEL PERFORMANCE AS MILLIMETER WAVE IMAGE CONVERTOR: M. H. Rahnavard and A. Habibzadeh, Electrical Engineering Department, School of Engineering, Shiraz University, Shiraz, Iran

Image conversion has been accomplished successfully in several regions of the electro-magnetic spectrum including millimeter and Infrared (IR) frequency bands. Because of the atmospheric attenuation at visible and infrared frequency bands under adverse weather conditions, image Conversion at wave-lengths longer than IR is increasing.

Many different methods of mm wave image conversion are suggested and discussed in the literature. A method that is of interest in this paper is the semiconductor mm wave image conversion. There are: (I) reflection mode of operation and (II) transmission mode of operation. In both cases a semiconductor panel is used and its response to illumination must be investigated.

So far the performance of illuminated semiconductor panel in millimeter band under uniform illumination and stationary spot is studied. In this paper excess carrier in semiconductor panel under moving spot illumination is developed. Using the developed excess carrier, the performance of the spot illuminated semiconductor panel (its reflection coefficient, transmission coefficient, attenuation, etc. vs. scanning velocity) in the millimeter wave region is studied.

F3-5
1540

QPSK DEGRADATION BY CLEAR AIR FILTERING

Jerry D. Hopponen
Lockheed Missiles and Space Company
O/62-47, B/562
P.O. Box 504
Sunnyvale, CA 94086-0504

QPSK communication links at EHF are subject to absorption by oxygen and water vapor in clear air. Attenuation and phase delay are dispersive, which suggests viewing the atmosphere as a filter. Following Weinberg's approach (IEEE Trans Comm.,Com-28, 1980), with the transfer function modelled as $(1 + a \cos w T) + j b \sin w T$, analysis shows that both amplitude and phase contribute to bit error rate degradation, and that the extent of the degradation depends upon the data rate (of each channel, in the more general case). Furthermore, I/Q crosstalk is introduced.

The absorption model of Liebe (e.g., Radio Science, 16, 1183-1199,1981) generates atmospheric filters for specific bands and path elevation angles, and these are introduced into a digital simulation program for calculation of BER. Illustrative cases of system performance,as well as atmospheric filters, are given.

F3-6
1600

POLARIZATION DIVERSITY IN THE PORTABLE COMMUNICATIONS ENVIRONMENT

S. A. Bergmann
Department of Electrical Engineering
Rutgers, the State University of New Jersey
New Brunswick, N. J. 08903

H. W. Arnold
Radio and Satellite Systems Research Division
Bell Communications Research, Inc.
Red Bank, N. J. 07701-7020

In today's highly mobile society it is becoming increasingly desirable to develop a portable communications system (D. C. Cox, "Universal Portable Radio Communications," National Communications Forum, NCF '84, Chicago, IL, September 24-26, 1984, pp. 169-174) that is reliable and ubiquitous. The transmitted signals of such a system, however, will suffer deep rapid fading due to random handset orientation and multipath propagation. This paper describes an experiment testing the feasibility of polarization diversity to mitigate these impairments.

Polarization diversity relies on the independence of signals received over two orthogonally-polarized antennas. Polarization diversity is both spectrally and spatially efficient. Frequency diversity requires the use of several frequencies and space diversity antennas must be separated by at least one-quarter wavelength, while polarization diversity uses a single frequency and the cross-polarized antennas can lie directly on top of one another.

Propagation measurements were made at 816 MHz in and around several buildings using a single linearly-polarized transmitting antenna and a dual-polarized microstrip receiving antenna. From these measurements the correlation between the envelopes of the two received signals was determined. Where a direct line of sight existed between transmitter and receiver, little fading and depolarization was observed; here polarization diversity offers protection against random receiving antenna orientation. Where no line of sight existed, deep and uncorrelated fading occurred on both polarizations. Polarization diversity can thus mitigate this signal impairment.

F3-7 1620 ATTENUATION DUE TO SINGLE TREES ALONG EARTH SPACE PATHS AT 869 AND 1500 MHz

Wolfhard J. Vogel and Geoffrey W. Torrence
Electrical Engineering Research Laboratory
The University of Texas at Austin
Austin, Texas 07558

Julius Goldhirsh and John R. Rowland
Applied Physics Laboratory
The Johns Hopkins University
Laurel, Maryland 20707

With the advent of future "Land-Mobile Satellite Systems", where a geostationary satellite will be communicating with a mobile vehicle, the question is raised as to the attenuating effects of transmissions passing through tree regions. For such a configuration the geometry is in general different than that of a land based configuration. Depending upon the elevation angle, the transmission path may intersect only the foliage portion of a single or at most a few trees located adjacent to the road. In this paper the results of an experiment are described in which the attenuation effects of various tree types were examined employing an 869 MHz transmitter system located on a remotely piloted aircraft. The circularly polarized transmissions were received at a nearby ground receiver-data acquisition system. The experiment was performed at Wallops Island, Virginia in June, 1985.

The results show median worst case attenuation levels for single trees varying, in general, between 10 and 20 dB. The instantaneous variations about these worst case levels were approximately +/- 3 dB (from the 25 to the 75 percentile signal levels). The trees were relatively mature with heights ranging from 14 to 28 M and foliage widths of approximately 8 M. Some of the tree types examined were Holly, Pine, and Oak. The approximate overall attenuation coefficient associated with transmission through the foliage portion of the tree was estimated to be 2 dB/m.

Results are also presented for simultaneous transmissions at 869 and 1500 MHz pertaining to an allied experiment in which signals emanating from a transmitter located on a stratospheric balloon were received at a moving vehicle. For equivalent tree path geometries, the average ratio of attenuation at the two frequencies was estimated to be 1.4 (ratio of 1500 MHz to 869 MHz values).

Session G-7 1355-Weds. CR0-30

IONOSPHERE MAPPING AND MEASUREMENTS

Chairman: Charles M. Rush, NTIA/ITS, Boulder, CO 80303

G7-1
1400

Mapping of Characteristics at the Peak of the F2 Layer

K. Davies
Space Environment Laboratory, NOAA
325 Broadway
Boulder, CO 80303

At the URSI General Assembly in Florence in 1984 a new working group was established with the following terms of reference "To suggest improvements in the present CCIR maps of F2 layer characteristics through theory and observation and, in particular, to investigate the possibility of incorporating space data". A progress report is presented of the work of the group to date.

G7-2
1420

APPLICATION OF COMPUTERIZED TOMOGRAPY TECHNIQUES TO IONOSPHERIC RESEARCH

J. R. Austen, S. J. Franke, and C. H. Liu
Department of Electrical and Computer Engineering,
University of Illinois, Urbana-Champaign, IL 61801

In this paper, we investigate the feasibility of using Computerized Tomography (CT) techniques to construct a two-dimensional picture of the electron density structure in the ionosphere. Transionospheric radio signals received on the ground will be used for this purpose. CT theory as applied to this study will be presented. The types of structures that can be seen from realisitic observational configurations, requirements for data, and limitations of this technique will be discussed. Examples of computer simulations will be presented. The possibility of reconstructing large-scale structures, such as the ionosphere trough and the equatorial bubble, using existing satellite beacon data will be investigated.

G7-3
1440

THE NUMERICAL MAPPING OF SCATTERED IONOSPHERIC DATA

J. S. Washburn and A. D. Spaulding
National Telecommunications and Information Administration, Institute for Telecommunication Sciences, U.S. Department of Commerce, Boulder, CO 80303

A set of ionospheric measurement data generally takes the form of a nonuniform net, usually sparce, of data points scattered over the Earth. Direct numerical mapping is usually impractical and/or inaccurate so that the generation of "additional data" is required. This paper discusses a C^1 interpolation to scattered data over a sphere developed at JPL and its application to ionospheric mapping procedures. Application to the estimation of worldwide atmospheric noise levels, based on only 27 measurement locations, is used as an example.

G7-4 1500 MAPPING OF THE STRUCTURE OF THE IONOSPHERE USING AUTOMATIC PATTERN RECOGNIZATION TECHNIQUES

R.D. Chaney, D.B. Odom and N.P. Viens
Raytheon Company, Equipment Division
Wayland, Massachusetts 01778

Abstract

The use of Automatic Pattern Recognization Techniques to map the structure of the ionosphere which lies in the vicinity of an HF radar or communication site has become increasingly important as the digital processing capability at these sites has grown. The complex manual scaling of this type of data has become a bottleneck in the otherwise automatic processing which is now being developed for use during real-time management of new radar and communication systems.

The automatic pattern recognization techniques used for speech pattern analysis and artificial intelligence decision making are potential candidates for this type of automatic processing. The direct application of pattern recognization theory to the task of scaling the many hours of vertical and backscatter ionospheric soundings which are manually processed to provide an update to the predicted ionospheric structure is expected to be extremely useful to HF radar and communication systems.

A review of the results obtained from an automatic pattern recognization technique used to provide an updated ionospheric model in the vicinity of an HF radar site is provided. A comparison is made with other techniques which are used to automatically obtain observed ionospheric profiles such as the ionospheric digitizing procedure developed at the University of Lowell (Reinisch, B.W., 1983). Improvements which are planned in the current pattern recognization process will be described along with the digital processing speeds which must be addressed during real-time system operations.

G7-5
1540

COMPARISON OF PREDICTED VALUES OF foF2

Margo PoKempner and Charles M. Rush
National Telecommunications and Information Administration, Institute for Telecommunication Sciences, Boulder, CO 80303

A set of numerical coefficients to represent foF2 on a global basis has been derived using observations of foF2 and data deduced from the time-dependent continuity equation (Rush et al., Radio Sci, 19, 1083-1097, 1984). The values of foF2 deduced from these coefficients have been compared with independent observations of foF2 and with values deduced using the existing CCIR coefficients (CCIR, Report 340-4, Vol. VI, Geneva, 1982). The values of foF2 determined from both sets of coefficients have been calculated using both the R_{12} and IG_{12} index. Results of comparisons between predicted and observed values of foF2 will be shown for both indices and for various locations around the globe.

G7-6 COMPARISON OF AURORAL ABSORPTION MODELS WITH RIOMETER DATA
1600

Nikhil Dave', Naval Ocean Systems Center,
Ocean and Atmospheric Sciences Division,
Code 542,
San Diego, CA 92152-5000

Models for calculating the Q1 statistic in auroral zones proposed by Foppiano and Bradley (Telecom. J., vol. 50 - X/1983, p. 547-560) and by Vondrak, et. al. (RADC-TR-78-7, January, 1978) were run on the computer and the results compared to riometer data as analyzed by Hartz, et. al. (Can, J. Phy., v. 41, 481-595, 1963) for the Alaskan/Canadian sector and by Driatskiy (Geom. & Aeron., v. 6, 828-834, 1966) for the Russian sector. Foppiano and Bradley propose two models: a long-term prediction scheme which depends only on the sunspot number R12 to determine solar activity, and a short-term scheme which depends only on three-hour values of KP to determine solar activity. Vondrak, et. al. propose a model incorporating both R12 and KP.

Comparison with riometer data indicates that the Vondrak model yields too large a forward shift in the time of peak drizzle particle precipitation (hence, peak auroral absorption) and an excessive latitudinal broadening of the auroral absorption zone for values of KP greater than 5. On the other hand, both models of Foppiano/Bradley give reasonable agreement with the published riometer data for a wide range of model parameters. The latter two models have the additional advantage that a program can be easily devised to run a long-term prediction based only on R12 or a complementary short-term prediction based only on KP for locally disturbed (magnetic substorm) conditions.

G7-7
1620

MODIFICATIONS OF MINIMUF-3.5 FOR APPLICATIONS IN POLAR REGIONS

W. Rix and D. B. Sailors,
Ocean and Atmospheric Sciences Division,
Naval Ocean Systems Center,
San Diego, CA 92152-5000

An improved version of MINIMUF-3.5 was developed to predict accurate maximum usable frequencies (MUFs) for paths having a portion of the path in the polar region. MINIMUF-3.5 encounters problems when predicting MUFs at polar latitudes. The physical basis for MINIMUF-3.5 is that all variations of the free election density are driven by the solar zenith angle (i.e., ionospheric free electrons are produced by solar photon induced dissociation). At high latitudes an important contribution to ionization is made by particle precipitation. A second reason for a weakness of MINIMUF-3.5 at high latitudes is that the fitting process in the development of MINIMUF-3.5 did not include paths with control points in the polar region.

The polar model developed by Chiu (J. Atmos. Terr. Phys., 37, 1563-1570, 1975) for inclusion in a global phenomenological model of the ionospheric election density was used to calculate foF2 in MINIMUF. The polar and non-polar functions in the Chiu model are welded together by means of a folding function. The folding function determines when polar effects (particle precipitation) become dominant and is used in MINIMUF. This polar model was also inserted into MINIMUF-85, an improved microcomputer MUF algorithm (R.A. Sprague and D.B. Sailors, 1985 North American Radio Science Meeting, June 1985).

The accuracy of the North polar model was determined from MOF's measured on five different paths; the data base was comprised of a total of 52 path months of MOF's. On these paths the value of the folding function at the control points varied from 0.20 to 1.0. For these paths MINIMUF-3.5 had a bias of 6.85 MHz low and an rms error of 10.9 MHz. With the polar model folded in the bias was 2.2 MHz low, and the rms error was 3.93 MHz. When the polar model was inserted in MINIMUF-85, the bias was 0.6 MHz low, and the rms error was 4.0 MHz. MINIMUF-3.5 consistently underestimated wintertime MUFs along polar paths to a greater degree than during other seasons. The errors in MINIMUF-3.5 along polar paths are positively correlated with sunspot number.

Session H-5 1355-Weds. CR2-26

WAVE GENERATION BY PARTICLE INJECTION - II

Chairman: W. J. Raitt, Center for Atmospheric and Space Sciences, Utah State University, Logan, UT 84322

H5-1
1400

A POSSIBLE CONNECTION BETWEEN SECONDARY ION STREAMS AND ELECTROSTATIC WAVES IN THE NEAR VICINITY OF SHUTTLE ORBITER

K. S. Hwang
ES-53, Space Science Laboratory, NASA/MSFC, Huntsville, AL 35812

N. H. Stone
ES-53, Space Science Laboratory, NASA/MSFC, Huntsville, AL 35812

K. H. Wright, Jr.
Physics Department, The University of Alabama in Huntsville, Huntsville,AL 35899

U. Samir
Dept. Geophys. & Planet. Science, Tel-Aviv Uni., Ramat-Aviv, Israel and Space Phys. Res. Lab., The University of Michigan, Ann Arbor, MI 48109

Recent measurements from the Shuttle mission show the presence of ion streams in the vicinity of the Orbiter at angle of attack as great as 50° with respect to the ram direction. These streams appear to be the source of observed electrostatic broadband noise between 30 Hz and 178 KHz.

A kinetic model for generating broadband electrostatic noise by an ion beam in a background plasma is investigated. We consider an infinite plasma permeated by a uniform magnetic field and a current with components normal and parallel to the magnetic field. Maxwellian velocity distribution functions are used for both electron and ion species in this derivation.

The generalized dispersion relation for the electrostatic waves is obtained by the linearized, collisionless Vlasov equation and Maxwell's equations. The numerical solutions predict the generation of waves over a broadband of frequencies (50 Hz-300 KHz) in agreement with STS-3 observations. Results also show that decreasing the temperature ratio Te/Ti decreases the wave growth rate as expected. Numerical examples with plasma parameters are presented.

H5-2
1420

MOTION OF AN ELECTRON BUNCH THROUGH A PLASMA

M. M. Shoucri
Institut de Recherche d'Hydro-Québec,
Varennes, Québec, Canada JOL 2PO

L. R. O. Storey
STAR Laboratory, Electrical Engineering Department,
Stanford University, Stanford, California 94305

The motion of a tenuous bunch of fast electrons through an isotropic plasma has been studied using a 1-dimensional Vlasov code [J. Comp. Phys. **27**, 315 (1978)]. Given a fairly large initial perturbation from equilibrium, the moving bunch sheds a train of nonlinear plasma oscillations, which appear to be sustained by a mild instability.

H5-3
1440

PLASMA RESPONSE TO THE INJECTION OF AN ELECTRON BEAM

Nagendra Singh and R. W. Schunk
Center for Atmospheric and Space Sciences
Utah State University
Logan, Utah 84322-3400

The response of a plasma to the sudden injection of an electron beam was systematically studied using a Vlasov-Poisson solver in one-dimension. The temporal response of the plasma was dramatic and included the following processes: (1) The formation of ion bursts; (2) The creation of electrostatic electron shocks and holes, depending on the beam density; (3) A strong plasma heating and the consequent plasma expulsion from the simulation region; (4) The creation of density gradients due to the plasma expulsion: (5) The formation of a caviton through the pondermotive force of long wavelength fast oscillations and the consequent steepening of the density gradient; (6) The propagation of the steep density front and solitary pulse down the density gradient; (7) The excitation of the Buneman mode and the subsequent formation of a virtual cathode and double layers. In the same simulation several types of double layers occur as the plasma evolves through various stages, including monotonic double layers, double layers with a dip on the low potential side, and double layers with a bump on the high potential side. When the electron current density is large, multiple double layers are common. On the other hand, when the electron current density decreases owing to disruptive plasma processes, a single strong double layer forms. Such double layers have localized negative potential dips at their low potential ends. Simulations carried out with several beam velocities indicate that the double layer strength approximately scales with beam energy.

H5-4
1520

PLASMA INSTABILITIES OF SEPAC ELECTRON BEAMS FROM THE SPACE SHUTTLE

C. S. Lin, Department of Space Sciences
Southwest Research Institute
P. O. Drawer 28510
San Antonio, TX 78284

The SEPAC (Space Experiments with Particle Accelerators) experiment conducted from the Spacelab-1 Shuttle mission indicated VLF noise up to 100 kHz during the electron beam emissions. The electron beams were injected with currents up to 300 mA and energies up to 5 keV. To understand the observed emissions, the general electromagnetic dispersion equation is derived for the SEPAC parameters using the vector potential formulation. The electron beam is represented by a drifting Maxwellian distribution function with temperature anisotropy. The beam profile is modelled by assuming that the current density is constant and the electron beam is space charge neutralized. The plasma instabilities for ion cyclotron, lower hybrid and whistler waves are examined as a function of ambient density, beam energy, and temperature anisotropy. The instability growth rates are then compared with the measured wave spectrum.

H5-5
1540

NEAR FIELDS GENERATED BY PULSED ELECTRON BEAMS IN SPACE

K.J. Harker and P.M. Banks
Space, Telecommunications, and
Radioscience Laboratory
Stanford University
Stanford, CA 94305

Far field theories for the generation of waves in space by electron beams are useful for predicting the strength of waves in the regions well removed from the beam. Near field theories are needed, on the other hand, to predict the field strength in the vicinity of beam itself. Such theories draw greater significance from the fact that the bulk of the observations on the emissions from such beams have been made in the near field.

The most recent results from our theoretical studies of the near fields in the vicinity of pulsed electron beams will be presented. The model, as in our previous studies, assumes that the electrons follow an idealized helical path through the space plasma in such a manner as to retain their respective positions within the beam, leading thereby to coherent spontaneous emission. The theory reported takes into account both propagating and evanescent waves and mutual coupling between modes in determining the field intensities.

Session J-5 1355-Weds. CR2-6

PROPAGATION EFFECTS IN RADIO ASTRONOMY - II: INTERPLANETARY MEDIUM AND INTERSTELLAR MEDIUM

Chairman: William J. Welch, Radio Astronomy Laboratory, University of California, Berkeley, CA 94720

J5-1
1400 RADAR SPECTRAL BROADENING OBSERVATIONS OF SOLAR WIND TURBULENCE NEAR THE SUN: J. K. Harmon, Arecibo Observatory, Arecibo, PR 00613; and W. A. Coles, University of California - San Diego, La Jolla, CA 92093

Spectral broadening of coherent radio waves is a useful remote probing technique for studying solar wind microturbulence within about 25 R_S (solar radii) of the Sun. Spectral broadening measurements have been made at Arecibo at both 2380 MHz and 430 MHz using radar echoes from Venus as the coherent probe signal. Previously reported results of 1979 and 1981 Arecibo radar observations confirmed earlier evidence from spacecraft beacons for flattening of the turbulence spectrum inside of 14 R_S, and provided some evidence for a 2 km inner scale at 5.4 R_S. More recently (1984) we made similar observations at both frequencies, but at smaller heliocentric distances R than in previous years. The 1984 results, besides reconfirming the spectral flattening, have strengthened evidence for a 1-2 km inner scale inside of 6 R_S. The Arecibo results are compared with other measurements in a brief review of the current state of (and deficiencies in) our knowledge of the radial evolution of the solar wind turbulence spectrum. In addition to spectral broadening, the Arecibo radar observations have also yielded measurements of group delay and refraction in the corona, the results of which are briefly reported.

J5-2
1420

PERTURBATIONS OF PLANETARY SPACECRAFT RADIO SIGNALS BY PROPAGATING INTERPLANETARY TRANSIENTS

R. Woo and J.W. Armstrong, Jet Propulsion Laboratory, California Institute of Technology, Pasadena, CA 91109

Propagating interplanetary transients manifest themselves in the amplitude and phase measurements of planetary spacecraft. Many of the major transients are shock waves (Woo et al., JGR 90, 154-162, 1985). The purpose of this paper is to present some statistics of the propagation effects and the transients observed in the S-band phase data of the Pioneer and Voyager spacecraft collected by NASA's Deep Space Network in 1979-1982. So far, 175 transients in a heliocentric distance range of 5-180 R_0 have been identified. These transients have values of R (ratio of peak scintillation level to pre-transient scintillation level) ranging from 4 to 100, and time durations varying from a few to tens of hours. Included in the data set are 22 interplanetary disturbances observed by two or more spacecraft. Propagation speeds of 200-2200 km/s are obtained for these disturbances based on the transit times from one radio path to the other. The propagation speed and R are found to be highly correlated (correlation coefficient of 0.9 for the 22 disturbances). Thus, the value of R serves as a rough indicator of the propagation speed. Owing to instrumental sensitivity, the majority (80%) of the transients were observed within 100 R_0, and the frequency of occurrence was highest within 40 R_0, about 0.25 transients/day.

J5-3
1440

RADIO SCINTILLATION MEASUREMENTS AND TURBULENT DENSITY VARIATIONS*

J. C. Higdon, Jet Propulsion Laboratory, California Institute of Technology, Pasadena, CA 91109

In interstellar and interplanetary media the presence of power spectra of electron density variations extending to scales, ℓ, much less than a Coulomb mean free path is required by analyses of scintillation measurements of radio signals that have propagated through such plasmas (e.g. R. Woo and J. W. Armstrong, J. G. R., 84, 7288, 1979; J. W. Armstrong et al., Nature, 291, 561, 1981). The spectral shape of these density distributions as a function of wavenumber, $2\pi/\ell$, is the same as that of the inertial range of turbulent velocity variations in incompressible fluids. The origin of plasma density variations with such spectral shapes is unknown.

I have developed a model of anisotropic magnetogasdynamic turbulence that reproduces well the measured properties of the density variations. This model does not employ small scale magnetoacoustic waves which dissipate efficiently in these plasma environments. In my model the small-scale density variations are generated by the convective distortion of initially large-scale isobaric entropy structures. Large-scale entropy structures are produced by any turbulent flow situated in a thermally heterogeneous fluid such as the interplanetary plasma or the interstellar medium. Due to the presence of strong mean magnetic fields the small-scale velocity fluctuations are concentrated in planes transverse to the directions of the mean magnetic fields. In these transverse directions the processes that dissipate the entropy and velocity structures, respectively thermal conductivity and viscosity, are dramatically reduced compared to the values found in the absence of mean magnetic fields. Thus the convective range of isobaric entropy structures can extend to very small scales before the diffusive action of thermal conductivity becomes significant.

*This research was carried out at the Jet Propulsion Laboratory, California Institute of Technology, under contract with the National Aeronautics and Space Administration. The author is a NAS/NRC Senior Resident Research Associate.

J5-4
1500 INTENSITY SCINTILLATIONS OF SPATIALLY EXTENDED, INCOHERENT SOURCES: J. L. Codona and R. G. Frehlich, Department of Electrical Engineering and Computer Science, University of California - San Diego, La Jolla, CA 92093

Using the Green's function formalism, a series solution is presented for the correlation of the intensity fluctuations of waves propagating through an extended random medium from a spatially-extended, incoherent source. The statistics of the random medium are assumed to be homogeneous in the direction transverse to the propagation but locally homogeneous in the propagation direction. Assuming the source emits a zero-mean complex Gaussian field that is delta-correlated in space, produces two terms for the intensity correlation. One is the "standard" intensity correlation obtained by summing the intensity contributions from different regions of the source. The second contribution describes the correlation of the rapid temporal fluctuations observed with a Hanbury Brown and Twiss intensity interferometer. The introduction of a model narrow-band receiver clarifies the role of these two contributions in a typical observation. The intensity spectrum of each contribution is expressed as a high and low spatial-frequency series. The effect of source averaging on the scintillation index and typical intensity correlation scales are presented for both weak and strong scattering. Where possible, these expressions are compared to previous results.

J5-5 THE SCATTERING SIZE OF CYGNUS X-3
1540

L. A. Molnar
Harvard-Smithsonian Center for Astrophysics
60 Garden Street, Cambridge, MA 02138

Cygnus X-3 presents a unique opportunity to study interstellar scattering sizes over 2 decades in wavelength. The small intrinsic size, large scattering size, and relatively flat spectrum make measurements of the scattering size possible from 1 to 100 cm wavelength. This enables a detailed test of the dependence of scattering size on wavelength predicted by models for the distribution of density fluctuations in the interstellar medium.

VLBI measurements at 1.3 cm made February 1985 suggest a 1.3 cm minimum size of 0.65(0.16) milliarcseconds. Comparison of this value with values from 20 cm measurements made simultaneously with the VLA in its largest configuration (A array) are consistent with the hypothesis that the 1.3 cm minimum size is the scattering size. We have scheduled further 1.3 cm VLBI measurements for October 1985 and proposed 90 cm VLA measurements.

J5-6
1600

INTERSTELLAR SCATTERING OF H_2O MASER RADIATION FROM SGR B2

J.M. Moran, M.J. Reid, C.R. Gwinn,
M. Schneps, E. Bloemhof
Harvard-Smithsonian Center for Astrophysics
60 Garden Street
Cambridge, MA 02138
R. Genzel
U. California
Berkeley, CA
D. Downes
IRAM
Grenoble, France

We have mapped the H_2O masers at 22 GHz towards Sgr B2 at five epochs with a VLBI network and identified a total of about 400 maser spots. The smallest angular size observed is about 0.3 milliarcseconds. This minimum size is probably set by scattering in the interstellar medium. The angular sizes of the OH masers at 1.6 GHz from the same region are about 0.1″. The ratio of sizes of OH masers to H_2O masers is about equal to the ratio of the wavelengths squared. The scattering sizes are about a factor of 3 smaller than those observed for Sgr A, which is located about 100 pc away. These results and those on other masers will be discussed.

J5-7 INTERPLANETARY SCINTILLATION
1620

Wm. A. Coles
Electrical Engineering and Computer Science,
University of California, San Diego,
La Jolla, Ca. 92093

The interplanetary medium (solar wind) has a number of measureable effects on radio astronomical measurements. Most of the propagation phenomena are caused by spatial fluctuations in electron density (microturbulence), although the effect of gradients in the mean density can be detected.

The basic underlying process is angular scattering from refractive index (density) fluctuations. This is observable directly as angular broadening of compact sources and in the form of VLBI phase fluctuations. It is also observable indirectly as spectral broading of narrow band sources. At present spectral broadening has only been observed in spacecraft telemetry and in planetary radar echos. Interference between components in the angular spectrum causes intensity fluctuations. Such diffractive intensity scintillation can also be modulated by large scale density fluctuations in a refractive manner. This process is not as important in the solar wind as it is in the interstellar medium.

Propagation processes can be used to study the solar wind and intensity scintillation, in particular, can also be used to estimate radio source diameters. In most cases unwanted effects can be avoided simply by observing at night, however this may not be sufficient at meter to decameter wavelengths. Of course there are also cases where the observation must be made near the sun.

A summary of our present understanding of the microturbulence will be given. This includes its spatial spectrum and anisotropy; its distribution with respect to the sun; and its changes with solar activity cycle. Recent observations of the inner region of the solar wind made with the VLA will be presented. These show rapid velocity changes and highly anisotropic structure near 4 solar radii. If possible new observations made within 2 solar radii (October 1985) will also be presented.

J5-8
1640

PULSAR FLUX STABILITY AND REFRACTIVE SCINTILLATION

D. R. Stinebring
Physics Department
Princeton University
Princeton, New Jersey 08544

J. J. Condon
National Radio Astronomy Observatory
Charlottesville, Virginia 22901

We have made continuum flux measurements of 25 pulsars over a 42 day period at 310, 416, and 750 MHz. Our observations place the refractive (slow) scintillation phenomenon (Rickett, Coles, and Bourgois, *Astron. Astrophys.*, 134, 390–5, 1984) on a firmer observational footing by extending the range of frequencies and dispersion measures probed. We find good agreement with refractive scintillation theory, indicating that it can explain fluctuations of compact extragalactic sources such as "low-frequency variables."

Seven high dispersion measure pulsars show flux stability in the range 5%–10%, demonstrating that intrinsic flux variations of pulsars are small on this timescale. Eight pulsars in our sample showed the effects of refractive scintillation. These pulsars show a clear correlation between fluctuations at 310 and 750 MHz, with little or no correlation between fluctuations at 310 and 750 MHz. The modulation depth is $\approx 20\%$ for the short timescale variations; there is no obvious trend in the modulation depth as a function of frequency. Refractive scintillation timescales, calculated on the basis of diffractive scintillation parameters, are in good agreement with the observed fluctuations for these pulsars. The remaining pulsars in the sample had flux variations that were dominated by diffractive scintillation.

These results show that pulsars are constant flux sources on timescales of days to weeks and that they are good probes of refractive scintillation. Unlike the observations of low disperion measure pulsars studied at 156 MHz (D. J. Helfand, L. A. Fowler, J. V. Kulhman, *Astron. J.*, 82, 701–5, 1977), we do not see modulation depths approaching 100%.

J5-9
1700

TIME DELAYS, IMAGE DISTORTIONS, AND INTERSTELLAR SCINTILLATIONS

James M. Cordes
Department of Astronomy
Cornell University, Ithaca, New York USA

Intensity scintillations in frequency and time, time of arrival fluctuations from pulsars, and multiple imaging due to propagation through the irregular interstellar plasma will be illustrated with observations of the millisecond pulsar PSR 1937+214 and other objects. The implications for the interstellar electron-density power spectrum and VLBI observations of compact galactic and extragalactic objects will be discussed.

Session A-3 0835-Thurs. CR1-42
GENERAL EM MEASUREMENTS
Chairman: M. Kanda, Electromagnetic Fields Division,
National Bureau of Standards, Boulder, CO 80303

A3-1
0840 SPACE-FREQUENCY SAMPLING CRITERIA FOR ELECTROMAGNETIC SCATTERING OF A FINITE OBJECT: Fredric Fok and Jonathan Young, The Ohio State University ElectroScience Laboratory, Department of Electrical Engineering, Columbus, OH 43212

This paper concerns the sampling criteria in the wave number space for generating the spatial impulse response of a finite target. The other purpose of this paper is in the management of large amounts of data for potential application in the presentation of scattered field data and construction of such images. A proper choice of canonical confinement for the target in space can greatly reduce the number of samples required to sufficiently characterize the target's spatial impulse response. Though a sampling lattice may be more efficient in the sense of a reduced number of measurement points, it may be less effective when digital processing is involved. Specifically, the time consuming interpolating step is required to put data presented in other types of sampling lattice into the proper type for the computer. Two dimensional impulse responses reconstructed from cubic sampled data are compared with those using Mensa et al.'s method. The responses obtained also indicate good potential for image reconstruction via the spatial impulse response.

A3-2
0900

THE MOON AS A CALIBRATION TARGET OF CONVENIENCE FOR VHF - UHF RADAR SYSTEMS*

J. K. Breakall
University of California
Lawrence Livermore National Laboratories, Livermore, CA

J. D. Mathews
Electromagnetic Waves and Wave Propagation Group
Case Western Reserve University, Cleveland, Ohio

M. P. Sulzer
National Astronomy and Ionosphere Center
Arecibo Observatory, Arecibo, Puerto Rico

This paper presents a convenient method for the necessary calibration to verify the performance of a radar system in an absolute sense using the moon as a radar target. As a result of work performed to calibrate the Arecibo 430 MHz incoherent scatter ionospheric radar system in an absolute power sense the idea occurred to use the moon as a reasonably general calibration target. In many geophysical applications such as ionospheric probing at Arecibo the absolute performance characteristics of VHF and UHF radars is often more important than relative characteristics. The lunar absolute radar scattering cross-section, σ_o, which is large and well known is about $0.07\pi\ r_\ell^2$ (r_ℓ is the lunar radius) and is nearly frequency independent for 6 m$\geq \lambda \geq$1 cm. In this paper the lunar radar equation will be derived in its various forms for wide and narrow beam scattering and pulsed and CW radars. The results of applying these derivations of the radar equation to the Arecibo 430 MHz moon bounce calibration experiments will be given. Summary and general discussion of how the moon may be used as a VHF - UHF calibration target will conclude this paper. The moon has been found to be a useful target for the absolute calibration of the Arecibo 430 MHz radar system. We suggest that calibration of other radar systems in a similar fashion seems feasible. The level of error to be expected in comparing two different radars would likely be $\pm$2 dB. To achieve better results than this would be difficult and probably expensive.

A3-3 MEASUREMENT OF THE SURFACE CURL OF THE SURFACE CURRENT DENSITY
0920

Carl E. Baum
Air Force Weapons Laboratory
Kirtland Air Force Base
Albuquerque, New Mexico 87117-6008

It is commonplace to measure the surface divergence of the surface current density on a perfectly conducting object. This is related to the surface charge density, or the normal electric field. This paper explores the measurement of a complementary quantity, the surface curl of the surface current density which can be related to an equivalent magnetic charge density, or the normal derivative of the normal magnetic field. Techniques and difficulties are discussed.

A3-4
0940

A RADIO-FREQUENCY POWER DELIVERY SYSTEM: PROCEDURES FOR ERROR ANALYSIS AND SELF-CALIBRATION

M. Kanda, W. J. Anson, and R. D. Orr
Electromagnetic Fields Division
National Bureau of Standards
Boulder, Colorado 80303

An expression is developed for net power delivered to a load in terms of the indicated forward and reflected power and the system S-parameters and reflection coefficients. The dual directional coupler is treated as nonideal with power reflections assumed between all ports. The system itself is used to evaluate the major S-parameter terms in net power computation, and uncertainty in the power meter readings and incompletely known S-parameters.

We derived an equation for computing the net power to a load antenna using a power delivery system for which all of the S-parameters are assumed to be nonzero. An S-parameter description of the system yields equations by which the system can be self-calibrated using two standard mismatch terminations. When the system used a dual channel power meter and is calibrated by the procedure described, the maximum uncertainty in P_{net} is ± 16% (for $|\Gamma_4| = 0.05$). This uncertainty can be reduced to 11.4 percent by using a single channel power meter. We have shown that a P_{net} computation based on the "ideal system" assumption may be sufficient if the reflection coefficient of the load is small.

A3-5
1020

THREE APPROACHES USED AT NBS TO DETERMINE THE GAIN OF EMC ANTENNAS

E. B. Larsen
Electromagnetic Fields Division
National Bureau of Standards
Boulder, Colorado 80303

The meaning and description of three independent techniques for determining antenna gain are discussed. Two definitions used in the EMC community are explained. One is "gain" (G), or true gain; the other is "realized gain" (G_{re}), or effective gain. G is an inherent property of an antenna, and is independent of its impedance, while G_{re} is the realized value after reduction by mismatch loss between the antenna and (50 Ω) system. If the antenna impedance is known (by measurement or theory), G_{re} can be converted to G. Other topics include the relations between antenna gain, antenna factor, effective length of a linear antenna, effective area of an aperture antenna, etc. Measured values are presented for typical EMC antennas.

Three approaches used at NBS to determine antenna gain are:

(1) "Relative gain." In this gain-comparison technique, an antenna under test (AUT) is compared experimentally with one that is known (by theory or measurement). For example, a reference field generated locally by a transmitting antenna (or ambient field) is employed. The pickup power or voltage of the AUT is compared with that of the "gain standard."

(2) "Absolute gain, insertion loss measurement." This technique involves two identical antennas, one transmitting and the other receiving. The gains of three general antennas can also be measured taking three sets of data for three pairs of antennas. In each case, the power received when the transmitter and receiver are directly connected is compared with the power received when the radiated path is inserted between the transmitting and receiving antennas. Refinements to the technique, such as the use of an "extrapolation range," are mentioned.

(3) "Absolute gain, theoretical calculation." The most common gain standards are horns or open-ended waveguides (OEG) for aperture antennas, dipoles or monopoles for linear antennas, and loops for H fields. The gains of a pyramidal horn (including near-zone reduction), thin dipole or monopole (self resonant or electrically short), and single-turn circular loop are given.

A3-6 1040 DOSIMETRY: A SURVEY OF THEORETICAL AND EXPERIMENTAL TECHNIQUES: Dr. Adel Abd El-Masieh Saleeb, Faculty of Electronic Engineering, Menouf, Egypt

Studies concerning the biological effects of electromagnetic radiation aim at linking the physical characteristics of EM fields and the magnitude of the effect. An important step toward this goal is quantifying the relationship between the properties of the exposure EM fields and the rate of energy absorption of fields in the exposed tissue. The process of finding this relationship is called "DOSIMETRY."

Theoretical techniques (analytical and numerical) are used to calculate the EM fields inside models of the human body. In the analytical techniques, Maxwell's equations are solved by some analytical methods while numerical techniques are characterized by the solution of large systems of simultaneous equations either by matrix inversion or by iterative techniques. The development of these techniques, their advantages and limitations are discussed.

Experimental techniques used for measuring the absorbed power in living and sacrificed animals (and recently in human volunteers) are reviewed.

A3-7
1100 ATTENUATION AND REFLECTION COEFFICIENT OF A SEMICONDUCTOR PANEL APPLIED TO THE SAMPLING OF MILLIMETER WAVE IMAGES: M. H. Rahnavard and A. Habibzadeh, Electrical Engineering Department, Shiraz University, Shiraz, Iran

The scattering image of an object illuminated by millimeter wave radiation is passed through a thin semiconductor panel. The mm wave image is sampled at the surface of the semiconductor by scanning a light beam across the panel surface to modulate the transmission/reflection properties of the panel. The modulation is produced by carrier generation due to the optical beam whose wavelength corresponds to an energy greater than the energy gap of the semiconductor. The transmitted/reflected mm wave radiation is collected by horn antennas, detected and electronically processed to construct the mm wave image. The excess carrier response due to the scanning (sampling) beam velocity, position, and the resultant mm wave transmission/reflection are studied.

A3-8
1120

INFRARED DETECTION OF MICROWAVE SCATTERING FROM CYLINDRICAL STRUCTURES

Ronald M. Sega and John D. Norgard
Department of Electrical Engineering
University of Colorado
Colorado Springs, CO 80933

A quantitative analysis is presented for scattered electric fields from cylindrical structures at 2-4 GHz using an infrared detection technique. The scattered fields interact with absorbing material screens resulting in joule heating. The material screens, essentially electric field detectors, are placed at a selected plane of the scattered field from which a direct or inverse scattering investigation can be performed. The associated infrared emission is detected, measured and related directly to the electric field strength at each pixel location of a multiple-frame averaged, digital presentation of the data. Thus, the scattered fields from the test structures are determined quickly, accurately and globally using a non-destructive, minimally-perturbing technique.

This experimental technique compliments classic theoretical methods and probe measurements. It is difficult to determine the scattered fields from complicated geometrical structures using existing analytical techniques. Only where a high degree of geometrical symmetry prevails, is it feasible to calculate the scattered fields exactly in closed mathematical form. With numerical solutions, many cases of practical interest remain unsolved or require extensive computer calculations. Experimental methods to determine the scattered field using electric and/or magnetic field probe techniques require multiple probe measurements and extensive correction procedures. Alternative methods, such as infrared detection, should be valuable in the investigations of direct and inverse scattering from complex structures.

The infrared detection technique provides a rapid method to determine fields scattered from objects such as finite metal plates, cylinders, or geometrically complex objects, with multiple layers of dielectric or magnetic coatings. To verify the accuracy of the infrared technique, simple canonical objects, viz., planes and cylinders, were tested in an anechoic chamber. The diffracted fields were detected with a carbon screen and the experimental data is compared with corresponding theoretical/numerical results. More complicated structures, for which there are no theoretical solutions, were also studied and the results are presented.

1120 Discussion

Session B-10 0835-Thurs. CR2-28

ANTENNAS - II

Chairman: S. A. Long, University of Houston, Houston, TX 77004

B10-1
0840 DETERMINATION OF RESONANT MODES FOR AN ARBITRARY MICROSTRIP PATCH ON AN ELECTRICALLY THIN SUBSTRATE

Edward F. Kuester and Thomas M. Martinson
Electromagnetics Laboratory
Department of Electrical and Computer Engineering
University of Colorado
Campus Box 425
Boulder, CO 80309

By using the quasi-static electric and magnetic fields near the edge of a half-plane on top of a grounded dielectric slab, we represent the fringing fields of the resonant modes of a microstrip patch of arbitrary shape. The correction to the resonant frequency predicted by the magnetic wall model involves not only an equivalent edge extension, but also some mutual interaction terms involving fields which couple opposite edges of the patch over the top, rather than underneath the patch. These interaction terms take the form of dynamic mutual inductance integrals which can be evaluated for several shapes of patch. A comparison will be made with several of the simpler theories of microstrip patch antennas, as well as with numerical solutions and experimental results. The strengths and weaknesses of other approximate theories will be discussed in light of our method. In particular, it will be seen to be compatible with the segmentation method for analyzing planar circuits, by improving the model used to account for field interaction over the top of the patch.

B10-2
0900

IMPEDANCE MATCHING OF MICROSTRIP ANTENNAS WITH REACTIVE LOADS

William F. Richards and Stuart A. Long
Department of Electrical Engineering
University of Houston - University Park
Houston, Texas 77004

Many possible applications of reactively loaded microstrip antennas have been reported in the literature. These include tuning the resonant frequency of a microstrip antenna, adjusting its polarization, producing dual bands spaced arbitrarily close to each other, and producing endfire microstrip elements. This paper will report on yet another application, the impedance matching of microstrip antennas. A theory and corroborating experimental results will be presented showing that for a fixed feed point, one can adjust the impedance of a microstrip element over a wide range *without changing* its resonant frequency or its pattern. This is done by appropriately loading the patch with two or more reactive loads. The simplest reactive load that can be used is a short circuit. By symmetrically loading the patch with one or more pairs of shorts, one can adjust the impedance without raising the level of cross-polarization over that of an unloaded element. Using PIN diodes to form the shorts allows one to dynamically change the input impedance to resopond to changing environmental conditions. For example, one may be able to re-match an array element as the beam scan angle is changed.

B10-3
0920

EFFECT OF MUTUAL COUPLING ON THE INPUT IMPEDANCE AND RESONANT FREQUENCY OF A RECTANGULAR MICROSTRIP PATCH ANTENNA

K.C. Gupta and Abdelaziz Benalla
Department of Electrical and Computer Engineering
University of Colorado
Box 425
Boulder, CO 80309

This paper discusses the effect of the mutual coupling between two radiating edges of a microstrip antenna on the input impedance and resonant frequency of a rectangular microstrip antenna.

The mutual coupling effect is taken into account by constructing a mutual admittance matrix to represent the interaction between two edges. The two edges are partitioned into number of sections (typically 20 on each edge). The mutual admittance element Y_{ij} (relating equivalent magnetic current at section j of one edge to the electric current induced at section i at the other edge) is obtained from the expressions for the fields of a magnetic current element. Two dimensional analysis method, for analyzing microstrip patches, has been modified to incorporate this mutual admittance matrix. For this purpose, the mutual admittance matrix is collapsed in a smaller matrix corresponding to the number of ports considered at the two edges for implementing the segmentation method. Diagonal terms of this reduced matrix are replaced by the self-admittance values used in antenna analysis without considering the mutual coupling. Segmentation procedure yields the overall input impedance of the patch antenna at the feed point.

It is found that mutual coupling reduces the input impedance of the patch and shifts its resonance frequency slightly. A detailed discussion of these effects and design modifications needed to compensate for them will be presented.

B10-4
0940

EDGE ADMITTANCE FOR MICROSTRIP ANTENNAS WITH A DIELECTRIC COVER LAYER

Yinggang Tu, K.C. Gupta and D.C. Chang
Department of Electrical and Computer Engineering
University of Colorado
Campus Box 425
Boulder, CO 80309

Conductive patches of microstrip antenna are often covered with a dielectric layer for protective purposes. In order to design microstrip antennas with a cover layer by transmission line method or two-dimensional analysis method, one needs to know the equivalent edge admittance at the radiating edges.

This paper reports the evaluation of edge admittance of microstrip antennas in the presence of a cover layer. The canonical problem of a grounded dielectric slab with a truncated upper conductor is solved by Wiener-Hopf technique. This is an extension of the Wiener-Hopf method employed earlier for microstrip antennas without a cover layer. The method yields the value of reflection coefficient at an open edge and the equivalent edge admittance is found therefrom.

Numerical results show that the presence of a cover layer increases both the conductance and the susceptance parts of the edge admittance. For example, value of edge admittance without a cover layer (at 9 GHz, for $\varepsilon_r = 2.5$, and substrate thickness 1/16 inch) is (0.32 + j0.98) mhos/m. When a cover layer of equal thickness (1/16 inch, and $\varepsilon_r = 2.5$) is placed over this microstrip antenna, the value of the edge admittance is modified to (0.53 + j1.39) mhos/m.

Increase in the value of edge conductance implies that the impedance bandwidth of the microstrip patch is increased. Increase in the value of the susceptance part corresponds to the increase in fringing capacitance at the edges. This results in reduction of the physical length of a rectangular patch. These changes in design and performance of rectangular patches caused by the presence of a cover layer would be discussed.

B10-5
1000

RADIATION CHARACTERISTICS OF MULTIPLY-FED DIPOLE ANTENNA

H. A. RAGHEB AND M. HAMID

Antenna Lab., Elec. Eng. Dept.
university of manitoba
winnipeg, canada, R3T 2N2

This paper presents an extension of Hurd's solution (Can. J. Phys., 44, 1723-1743,1966) for the input admittance of a long linear antenna to the general case of an arbitrarily and multiply-fed dipole antenna. The arbitrarily fed dipole shown in Fig. (c) is solved using a superposition of the two cases shown in Figs. (a) and (b), while the multiply-fed dipole (not shown) is considered as a superposition of the arbitrarily fed dipole. Accurate expresions for the radiation pattern, current distribution and input admittance of the arbitrarily fed dipole antenna are derived by the Wiener-Hopf technique. The results are compared with Harrington's solution (IEEE Trans. on Ant. and Prop., 15, 502-515, 1967) for the case of an arbitrarily fed dipole and very close agreement is observed. For a multiply-fed dipole a comparison with Strait's numerical solution (IEEE Trans. on Ant. and Prop., 18, 699-700,1970) indicates that our expression for the radiation pattern is highly accurate even when it only corresponds to the first order expression for the current distribution. The current distribution and the input adimttance are calculated up to the third order and include terms of $O(1/h^2)$ where h is half the tip to tip length of the antenna.

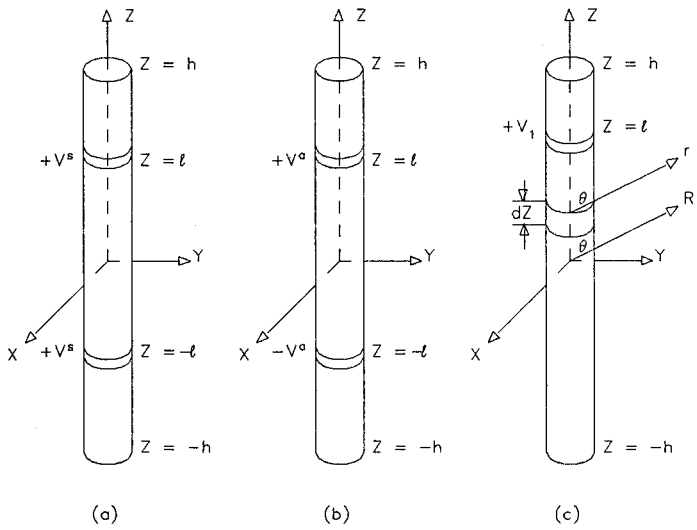

Geometry of the problem.

B10-6
1020

AN INVESTIGATION OF A MONOPOLE ANTENNA ATTACHED TO A CONDUCTING BOX

Shyamal Bhattacharya, Stuart A. Long, and
Donald R. Wilton
Department of Electrical Engineering
University of Houston - University Park
Houston, Texas 77004

The problem of a monopole antenna over a large ground plane has been throughly investigated in the past, and even the case of finite sized ground planes has received attention. In many practical applications, however, monopoles are mounted on quite arbitrarily shaped conducting bodies (eg. aircraft, vehicles, ships, buildings, etc.). For this reason an investigation has been undertaken to determine the circuit and radiation properties of monopoles attached to more generally shaped conductors. This study includes both numerical analysis techniques to attack the problem theoretically and experimental measurements on actual physical models.

As a beginning experimental study, a conducting cubical box was constructed and attached to a ground plane. A monopole was then attached to the top surface of this structure and the input impedance of the monopole was measured using an automated network analyzer. The fixture was fabricated in such a fashion that the position of the monopole could be varied from the center of the top surface both along a line to a point near the center of one edge and along a diagonal line to a point near one corner. The resonant frequency and the input impedance was recorded for each location using a constant length monopole. The size of the monopole is then changed and the procedures repeated. Examining the impedance as a function of frequency near the point where the monopole was a quarter wavelength long, allows an effective investigation of the functional dependence of the impedance on the electrical size of the box. The range of sizes of monopoles resulted in box edge lengths from one to one-quarter wavelength. Comparisons with results calculated from a patch model of the structure were made and reasonable correlation was found.

B10-7 1040 ANALYSIS OF PARALLEL MONOPOLE ANTENNAS RESIDING IN CONTIGUOUS MEDIA

K.A. Michalski and C.E. Smith
Department of Electrical Engineering
University of Mississippi
University, MS 38677

An integral equation is formulated and solved numerically for the current distribution on two parallel monopole antennas mounted on a ground plane and residing in two contiguous media. The monopoles, one of which is driven by a coaxial cable, are perpendicular to the ground plane and are parallel to and on opposite sides of the interface. Numerical results are presented for several cases of interest and are compared with measured data in the case where the lower, driven monopole resides in fresh or salt water and the upper, parasitic monopole resides in air (see figure below).

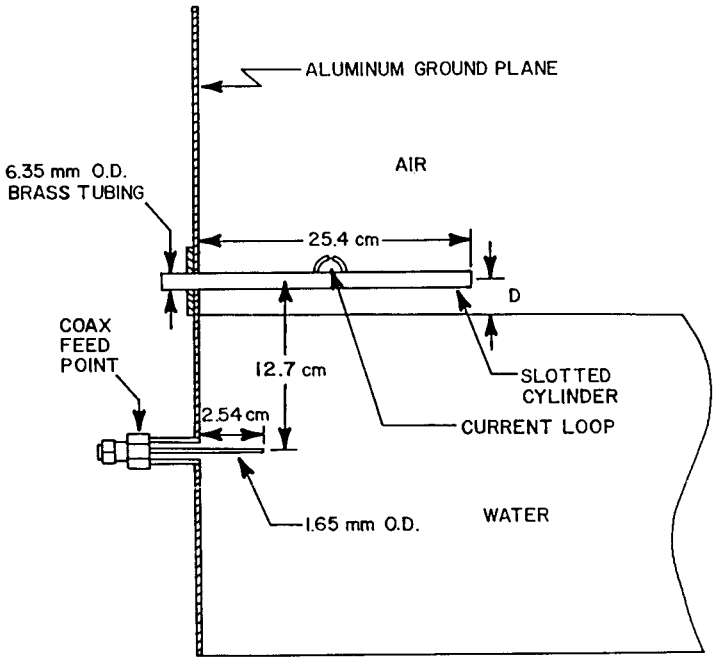

B10-8
1100

AN EQUIVALENT CIRCUIT FOR MULTIPORT RECEIVING ANTENNAS

A.T. Adams
Department of Electrical and Computer Engineering
Syracuse University
Syracuse, NY 13210

Equivalent circuits are derived for multiport receiving antennas in the presence of incident fields. The multiport antennas may thus be considered as an active linear device. Equivalent circuits which are generalizations of the Thevenin's and Norton's equivalent circuits for the one-port device are obtained. Equivalent circuits involve open-circuit voltages, short-circuit currents, mixed-source representations. The elements of the equivalent circuits may be related to incident fields and to the properties of the passive system under various transmitter excitations.

B10-9
1120

THE EFFECTS OF COVER-LAYER ON RADIATION AND SURFACE-WAVES OF A MICROSTRIP PATCH ANTENNA

Ahmad Hoorfar, K.C. Gupta and D.C. Chang
Department of Electrical and Computer Engineering
University of Colorado
Campus Box 425
Boulder, CO 80309

The effects of a thick cover-layer on the radiation pattern, surface-wave modes and efficiency of a microstrip-patch antenna are investigated. Assuming a very thin substrate, the patch is modeled with a magnetic line source on a conducting plane with a possibly thick dielectric cover of thickness, t. This model is used to calculate the (space-wave) radiation pattern as well as the radiated and surface-wave power as a function of cover-layer thickness, $k_0 t$. It is found that the beamwidth in E-plane will initially decrease and then increase upon increasing $k_0 t$. It is also shown that for the values of $k_0 t \gtrsim 1$, the power carried by the surface-waves is almost entirely contained inside the cover-layer; this suggests the possibility of placing a graded lossy thin-film between the substrate and the cover layer in order to attenuate the surface-waves propagation (and their eventual radiation as a side lobe). Numerical results will be presented to show the effects of a lossy dielectric cover-layer on the surface-waves and the radiated power.

B10-10 1140 EFFECTS OF CYLINDRICAL-CURVATURE ON RADIATION PATTERN OF A MICROSTRIP ANTENNA WITH A COVER-LAYER

Ahmad Hoorfar, K.C. Gupta and D.C. Chang
Department of Electrical and Computer Engineering
University of Colorado
Campus Box 425
Boulder, CO 80309

The fundamental effects of cylindrical curvature on the radiation pattern and radiated power of a microstrip patch antenna with a cover-layer are investigated. The method of analysis is based on modeling the patch with a magnetic line source on a conducting cylinder. This model is valid for a thin-substrate with a possibly thick cover-layer (superstrate). Extensive numerical results for the radiation pattern in the azimuthal-plane and for various cover-layer thickness $k_0 t$ and cylinder diameter to wavelength ratio d/λ_0 are obtained. Significant rippling effects and distortions in radiation patterns and sharp peaks in total radiated power appear for specific values of d/λ_0 and $k_0 t$. This behavior is due to surface-waves going around the cylinder. Also beamwidth increases by decreasing the value of d/λ_0. The above effects are most pronounced in the range $0.5 \leq k_0 t \leq 1.5$ and $5 \leq d/\lambda_0 \leq 20$. As will be discussed, the ripples in the radiation pattern can be substantially reduced by making the dielectric cover lossy.

B11/F4-1
0840 A COMPARISON OF SMOOTHING AND ITERATION FOR RANDOM SURFACE SCATTERING

Gary S. Brown
Department of Electrical Engineering
VPI & State University
Blacksburg, VA 24061

In a recent paper (G. S. Brown, IEEE Trans. Antennas & Propg., AP-32, 1308-1312, 1984), the method of smoothing was applied to the rough surface scattering problem. A series solution was obtained which appeared to be significantly different from the standard iterative solution and only under a very restrictive approximation could the smoothing and iterative series be reconciled. Thus, the relationship between the results generated by these two different techniques is still largely an open question. This paper will shed some new light on this subject.

In the process of simplifying the smoothing result, it was found that one of the series contained in the result was, in fact, a null series, i.e. the full infinite series summed to zero. This discovery has led to a new series solution for both the coherent and incoherent scattered fields. This new solution shows certain advantages relative to conventional series solutions and particularly in regard to the satisfaction of extinction. Furthermore, when the null series is fully removed from the smoothing series, it can be shown that the result is identical to the iterative series solution after the null series is fully removed from it. Thus, the primary conclusion of this paper is that smoothing and iteration series are identical, but only after certain null series are removed from each solution. The removal of the null series also appears to give rise to a series (either through smoothing or iteration) which converges more rapidly; however, this point requires more detailed study.

B11/F4-2
0900

SCATTERING BY ROUGH SURFACES: PERTURBATION THEORY REVISITED

C. Eftimiu
McDonnell Douglas Research Laboratories
P.O. Box 516
St. Louis, MO 63166

Perturbation theory can be applied to study the scattering of electromagnetic waves by surfaces which are statistically characterized by small variances and large correlation lengths. Most of the previous work based on perturbation theory reported in the literature has made use of the Rayleigh hypothesis, and is therefore partly incorrect. A notable exception is the work of M. Nieto-Vesperinas, based on the extinction theorem.

We show that the same correct results can be obtained by using the Electric Field Integral Equation in a consistent manner. In the process, we point out the possibility of relaxing the assumption of large correlation lengths, i.e. of small slopes.

B11/F4-3
0920

SCATTERING AND DEPOLARIZATION BY CONDUCTING CYLINDERS WITH ROUGH SURFACES

Ezekiel Bahar and Mary Ann Fitzwater
Electrical Engineering Department
University of Nebraska--Lincoln
Lincoln, NE 68588-0511

ABSTRACT

The problem of electromagnetic scattering by finitely conducting cylinders or spheres has been dealt with extensively in the technical literature. Perturbation theory has been used to extend these results to scattering by slightly rough circular cylinders or spheres (D. E. Barrick et al. Radar Cross Section Handbook, Chapter 8, Plenum Press, 1970). However, perturbation theory is limited to surfaces for which the roughness parameter $\beta = 4k_o^2\langle h_s^2\rangle < 0.1$ (k_o is the electromagnetic wavenumber and $\langle h_s^2\rangle$ is the mean square height of the rough surface (G. S. Brown, IEEE Trans. Ant. and Prop. AP-26 (3) 472-482, 1978). For $\beta < 0.1$ the scattering cross sections are not significantly different from those for smooth conducting circular cylinders.

In this work the full wave approach (E. Bahar, Radio Sci. 16(6), 1327-1335, 1981), is used to determine the like and cross polarized scattering cross sections at optical frequency for finitely conducting cylinders with roughness scales that significantly modify the scattering cross sections. The radii of curvature of the unperturbed cylinders considered are large compared to wavelength λ. (However, the cross section of the unperturbed cylinder need not be circular). Both specular point scattering and diffuse scattering are accounted for in the analysis in a self-consistent manner and the scattering cross sections are expressed as a weighted sum of two cross sections.

The full wave solutions are presented for long cylinders with mean circular cross sections and both the specular point and diffuse contributions are identified. Several illustrative examples are considered for cylinders with roughness parameter $\beta = 1$. The rough surface is characterized by its surface height spectral density function. The like and cross polarized cross sections as well as the albedos for smooth and rough cylinders are compared.

B11/F4-4
0940

A MULTIPLE-SCATTERING LAYER APPROXIMATION FOR PROPAGATION IN DISCRETE RANDOM MEDIA

C. L. Rino
SRI International
333 Ravenswood Avenue
Menlo Park, CA 94025

An iterative method has been developed for computing the successive interactions of a directed wavefield with random planar distributions of discrete scatterers. Effectively, the method is a generalization of the multiple-phase-screen method that has been applied to propagation problems in continuous random media. For symmetric scatterers, coupled difference equations for the forward and backscattered signal moments through second order can be derived and solved. The computational method and some results that have been obtained for both lossless scatterers and lossy scatterers are described. The results are compared with other computational methods that predict power transmission and reflection coefficients for slabs of discrete scatterers.

B11/F4-5 RADIATIVE TRANSFER EQUATIONS MODIFIED FOR
1020 APPLICATION TO DENSE NONTENUOUS MEDIA

Leung Tsang and Akira Ishimaru
Department of Electrical Engineering
University of Washington
Seattle, WA 98195

The classical radiative transfer equation has been used extensively in studying volume scattering in remote sensing problems. The advantages of using the radiative transfer theory are that (i) multiple scattering of the incoherent intensities are included in the theory, (ii) energy conservation is satisfied, and (iii) numerical solutions are tractable. However, the transfer equation, in its classical form, is not applicable for dense nontenuous media.

In a dense medium, the particles occupy an appreciable fractional volume. In a nontenuous medium, the permittivity of the particles is significantly different from that of the background medium. In a dense nontenuous medium, the assumption of independent scattering of the particles no longer holds so that the classical transfer equation is not valid. In this paper, we derive a set of "new" transfer equations from analytic wave theory. The approximations made on the analytic wave theory are (i) quasi-crystalline approximation with coherent potential on the first moment of the field and (ii) a modified ladder approximation for the second moment of the field. These two approximations are shown to satisfy energy conservation. The differences between the "new" set of transfer equations and the classical ones will be discussed. Both the scalar wave equations and the vector electromagnetic propagation will be studied.

B11/F4-6 **Intensity Scintillations of Spatially Extended, Incoherent Sources**
1040

J. L. Codona and R. G. Frehlich †
Dept. of Electrical Engineering and Computer Science
C-014
University of California, San Diego
La Jolla, CA 92093

Using the Green's function formalism, a series solution is presented for the correlation of the intensity fluctuations of waves propagating through an extended random medium from a spatially-extended, incoherent source. The statistics of the random medium are assumed to be homogeneous in the direction transverse to the propagation but locally homogeneous in the propagation direction. Assuming the source emits a zero-mean complex Gaussian field that is delta-correlated in space, produces two terms for the intensity correlation. One is the "standard" intensity correlation obtained by summing the intensity contributions from different regions of the source. The second contribution describes the correlation of the rapid temporal fluctuations observed with a Hanbury Brown and Twiss intensity interferometer. The introduction of a model narrow-band receiver clarifies the role of these two contributions in a typical observation. The intensity spectrum of each contribution is expressed as a high and low spatial-frequency series. The effect of source averaging on the scintillation index and typical intensity correlation scales are presented for both weak and strong scattering. Where possible, these expressions are compared to previous results.

† Present Address:
University of Colorado, Boulder
CIRES
Campus Box 449
Boulder, CO 80309

B11/F4-7
1100

WAVE-KINETIC NUMERICAL SIMULATION OF BEAMS IN INHOMOGENEOUS MEDIA

D. A. de Wolf and J. K. Pack
Department of Electrical Engineering
VPI&SU
Blacksburg, VA 24061

A novel and efficient technique for computer simulation of electromagnetic beams in (randomly) inhomogeneous media has been applied to several canonical problems. The irradiance of the beam is calculated from the Wigner distribution function (WDF), which is approximately conserved in forward scattering media over long distances - well into the diffraction region. Instead of constructing a beam from very many rays, the method uses a relatively small number of ray trajectories which obey the equations of geometrical optics. A Gaussian interpolation scheme in 4 dimensions fills out the WDF, and allows efficient computation of the irradiance.

Two canonical problems tested with this method are: i) diffraction of a Gaussian beam in free space (for which analytical approximations are available), and ii) scattering of a plane wave by a Gaussian inhomogeneity in the permittivity. In the latter case, Monte-Carlo generation of very many rays as well as a Born approximation (less accurate) was used for comparison. The comparisons, and further tests (if available) will be discussed.

B11/F4-8 1120 THE CLOSURE PROBLEM FOR THE STOCHASTIC CUBIC PARABOLIC EQUATION

I. M. Besieris and M. E. Sockell
Department of Electrical Engineering
Virginia Polytechnic Institute and
State University
Blacksburg, Virginia 24061

Exact solutions for representative stochastic nonlinear problems arising in physical applications are practically impossible. As a consequence, a serious effort must be made to develop formal asymptotic or perturbative techniques which will yield reasonable approximate solutions. Such solutions, in connection, e.g., with the transmission of a thermally self-stressed laser beam in a turbulent medium, should provide insights into physical effects such as nonlinear refraction, attenuation of radiation, and incoherent degradations on the phase and amplitude of the beam.

Our specific aim in this exposition is to examine the closure problem for the stochastic cubic parabolic equation under conditions of strong field fluctuations and finite range correlation lengths. Closed coupled equations for the second and fourth order moments are derived by working in phase space via a Wigner distribution function. Our work extends previous results by Kraichnan, Weinstock, Balescu and Misquich on hydrodynamic (Navier-Stokes) and plasma (Vlasov) turbulence.

Session G-8 0835-Thurs. CR0-30

MATSUSHITA MEMORIAL

Co-Chairmen: E. K. Smith, California Institute of Technology, Jet Propulsion Laboratory, Pasadena, CA 91109; and B. B. Balsley, Aeronomy Laboratory, ERL/NOAA, Boulder, CO 80303

G8-1
0840

DR. MAT - A GRADUATE STUDENT'S PERSPECTIVE

D.N. Anderson
Air Force Geophysics Laboratory
Hanscom AFB MA 01731

My introduction to Dr. Mat was through his course on Geomagnetism. For whatever reasons, this course convinced me that my interest in atmospheric sciences - aeronomy and ionospheric physics - was for real. Only later, after he became my thesis advisor, did I come to fully appreciate Dr. Mat's support, encouragement and enthusiasm.

G8-2
0900

WHAT GEOMAGNETISM OWES TO S. MATSUSHITA

Wallace H. Campbell
U. S. Geological Survey
Federal Ctr., MS 964, Box 25046
Denver, CO 80225

Sadami Matsushita, of the National Center for Atmospheric Research, died in Boulder on 15 March 1984, at the age of 64. His first scientific article (on F-region lunar tides) appeared in the *Journal of Geomagnetism and Geoelectricity* in 1949. By the time of his death he had published 153 articles of which 94 concerned geomagnetism topics. Although he studied a broad range of geomagnetic subjects such as sudden field impulses, solar eclipse effects, geomagnetic storms, rapid field pulsations and interplanetary field sector effects, his major contributions focused upon the ionospheric currents driven by gravitational, thermal, and wind processes. The complexities of the origins and behaviors of Sq (solar-quiet) and L (lunar) geomagnetic field changes were resolved through the publications of Dr. Matsushita during his 35 years of diligent research. His publications spanned a broad range from mathematical representations to semipopular movie films of the current systems. Numerous highlights of the Matsushita geomagnetic studies will illustrate the presentation of this tribute to his memory.

G8-3
0920

MEMORIES OF SPORADIC E AND S. MATSUSHITA

Ernest K. Smith
California Institute of Technology
Jet Propulsion Laboratory
Pasadena, CA 91109

The author's attention was first drawn to Dr.Matsushita in 1953 when, as a graduate student working on a sporadic-E thesis at Cornell, he thought he was the first to definitively tie down the geographical relationship between equatorial sporadic E (dubbed q-type for the IGY) and the equatorial electrojet, only to discover that Dr. Mat had already published the connection in an obscure Japanese journal. When we both ended up in Boulder our friendship ripened and, during the sixties we co-edited a book and jointly ran three triennial sporadic-E symposia. As well as being a careful and indefatigable researcher, Dr. Mat was also the perfect collaborator. Whenever faced with a difference in viewpoint over any of the multitude of inconsequential details of a conference, Dr. Mat had a standard answer: "No problem, you decide", but where it impacted his scientific integrity that was another matter.

Temperate latitude sporadic E does not appear to have received the attention in the last 15 years that it did in the prior three decades. Yet there were still many unanswered questions when interest slackened around 1970. Therefore an attempt is made in this paper to determine which of these unanswered questions have now safely been laid to rest and which are still with us. Principal among these questions are whether the proposed causes can explain the observed statistics, in particular: 1) the seasonal distribution of Es, 2) the diurnal distribution, 3) the geographic variation, 4) the magnetic correlation, and 5) the year-to-year variability.

G8-4
0940

PROFESSOR S. MATSUSHITA: PERSONAL REFLECTIONS OF A WOMAN SCIENTIST

Sunanda Basu
Emmanuel College
Boston MA 02115

I had the privilege of working with Professor S. Matsushita at several of the Equatorial Aeronomy Conferences. He strongly felt that women scientists should have an active role at international meetings. Some personal reflections are shared.

G8-5
1000

Dr. Sadami Matsushita: His Contributions to the International Symposium on Equatorial Aeronomy (SEA)

Ben B. Balsley

One of the many contributions of Dr. Sadami Matsushita to the international community of science was his active participation in and careful guidance of the quasi-periodic meetings of the International Symposium on Equatorial Aeronomy (ISEA). These symposia, which are convened roughly every four years, were initiated as a forum for the presentation of studies on the equatorial ionosphere. In the course of this presentation, we will present a brief history of the ISEA, as well as some of the highlights of this rather unique symposium.

Session G-9 1020-Thurs. CR0-30

ROUND TABLE DISCUSSION ON GLOBAL IONOSPHERE AND AERONOMY STUDY PROGRAM

Moderator: Jules Aarons

G9 1020 Panel Members: H. C. Carlson, A. J. Ferraro, iu, C. H. Liu, C. M. Rush and R. W. Schunk

An exciting opportunity to focus on the physics and technology of the ionosphere will be presented by the Global Ionosphere and Aeronomy Study to be pursued at the end of this decade. Suggestions as to programs, needs of the technology community, unknown physical relationships etc. will be discussed by members of a round table and the audience. The concept is to begin to put together a program for URSI and the community involved in ionospheric physics and technology to pursue.

Session H-6 0835-Thurs. CR0-26

WAVE PROCESSES STIMULATED BY CHEMICAL RELEASES

Chairman: P. A. Bernhardt, Los Alamos Scientific Laboratory, Los Alamos, NM 87545

H6-1
0840

A COMPARISON OF THE PLASMA WAVE SPECTRA FROM 100 HZ TO 100 KHZ FOR THE EIGHT AMPTE CHEMICAL RELEASES

H.C. Koons and J.L. Roeder
Space Sciences Laboratory, The Aerospace Corporation, P.O. Box 92957, Los Angeles, CA 90009
O.H. Bauer, G. Haerendel, and R. Treumann
Max-Planck-Institute for Physics and Astrophysics
Institute for Extraterrestrial Physics
Garching by Munich, Germany
R.R. Anderson and D.A. Gurnett
Department of Physics and Astronomy
University of Iowa
Iowa City, IA 52242
R.H. Holzworth
Space Sciences Division, University of Washington, Seattle, WA 98195

The AMPTE IRM spacecraft performed a series of eight chemical releases at high altitudes. There were two lithium releases in the solar wind, two lithium and two barium releases in the near-earth magnetotail , and two barium releases to simulate artificial comets, one in the solar wind and the other in the magnetosheath. A variety of plasma waves were observed in conjunction with each of the releases. The releases were performed essentially in comparable pairs. Although there were unique features associated with some of the individual releases, the comparable releases generally produced similar wave emissions. This paper will discuss the similarities and differences among the releases.

A dominant feature of all of the releases was the presence of Langmuir waves. These waves have been used to determine the temporal and spatial variation of the local plasma density. Natural electromagnetic radiation such as continuum radiation and kilometric radiation was excluded from the plasma clouds at all frequencies below the electron plasma frequency. Ion-acoustic and electron cyclotron harmonic waves were observed in the transition region between the lithium ion cloud and the solar wind

The barium releases all produced radiation at the barium ion plasma frequency inside of the barium cloud. Broadband bursts of electrostatic noise were encountered on the sunward side of the compression region. This noise was similar to the noise observed in the earth's bow shock. The barium releases in the tail produced a plasma cloud whose density remained above ambient levels for 20 minutes. The density displayed considerable temporal structure as it decayed to ambient levels.

H6-2
0900

NUMBER DENSITY OBSERVATIONS OBTAINED FROM THE PLASMA WAVE EXPERIMENT DATA DURING THE AMPTE BARIUM AND LITHIUM RELEASES IN THE SOLAR WIND, MAGNETOSHEATH, AND TAIL

R.R. Anderson and D.A. Gurnett
Department of Physics and Astronomy
The University of Iowa
Iowa City, Iowa 52242
R.A. Treuman, O.H. Bauer, and G. Haerendel
Max-Planck-Institut fur Extraterrestrische Physik
D-8046 Garching, West Germany
R.H. Holzworth
Geophysics Program, University of Washington
Seattle, Washington 98195
H.C. Koons
Space Sciences Laboratory
The Aerospace Corporation
P.O. Box 92957
Los Angeles, California 90009

From September 1984 through July 1985 the AMPTE Project carried out eight chemical releases of either barium or lithium in the solar wind, magnetosheath, and geomagnetic tail. A Plasma Wave Experiment consisting of several receivers covering a total frequency range of DC to 5.6 MHz was included as part of the diagnostic instrumentation on the AMPTE/IRM spacecraft. Data from the AMPTE/IRM Plasma Wave Experiment's high time resolution and very sensitive electric field receivers have provided detailed information on the electron number densities observed both near the center of the releases (as determined from the observations of electron plasma oscillations) and at the boundaries of the expanding clouds (from the observed shadowing of electromagnetic radiation existing external to the clouds). The large frequency range of the receivers allowed the observation of number densities as high as 4×10^5 cm^{-3} encountered during the earliest seconds of the barium releases. During the diamagnetic cavity phase of the releases the number density measurements provided important information about the efficiency of the reactions and the rate of ionization. Higher number densities were observed at the outer edges of the clouds than at the center of the clouds for all of the releases. Dramatic increases in number densities were also observed when the magnetic field re-entered the clouds for all of the releases except the two lithium releases in the tail. The subsequent observations of the number densities following the re-entry of the magnetic field were quite structured and varied considerably for the different releases.

H6-3
0920

BARIUM RELEASES IN THE MAGNETOTAIL DURING AMPTE

P.A. Bernhardt, R.A. Roussel-Dupre, S.P. Gary and M.B. Pongratz
Los Alamos National Laboratory
Los Alamos, NM 87545

The release of 10^{25} barium atoms in the magnetotail occurred on two occasions, March 21, 1985 and May 13, 1985. The first release occurred at 12 earth radii geocentric distance in a 8 nT background field. The second release occurred at 14.4 earth radii in a 17.6 nT background field. In each case, the expanding barium ions formed a magnetic cavity. The maximum size of the cavity was dependent on the strength of the ambient magnetic pressure. We have successfully modeled the formation and collapse of the cavities with MHD theory.

The surfaces of the diamagnetic cavities were rippled with field aligned irregularities. The scale size of the irregularities is in agreement with the theory of the lower-hybrid-drift instability. Both kinetic instabilities and fluid instabilities are being examined as sources for the irregularities.

H6-4 MODELING OF ION CLOUD EXPANSION IN SPACE
0940
A.T.Y. Lui
Applied Physics Laboratory
Laurel, MD 20707
A. Mankofsky, R.A. Smith
A.T. Drobot, L. Linson, K. Papadopoulos*
and C. Goodrich*
SAIC
McLean, VA 22102

Computational and theoretical studies of ion cloud expansion under conditions of high and low kinetic beta will be presented. The modeling is performed by using a two dimensional hybrid (kinetic ions and magnetized fluid electrons) code that includes anomalous transport as well as a simplified description of the collisional plasma neutral gas interactions. Emphasis is given to the physical processes controlling the formation of diamagnetic cavities due to the cloud-plasma interactions, the accompanying collisionless momentum coupling and the resulting cloud morphology. The results will be applied to the recent AMPTE releases for the high kinetic beta situation, and to the future CRESS program for the low kinetic beta interaction.

*Permanent Address: University of Maryland, College Park, MD 20742

H6-5
1020

WAVE PHENOMENA DURING ARTIFICIAL GAS RELEASES IN THE MAGNETOSPHERE

Adam Drobot, Alan Mankofsky, Lewis Linson,
K. Papadopoulos*
SAIC
McLean, VA 22102
A.T.Y. Lui
Applied Physics Laboratory
Laurel, MD 20707

Two dimensional hybrid (kinetic ions, magnetized fluid electrons) and particle codes are used to study electrostatic wave phenomena resulting from the interaction of an expanding ionized gas release in the magnetosphere. Instabilities due to counterstreaming ion distributions and due to relative electron-ion drifts such as the ion-ion instabilities, the modified two stream instability and the lower hybrid drift instability are examined within the context of the expanding releases and the resulting nonlinear wave spectra and global structures are predicted. The results are compared with the structures and wave spectra observed during the AMPTE releases in the magnetosphere.

Permanent Address: University of Maryland,
College Park, MD 20742

H6-6
1040

SHORT WAVELENGTH ELECTROSTATIC NOISE OBSERVED IN THE VICINITY OF THE SHUTTLE DURING THE SL-2 MISSION

D. A. Gurnett, J. T. Steinberg and W. S. Kurth
Dept. of Physics and Astronomy
The University of Iowa
Iowa City, IA 52242

Intense broadband electrostatic emissions were observed by the University of Iowa Plasma Diagnostics Package (PDP) during a fly-around of the Shuttle as part of the Spacelab-2 mission. The noise mainly occurs at frequencies below 10 kHz, but a weak component can be detected at frequencies up to 100 kHz. The spectrum is similar to spectrums observed during the previous STS-3 mission. The intensities increase during firings of the thrusters, and during water dumps, which shows that the noise is associated with neutral gas emissions from the Shuttle. Broadband intensities are typically in the range from 1 to 10 mVolts/m.

The principal new results from the Spacelab 2 flight have to do with the spatial distribution of the noise around the Shuttle and the wavelength of the waves. The fly-around shows that the highest intensities occur in the wake behind the Shuttle, and near the magnetic flux tube through the Shuttle. The noise intensities are quite low upstream of the Shuttle. Antenna interference pattern effects, observed as the PDP rotates, show that the noise has very short wavelengths, only a fraction of a meter at the highest frequencies. It seems likely that this noise is produced by ionization of the neutral gas cloud around the Shuttle. Possible mechanisms for generating the noise are discussed.

H6-7
1100

INFLUENCE OF PARALLEL DYNAMICS ON THE STABILITY OF IONOSPHERIC PLASMA CLOUDS: A 2D WATERBAG MODEL

J.F. Drake*, J.D. Huba, and S.T. Zalesak
Naval Research Laboratory (Code 4780)
Washington, DC 20375-5000

We present a stability analysis of ionospheric plasma clouds based on 2D waterbag model. In particular, we investigate the evolution of the $\underset{\sim}{E} \times \underset{\sim}{B}$ gradient drift instability. The new feature of this analysis is the inclusion of parallel dynamics, i.e., density and potential fluctuations along the ambient field. It is found that parallel effects can be very important and can stabilize the $\underset{\sim}{E} \times \underset{\sim}{B}$ instability in the long wavelength limit ($kL < 1$ when k is the wavenumber and L is the scale length of the density gradient). The relevance of this work to barium cloud observations will be discussed.

*Science Applications International Corporation, McLean, VA 22102 and University of Maryland, College Park, MD 20742

H6-8
1120 COLLECTIVE PROCESSES DURING CRITICAL IONIZATION VELOCITY INTERACTIONS

R. Smith, A. Drobot and K. Papadopoulos*
Science Applications International Corporation
McLean, VA 22012

The instabilities responsible for the electron heating causing ionization during critical ionization velocity (CIV) experiments are revisited. A linear analysis of the situation is performed that includes the role of the finite system size, finite beta effects as well as highly collisional interactions. It is found that:

(i) The system size plays an important role, not only in controlling the electron confinement time, but more importantly in the structure of the unstable eigenmodes and the allowable electron energization.
(ii) The cross field instabilities that produce the electron energization are substantially weakened and even completely stabilized for high kinetic beta situations.
(iii) When the electron-neutral collision frequency is comparable with the lower hybrid frequency the C.I.V. is driven by collisional electron heating in the oscillatory electric fields caused by the counterstreaming ion-ion interaction.

*Permanent Address: University of Maryland, College Park, MD 20742

Session A-4 1355-Thurs. CR1-42
NEAR FIELD MEASUREMENTS
Chairman: R. C. Baird, Electromagnetic Fields Division,
National Bureau of Standards, Boulder, CO 80303

A4-1
1400 THE RECEIVING ANTENNA AS A LINEAR DIFFERENTIAL OPERATOR

Arthur D. Yaghjian
Electromagnetic Sciences Division
Rome Air Development Center
Hanscom AFB, MA 01731

Ronald C. Wittmann
Electromagnetic Fields Division
National Bureau of Standards
Boulder, CO 80303

The general receiving antenna is represented as a linear differential operator converting the incident field and its spatial derivatives at a single point in space to an output voltage. The differential operator is specified explicitly in terms of the multipole coefficients of the antenna's complex receiving pattern. When the linear operator representation is applied to the special probes used in spherical near-field measurements, a probe-corrected spherical transmission formula is revealed that retains the form, applicability, and simplicity of the nonprobe-corrected equations. The new spherical transmission formula is shown to be consistent with the previous transmission formula derived from the rotational and translational addition theorems for spherical waves.

A4-2 1420 **MEASUREMENT OF ARRAY ELEMENT EXCITATIONS USING A PLANAR NEAR-FIELD RANGE.**

K. N. Sherman, Member Technical Staff
HUGHES AIRCRAFT COMPANY
P.O.B. 92919 S12/W319
LOS ANGELES CA 90009

It is often useful to know the element excitations of an array antenna. This information may be used to adjust the phase shifters of an electronically scanned array, or to verify the design of an antenna with a fixed excitation. It can be difficult, however, to measure the element excitations directly without disturbing the field of the antenna.

This paper describes a proceedure to calculate the excitation of each radiator from a near-field scan of the antenna. First, the plane wave spectrum of the antenna is computed from the near-field data. This is divided through by the spectrum of a typical array element. Integration then yields the complex element excitations, which include any mutual coupling effects that may be present. The precise location of each radiator relative to the near-field data is essential for this calculation.

Results are given for measurements of a C-band circularly polarized array of 146 potter horns fed by a squareax network. Results are also given for a linearly polarized array of waveguide fed dielectric horns.

A4-3
1440

Improved Spherical and Hemispherical Scanning Algorithms

Richard L. Lewis and Ronald C. Wittmann

Electromagnetic Fields Division
National Bureau of Standards
Boulder CO 80303

ABSTRACT

A probe-corrected hemispherical-scanning algorithm has been developed which is applicable when the antenna under test radiates negligibly into its rear hemisphere. Compared to an efficient version of the best previously described full-sphere scanning algorithm, our hemispherical scanning algorithm is over three and a half times more efficient. Improvements have also been made to full-sphere scanning, resulting in a new algorithm which is twice as efficient as the best previous full-sphere algorithm. Moreover, our new formulations exactly invert the band-limited spherical-coordinate representation of the received signal (i.e., no aliasing errors are introduced).

A4-4
1520

THE DETERMINATION OF ROOM SCATTERING ON A NEAR-FIELD RANGE

Allen C. Newell, Michael H. Francis
National Bureau of Standards
Electromagnetic Fields Division
Boulder, Co 80303

The NBS has developed a method for determining the level and character of the signals scattered by the room and subsequently received by the probe.

Conceptually one wants to fix the x-y-z position for both the probe and antenna and move the room. Changes in signal are then due to room scattering. This can be accomplished by moving both the probe and antenna together relative to the room. Various averaging techniques are used to estimate and correct for errors other than room scattering. After correcting for these errors an estimate of the room scattering is obtained.

A4-5
1540

MODIFIED PLANAR NEAR-FIELD MEASUREMENT FACILITY TO ACCOMMODATE LARGER ANTENNAS

Allen C. Newell and Douglas Kremer
Electromagnetic Fields Division
National Bureau of Standards
Boulder, CO 80303

In almost all planar near-field measurement facilities, the antenna remains stationary and the probe is moved in x and y to obtain the amplitude and phase data used in the calculation of antenna patterns. Since data must be obtained over an area somewhat larger than the antenna under test, the size of the scanner determines the antenna sizes that can be accommodated.

This has been the case with the NBS scanner which has a measurement area coverage of approximately 4 meters in both directions. Recently the facility was modified by adding a pair of precision rails in front of, and running parallel to the scanner. The rails are 15 m long and the antenna tower moves on these rails. By positioning the antenna in a sequence of three positions as shown in the figure below, the effective scan area has been increased to approximately 12 m X 4 m.

Techniques will be described to accurately align the rails, measure the probe/antenna position and guarantee continuity of the data for the three antenna positions.

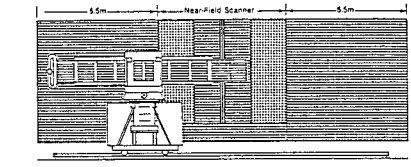

ANTENNA ON NEAR-FIELD SCANNER, POSITION 1

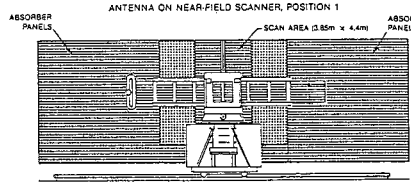

ANTENNA ON NEAR-FIELD SCANNER, POSITION 2

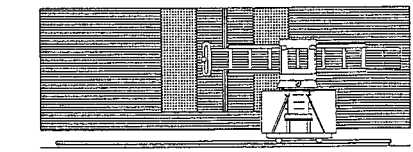

ANTENNA ON NEAR-FIELD SCANNER, POSITION 3

A4-6 1600

SPHERICAL NEAR-FIELD SCANNING MEASUREMENTS: COMPUTATION BASED ON THE PROBE-OPERATOR CONCEPT

R. C. Wittmann and R. H. Cormack
Electromagnetic Fields Division
National Bureau of Standards
Boulder, CO 80303

Recently it has been shown that that it is possible to represent a probe as a linear operator which interacts with the incident field at a given point in space to produce a scalar output. While this idea allows an intuitive derivation of spherical scanning theory from a measurement oriented point of view, one is ultimately faced with the practical problem of evaluating lengthy expressions involving differential operations.

In the past analytical calculations have not been considered in the domain of automatic computing, but with the advent of symbolic manipulation programs it is possible to perform much tedious algebra in a straightforward and elegant manner. We would like to demonstrate the use of computer aided symbolic manipulation, both as a practical computational tool in the case of "simple" probes, and as a useful alternate check in the more general case.

A4-7 Discussion
1620

Session G-10 1355-Thurs. CR0-30
SCINTILLATION MODELING
Chairman: Steve J. Franke, University of Illinois, Urbana, IL 61801

G10-1
1400

SCINTILLATION THEORY AND NUMERICAL SIMULATIONS

C. L. Rino
SRI International
333 Ravenswood Avenue
Menlo Park, CA 94025

The diffraction theory of power-law phase screens has been exploited effectively to characterize the scintillation structure in single power law environments, particularly in the scale-free or fractile limit. However, some of the more interesting tests of the theory in practical situations, as well as extensions to multiple power-law environments and to other situations that are not readily treated analytically, have been studied by using numerical simulations. In this paper we review these results and discuss their ramifications.

G10-2
1420

SCINTILLATION SIMULATION FOR THE IONOSPHERIC REFLECTION CHANNEL

J.-F. Wagen and K. C. Yeh
Department of Electrical and Computer Engineering
University of Illinois, Urbana-Champaign, IL 61801

A numerical scheme has been developed to study the effect of HF waves reflected by a turbulent stratified ionosphere. The scheme uses the phase-screen-diffraction layer method with particular attention to the turning point where the classical WKB solutions are known to be inappropriate.

Previously, results [Kiang and Liu, 1985] have been published for the case of vertically incident waves. After generalizing the method to the case of an oblique incidence, new results are obtained and compared with these earlier results. The results will depict scintillation characteristics such as the power spectrum, scintillation index, and two-frequency mutual coherence function. The last quantity is of interest in applications to HF communications.

G10-3 1440 APPLICATION OF A THEORETICAL MODEL OF FIELD-ALIGNED SCATTER TO VHF SCATTERING BY AURORAL IRREGULARITIES

A. Malaga
SIGNATRON, Incorporated
12 Hartwell Avenue
Lexington, MA 02173

In this paper we discuss a theory for VHF scattering by field-aligned ionospheric irregularities and present results which illustrate the geometrical (aspect) sensitivity of the scattering by field-aligned irregularities at E-layer heights (90-140 km) in the auroral region. The theory developed is very general, though, and also applies to scattering by field-aligned irregularities induced by high-altitude nuclear bursts at arbitrary latitudes. The main difference between auroral scatter and scattering at lower latitudes is that at high latitudes only energy scattered by irregularities in the E-layer (90-140 km heights) can be received by a terminal on the surface of the earth. Energy scattered by irregularities in the ionization of the F-layer (200-500 km) does not intersect the surface of the earth because of the directionality caused by the anisotropy of field-aligned irregularities. At lower latitudes field-aligned irregularities in the E- and F-regions contribute to the total received scattered field. However, the scattering cross-section of the irregularities in the F-layer is greater than that of the E-layer irregularities so that, at lower latitudes, most of the received energy is due to F-layer irregularities.

In addition to the aspect sensitivity (geometry) of field-aligned scatterer we also present results which illustrate polarization effects, antenna height, pointing and beamwidth effects, frequency dependence, and the delay spread or coherence bandwidth of the scattered signal.

G10-4
1520 AN INVESTIGATION OF 4 GHZ SCINTILLATION IN THE ASIAN REGION

T. A. Mollen and C. H. Liu
Department of Electrical and Computer Engineering
University of Illinois, Urbana-Champaign, IL 61801

In this paper, a detailed study is carried out in an attempt to understand the morphology of equatorial ionospheric irregularities causing scintillation at C-band. The study is based on data of 4 GHz downlink signal received at Hong Kong during the solar maximum period of 1979-80 from the Intelsat satellites located at 63°E in the Pacific Ocean Region (POR) and 174°E in the Indian Ocean Region (IOR). The scintillation index, power spectrum, correlation function as well as distribution of signal level are computed from the data for over a fifteen month period. Statistics of power spectral index (PSI) for the spectrum and the coherence time of the autocorrelation function are investigated to find the seasonal and diurnal behavior. The results are applied to study the evolution of irregularity spectrum and the drift velocity. A study of the statistics of signal fluctuation is also conducted. Experimental relations between signal enhancements and fade levels to the scintillation index S_4 will be presented.

G10-5 HF SIGNAL DISTORTION IN THE POLAR IONOSPHERE
1540

R.P. Basler, G.H. Price, C.L. Rino, and R.T. Tsunoda
Radio Physics Laboratory
SRI International
Menlo Park, California 94025

An experiment in Greenland has measured the transfer characteristics for HF signals propagating through disturbed regions of the ionosphere. Transmissions over the 1-hop path from Narssarssuaq to Thule have suffered distortions in the range (propagation time) and Doppler domains on the order of hundreds of microseconds and tens of Hertz, respectively. A frequency-modulated continuous wave (FMCW) waveform was used for oblique sounding purposes, and a pseudorandom noise modulation with a 20-kHz bandwidth was used to measure range and Doppler spreads. Spaced receivers were used to measure azimuthal angle of arrival, and independent ionospheric diagnostic data for points along the path were provided by the incoherent-scatter radar at Sondre Stromfjord. The results are interpreted in terms of scatter effects produced by high-velocity plasma irregularities encountered along the mean ray paths.

G10-6
1600

ANALYSIS AND INTERPRETATION OF DRIFTING IONOSPHERIC IRREGULARITIES USING SPACED RECEIVER DATA

J. D. Vacchione, S. Franke
Department of Electrical and Computer Engineering
University of Illinois, Urbana-Champaign, IL 61801
M. R. Paulson
Naval Ocean Systems Center
Code 544
San Diego, CA 92152

An analysis of equatorial scintillation at VHF is carried out using spaced receiver (457.2 meters east-west) data taken in Guam at the Naval Communication Area Master Station. The data was received during both pre- and post-midnight hours from April 1982 through May 1983 and was transmitted by the Pacific Fleet Satellite at a frequency of 250.55 MHz.

By using the Briggs full correlation method, the drift velocity and "characteristic random velocity" is tabulated for multi-hour data segements. These calculations are compared with values found by using two other methods (based on Brigg's assumptions) and are found to be in strong agreement. Four case studies, during both strong and weak scintillation, involving interesting velocity trends are examined.

The results from the "characteristic random velocity" calculations will be discussed and some possible interpretations of this parameter will be proposed.

+

G10-7
1620

SPACED RECEIVER ANALYSIS IN THE SPECTRAL DOMAIN

Emanoel Costa
Physics Research Div.
Emmanuel College
400 The Fenway
Boston, MA 02115

Paul F. Fougere
Ionospheric Physics Div.
Air Force Geophysics Lab.
Hanscom AFB MA 01731

It has recently been agreed that Tromso/HILAT spaced receiver data often are degraded by multipath and/or equipment malfunction. As a result the intensities of the received signals are not generally useful for correlation analysis, at the scintillation levels currently observed at 413 MHz. These problems manifest themselves in the form of quasi-sinusoidal components with a slowly-drifting frequency superposed with (and sometimes masking) the expected scintillation. In the frequency domain, the maximum entropy power spectra of the combined signal frequently display narrow and intense peaks on top of the usual scintillation spectrum. Fortunately, the phases of the signals, although not entirely free from, are less affected by multipath contamination and thus look more promising from the correlation analysis standpoint.

In an additional attempt to circumvent some of those difficultities, this contribution will initially describe how a single-scattering scintillation theory has been used to express the auto and cross spectra of the signals in the spaced receiver experiment in terms of those parameters which characterize surfaces of constant correlation levels in the correlation analysis (G.S. Kent and J.R. Koster, Ann. Geophys., 22(3), 405-417, 1966; C.L. Rino and R.C. Livingston, Radio Sci., 17(4), 845-854, 1982). It will then be shown that these calculations provide a straightforward interpretation for the apparent velocity measured by the dispersion analysis (B.H. Briggs, J. Atmos. Terr. Phys., 30, 1789-1794, 1968) in terms of the same parameters.

A scheme which enables us to estimate the anisotropy and the drift of the diffraction pattern defined on the ground by using only the common sections of the spectra which are free from contamination effects will then be briefly described. Finally, comparisons will be made between results provided by the above method and those yielded by applying the standard correlation analysis either to uncontaminated data or to data previously processed by conventional techniques (such as filtering). Signals transmitted by the HILAT satellite at 413 MHz will be used in this comparison.

Session H-7 1355-Thurs. CR2-26
WAVE INJECTION BY ELECTRODYNAMIC TETHER
Chairman: R. D. Estes, Smithsonian Institution Astrophysical Observatory, Cambridge, MA 02138

H7-1
1400

E.M. EMISSIONS FROM THE T.S.S. SHUTTLE-BORNE ELECTRODYNAMIC TETHER: PREPARING FOR GROUND-BASED OBSERVATIONS

R.D. Estes and M.D. Grossi
Harvard-Smithsonian Center for Astrophysics
Cambridge, Massachusetts 02138

The first demonstration flight of the Shuttle-borne Tethered Satellite System (T.S.S.), presently scheduled for mid 1988, will be equipped with a 20 Km-long electrodynamic tether, to be deployed upwards from the Shuttle that will be in an orbit of approximately 250 Km height. The electromotive force that the tether generates by its electrodynamic interactions with the medium will be about 4 KV, while the tether current will be $\lesssim$0.5 A.

It is expected that the tether will generate and radiate electromagnetic emissions in a broad band of frequencies, spanning from well above the gyrofrequency of the ionospheric electrons to well below the ion gyrofrequency. Of particular interest in our research are the wave frequencies below the hybrid resonant frequency (tether-induced whistlers).

Signal intensities at the Earth surface are expected to be detectable above noise, with an integration time shorter than one minute at least for those passes in which the T.S.S. will be directly overhead above the receiving site. Our plans call for "listenings" at ULF (tether-induced micropulsations) by the world-wide network of magnetic observatories (that will be alerted through IAGA about the orbital position of the T.S.S. at specific times), as well as at ELF and at VLF, by receiving sites suitably located and appropriately instrumented. A submersible station will also be utilized in the observations, at the initiative of the University of Genova, Italy, that participates in the experiment.

These observations will be determinant in sorting out the correct theory among the several formulations that have been put forward by various authors on the mechanisms of e.m. wave emission by the electrodynamic tether.

H7-2
1420

PROPAGATION FROM AN ULF/ELF/VLF TETHER ANTENNA SOURCE IN THE IONOSPHERE TO THE EARTH SURFACE

Francis J. Kelly
E.O. Hulburt Center for Space Research
Naval Research Laboratory
Washington, D.C. 20375

The methods for calculating the expected e.m. field on the Earth surface from an ULF/ELF/VLF tether antenna source in the ionosphere are reviewed.

Sample calculation results are presented.

H7-3
1440

RADIATION OF PLASMA WAVES BY A CONDUCTING BODY MOVING THROUGH A MAGNETIZED PLASMA

A. Barnett and S.Olbert
Center for Space Research
Massachusetts Institute of Technology
Cambridge, Massachusetts 02139

There are many situations of interest in space and astrophysics which consist of a conducting body moving through a magnetized plasma. It is well known that large conducting objects which move slowly across magnetic field lines radiate low frequency (Alfvèn) waves. In this paper we study the interaction between a plasma and a moving conductor in order to estimate the total power radiated at all frequencies. Toward this end, we develop a formalism which permits us to compute the response of the plasma to an external current source. We then derive an integral equation which relates the source current to the electrical properties of the conducting body. This formalism enables us to estimate the total radiated power for simple geometries.

We find in general that radiation is produced at all frequencies for which one of the plasma modes has zero phase velocity in some direction. The mechanism by which this radiation is produced is analogous to Cherenkov radiation. In the cold plasma approximation, in a plasma for which

$$\omega^2 >> \Omega_e^2 \quad \text{and} \quad V^2 << c_A^2 << c^2 ,$$

there is radiation in three frequency bands : $\omega < \Omega_i, \omega_{LH} < \omega < \Omega_e$ and $\omega_p < \omega < \omega_{UH}$, where V is the speed of the body, c_A is the Alfvèn speed, c is the speed of the light in vacuum, ω is the frequency of the radiation, and Ω_i, ω_{LH}, Ω_e, ω_p, ω_{UH} are the ion cyclotron, lower hybrid, electron cyclotron, plasma, and upper-hybrid frequencies, respectively.

To gain a better understanding of the properties of the plasma waves in these frequency bands, we present polar plots of the phase and group velocities of these waves. Finally, we present estimates of radiated power for a sphere and a cylinder of arbitrary size. We find that a wire 10 Km long and 3 mm radius, such as the tether for a tethered satellite system, radiates about 65 watts. The Jovian Satellite Io, known to be a strong source of Alfvèn waves, also radiates 10^{-7} times as much power in the second frequency band.

H7-4
1520

WAVE INJECTION FROM THE ELECTRODYNAMIC TETHERED SATELLITE SYSTEM

A.T. Drobot, C.K. Goertz[1], L.M. Linson, K. Papadopoulos and R.A. Smith
Science Applications International Corporation
McLean, VA 22102

The electrodynamic Tethered Satellite System (TSS) provides an unusual opportunity for studying fundamental aspects of the interaction between highly charged moving conductors and a tenous plasma. The operation of the TSS results in a global current circuit which consists of the satellite sheath, the conducting tether, the orbiter sheath, and field aligned ionospheric currents which close in the E-region. We will discuss the mechanisms which can lead to ionospheric wave injection from the TSS. The sources of wave injection that we consider are: i) the natural spectrum of Alfven and whistler waves which propagate along the ionospheric transmission line represented by the field aligned currents which close the TSS circuit at the satellite and at the orbiter; ii) current fluctuations in the conducting tether; iii) instabilities in the orbiter or satellite sheaths; and iv) current driven instabilities in the ionospheric plasma.

---

(1) Permanent Address: University of Iowa

INDEX